Online Supplementary Material for

Distributional and Temporal Heterogeneity in the Climate Change Effects on U.S. Agriculture*

Emir Malikov[1]   Ruiqing Miao[2]   Jingfang Zhang[2]

[1]University of Nevada, Las Vegas   [2]Auburn University

September 19, 2020

Abstract

Existing studies on climate change effects on crop yields mainly focus on the *average* climate–yield relationship that is typically assumed to be time-invariant. We apply a flexible panel-data quantile regression with time-varying coefficients to examine distributional heterogeneity and temporal variation in this relationship. We find that U.S. corn and soybean yields have gradually become less sensitive to temperature and precipitation over 1948–2010, which is especially the case for upper yield quantiles. Consequently, the negative impacts of future climate change are of larger magnitudes at the lower yield quantiles. Failure to accommodate temporal changes in the climate–yield relationship leads to significantly overestimated responsiveness of crop yields to weather variation and, therefore, overestimated negative impacts of future climate change. On many occasions, the corn yield decline projections from such time-invariant specifications are about twice as large as (and sometimes triple) the predictions from our time-varying-coefficient model.

Keywords: Adaptation, Agriculture, Climate Change, Crop Yields, Heterogeneity, Quantile Regression

JEL Classification: Q16, Q54

This supplementary material is an extended version of the paper.

* *Email*: emir.malikov@unlv.edu (Malikov), miaorong@auburn.edu (Miao) and jzz0080@auburn.edu (Zhang).

1 Introduction

Since the publication of the *Changing Climate* report by the U.S. National Research Council in 1983,[1] which raised serious concerns about adverse climate change impacts on agricultural production following a comprehensive assessment of potential consequences of the increasing CO_2 levels in the atmosphere, the link between climate and agricultural outcomes (e.g., land values, farming returns, and crop yields) has garnered much attention from economists. Starting with Mendelsohn et al.'s (1994) seminal work, numerous studies have applied regression analyses to examine climate change effects on agriculture (e.g., Schlenker et al., 2005; Deschênes & Greenstone, 2007; Schlenker & Roberts, 2009; Lobell et al., 2014; Burke & Emerick, 2016; Chen et al., 2016; Miao et al., 2016; Zhang et al., 2017).[2] However, prior studies have mainly focused on the *average* climate–agriculture relationship, which inhibits our understanding of potential distributional heterogeneity in climate change effects. Although knowing how climate may affect mean agricultural outcomes are important, it is no less critical to examine potentially differential impacts of climate on lower and upper tails of the outcome distribution, particularly as agricultural outcomes are highly heterogeneous. Not least importantly, the existing literature also largely assumes time-invariance of the climate–agriculture relationship, which cannot capture the evolution of climate impacts on agriculture over time.

In this paper, we examine the reduced-form relationship between climate and agricultural outcomes (namely, crop yields) by addressing the aforementioned research gaps. We choose crop yields as outcome variables because they are a simple and direct measure of crop production with detailed historical data for many decades in the United States. Moreover, crop yields have been widely used in the climate change literature to examine the impact of climate change on agriculture. We did not choose agricultural profits as an outcome variable due to data limitation as the calculation of agricultural profits requires U.S. Census

[1] See National Research Council (1983).

[2] We refer readers to Hsiang (2016), Mendelsohn & Massetti (2017), and Blanc & Schlenker (2017) for comprehensive reviews of this literature. A closely related literature centered on the agronomic-economic analysis combines process-based agronomic simulation models and farm-level economic analyses to quantify climate change effects on agriculture while accounting for farmers' adaptation (see Antle & Stöckle (2017) for an excellent review).

of Agriculture Data which are available only every five years and for a shorter period time (Deschênes & Greenstone, 2007). In a pursuit of robust estimates of the climate change effects on crop yields, we estimate a flexible, yet parsimonious, time-varying-coefficient panel-data quantile regression model which explicitly allows for (*i*) distributional heterogeneity in the effects of climate on yields in low-, medium- and highly-productive areas, (*ii*) temporal variation in the dependence of crop yields on climate (i.e., technological adaptability), and (*iii*) unobservable county-level confounders.

We employ a quantile regression approach to capture distributional heterogeneity of the climate change impacts on crop yields. Quantile regression has become increasingly popular in various fields of economics including education, health, and labor (see Koenker & Hallock, 2001). Unlike traditional regression models that focus on the first moment, quantile regression provides a complete description of the relationship between the distribution of outcome variable and its regressors. Given the advantages of quantile regression over the customarily employed conditional-mean models especially with regard to its ability to better accommodate distributional heterogeneity, it is surprising that the technique has not attracted much attention among applied economists interested in studying the climate–agriculture linkage. Since agricultural outcomes are highly heterogeneous across space, there remains much untapped benefit of examining the link between climate and agriculture via quantile analysis. Thus, contrary to previous studies in the literature which estimate climate change effects on the *average* crop yields via popular conditional-mean models (e.g., Schlenker & Roberts, 2009; Miao et al., 2016; Burke & Emerick, 2016; Chen et al., 2016; Zhang et al., 2017), we focus our analysis on conditional *quantiles* of the (log) yield distribution.[3] Not only does this approach enable us to examine potential heterogeneity in the climate-yield relationship across areas of varying agricultural productivity, but it is also more robust to the error distributions including the presence of outliers in the data. Furthermore, it exhibits a useful equivariance property thereby letting us avoid biases in the "level-of-yield" predictions based on the model estimated in logs that numerous earlier studies suffer from (to be discussed

[3]Within this line of literature that uses conditional-mean models, Schlenker & Roberts (2009) is a representative study in which the authors utilize fixed-effects panel data models to identify the non-linear effects of climate change on U.S. crop yields.

later).

Borrowing from Baltagi & Griffin (1988), we devise a flexible, yet parsimonious, model that allows parameters of the conditional quantile to vary with time, which enables us to investigate the evolution of sensitivity of crop yields to climate variation. Such temporal changes in the climate-yield relationship are meant to reflect farmers' technological adaptability to the changing climate and, more generally, technological progress in the agricultural production whereby yields may improve over time *ceteris paribus*. Most existing studies of the climate-yield relationship estimate models with time-invariant coefficients, implicitly assuming that the relationship is fixed or static. Although Burke & Emerick (2016) investigate the potential of farmers' adaptation to climate change by utilizing an innovative long-difference approach, they still implicitly assume that the climate change impact on crop yields does not vary over time and do not explore temporal changes in the climate-yield relationship. Few exceptions include Mendelsohn et al. (2001) and Lobell et al. (2014) who quantify changes in the sensitivity of agriculture to climate by comparing coefficients estimated using data from different time periods. Although convenient, such a sample-splitting approach suffers from reduced degrees of freedom and is more likely to yield noisier estimates as a result of giving up valuable information embedded in a panel structure of the data. Alternatively, other studies interact time trend with weather variables to capture temporal variability in their marginal effects (e.g., Yu & Babcock, 2010). However, the latter approach effectively requires an *a priori* assumption about the smoothness and a functional form of the dependence of marginal impacts on time (usually, linear). In contrast, we employ flexible non-neutral time indices à la Baltagi & Griffin (1988) to let the coefficients vary with time in an arbitrary fashion. These time indices are unobservable functions of time, and we effectively model them nonparametrically via discretization using a series of time dummies. Overall, by having the time indices enter the quantile function, we are able to accommodate temporal changes in the *entire* conditional log-yield distribution.

We control for unobservable cross-county heterogeneity via fixed effects which absorb time-invariant confounding variation and therefore let us identify the climate-yield relationship by relying on within-county climate deviations from the mean that are plausibly exogenous.[4] However, the direct estimation of quantile regressions with fixed effects using routine estimators is not trivial due to nonlinearity of the quantile operator which makes it impossible to purge fixed effects from the regression via any transformation (e.g., see Koenker, 2004; Galvão & Kato, 2018). We tackle this problem by adapting the recently developed approach by Machado & Santos Silva (2019) that allows an easy-to-implement indirect estimation of the quantile parameters via moments and is more fitting for nonlinear specifications.

In our analysis, we use the annual county-level data on weather variables as well as corn and soybean yields over 1948–2010 in the rainfed region of the United States. The data consistently reject the fixed-coefficient specification in favor of our time-varying-coefficient model. Overall, our empirical results show that yields have gradually become less sensitive to temperature (both the normal-range and overheat) and precipitation over the years. This is especially the case for upper yield quantiles. We find that, compared to our time-varying-coefficient model, a more restrictive fixed-coefficient model tends to significantly overestimate the responsiveness of crop yields to climate variation. For instance, such a model overestimates negative effects of the overheat temperature (29°C+) on corn yields in 1990–2010, with the overestimation being particularly large (more than 50% of the effect size) at lower yield quantiles. Owing to our model's ability to capture temporal change in the climate-yield relationship, we are also able to isolate changes in agricultural productivity that are due to factors other than underlying climatic determinants and county-level effects. Our estimates suggest that, over the course of a sample period, the average annual rate of technology-driven yield improvements for corn have ranged from 1.14% to 1.92% depending on the quantile, with the upper yield quantiles exhibiting higher improvement rates.

Based on forecasts from two popular global climate models (HadGEM2-ES365 and NorESM1-M) under two greenhouse gas representative concentration pathways (RCPs) (RCP4.5 and RCP8.5), we compute crop yield reductions attributed to future climate change at the medium-term (2040–2059) and long-term (2080–2099) horizon by using both the time-varying-coefficient and the more restrictive fixed-coefficient models. We find that using the fixed-

[4]Failing to control for such fixed effects will cause omitted variable bias because the unobservable confounders (such as soil quality, for instance) may correlate with weather variables in a county. We refer readers to Blanc & Schlenker (2017) for a comprehensive discussion about panel models in assessing the impact of climate change on agriculture.

coefficient model highly overestimates (on many occasions, double) the negative impact of future climate change on corn yields. Our projections also show that the negative future climate change effects are of larger magnitudes for corn yields at lower quantiles, thereby suggesting that climate change has the potential to make corn yields even more negatively skewed in the future. Although our data are for the corn production in the U.S., where the most advanced technologies and management practices are employed, this finding also sheds light on the distributional heterogeneity of climate change effects on agriculture in the world more generally: less productive regions (read, developing countries) are expected to be hit by climate change the most, whereas more productive regions (read, developed countries) may be more immune to the negative climate change effects. We obtain similar findings about future soybean yield declines, although the magnitudes of future soybean yield reduction are typically larger than those for corn, especially at lower yield quantiles.

The remainder of the paper proceeds as follows. Section 2 discusses our econometric strategy, followed by Section 3 that describes the data used in the analysis. Section 4 contains the empirical results, robustness checks, and projections of future climate change effects on crop yields. The last section concludes.

2 Econometric Strategy

In a pursuit of robust estimates of the yield–climate relationship, our econometric strategy is to devise a flexible model that is capable of accommodating distributional heterogeneity across counties of varying productivity, potential time variability in the said relationship as well as unobservable county-level confounders, while still maintaining parsimony of the specification. In what follows, we describe our model as well as the associated procedures for statistical inference that we employ in our analysis.

2.1 Panel Data Quantile Estimation

We model the reduced-form relationship between the county-level climate and crop yield at different conditional quantiles of the latter. Let $\log y_{it}$ be the log-yield in county $i = 1, \ldots, n$

in year $t = 1, \ldots, T$, μ_i be the county fixed effect, and $\mathbf{x}_{it}$ be the vector of strictly exogenous weather variables and, possibly, their higher-order polynomial terms. Now, consider the following location-scale regression à la Koenker & Bassett (1982) with fixed effects and time-varying coefficients:

$$\log y_{it} = \mu_i + \beta_0 + \mathrm{B}(t) + \mathbf{x}_{it}' \big[\boldsymbol{\beta}_1 + \boldsymbol{\varphi}_1 \mathrm{B}(t)\big] + u_{it}, \quad u_{it} = \big(\gamma_0 + \Gamma(t) + \mathbf{x}_{it}'\boldsymbol{\gamma}_1\big)\varepsilon_{it}, \tag{2.1}$$

where β_0, $\boldsymbol{\beta}_1$, $\boldsymbol{\varphi}_1$, γ_0 and $\boldsymbol{\gamma}_1$ are unknown fixed coefficients and, to allow for temporal variability in the relationship, we borrow from Baltagi & Griffin (1988) and introduce two scalar time indices $\mathrm{B}(t)$ and $\Gamma(t)$. Both time indices are unobservable and one may think of them as the unknown functions of time. These time indices are advantageous over simple time trends (including quadratic) in modeling temporal changes because they provide richer variation in the measurement of technological change and much closer approximation to observed temporal changes than do the simple time trends (Baltagi & Griffin, 1988). Furthermore, index $\mathrm{B}(t)$ enters the location function *non*-neutrally, shifting not only the intercept $\beta_0 + \mathrm{B}(t)$ but also the slopes $\boldsymbol{\beta}_1 + \boldsymbol{\varphi}_1\mathrm{B}(t)$, thereby allowing for flexible locational shifts over time. Scale changes over time are also allowed by means of $\Gamma(t)$ but, for computational ease and parsimony, we assume additive separability of $\Gamma(t)$ from other variables in the scale function. In all, by means of the time indices in both the location and scale function, we are able to accommodate temporal changes in the *entire* conditional log-yield distribution.

Along the lines of Machado & Santos Silva (2019) upon whom we build our estimation procedure, we assume that ***(i)*** ε_{it} is *i.i.d.* across i and t with some cdf F_ε; ***(ii)*** $\varepsilon_{it} \perp \mathbf{x}_{it}$ with the normalizations that $\mathbb{E}\left[\varepsilon_{it}\right] = 0$ and $\mathbb{E}\left[|\varepsilon_{it}|\right] = 1$; and ***(iii)*** $\Pr\left[\gamma_0 + \Gamma(t) + \mathbf{x}_{it}'\boldsymbol{\gamma}_1 > 0\right] = 1$. Then, for any given quantile index $\tau \in (0, 1)$, from (2.1) it immediately follows that the τth conditional quantile of the log-yield is

$$\mathbb{Q}_\tau\left[\log y_{it} | \mathbf{x}_{it}\right] = \mu_i + \underbrace{\Big[\beta_0 + \gamma_0 q_\tau + \mathrm{B}(t) + \Gamma(t) q_\tau\Big]}_{\text{time-varying quantile interecept}} + \mathbf{x}_{it}' \underbrace{\Big[\boldsymbol{\beta}_1 + \boldsymbol{\gamma}_1 q_\tau + \boldsymbol{\varphi}_1 \mathrm{B}(t)\Big]}_{\text{time-varying quantile slopes}}, \tag{2.2}$$

where $q_\tau = F_\varepsilon^{-1}(\tau)$ is the (unknown) τth quantile of ε_{it}, and both the intercept and slope coefficients vary with the quantile of log-yield as well as time.

We opt to begin with the location-scale model to derive the conditional quantile function of interest in (2.2) as opposed to postulating a quantile regression *prima facie* because we seek to estimate these quantiles *indirectly*. This is motivated by the presence of unobserved fixed effects in the model. Namely, the direct estimation of quantile regressions with fixed effects using the routine check-function-based estimator is not trivial due to nonlinearity of the quantile operator that makes it impossible to purge $\{\mu_i\}$ from the equation via any transformation (e.g., see Koenker, 2004). We therefore adopt the approach recently proposed by Machado & Santos Silva (2019) that allows an easy-to-implement indirect estimation of the quantile parameters via moments, where all quantile parameters are estimated based on the moments implied by the location-scale model in (2.1).

To operationalize the estimator, per Baltagi & Griffin's (1988) idea, we model unobservable $\mathrm{B}(t)$ and $\Gamma(t)$ via discretization. Specifically, for each $\kappa = 1, \ldots, T$, define the dummy variable $d_{\kappa,t}$ that is equal to 1 in the κth time period and 0 otherwise. Then, we set $\mathrm{B}(t) = \sum_{\kappa=2}^{T} \eta_\kappa d_{\kappa,t}$ and $\Gamma(t) = \sum_{\kappa=2}^{T} \theta_\kappa d_{\kappa,t}$, where $\mathrm{B}(1) = \eta_1 = 0$ and $\Gamma(1) = \theta_1 = 0$ are normalized for identification.[5] The feasible analogue of (2.1) is then given by

$$\log y_{it} = \mu_i + \beta_0 + \sum_{\kappa=2}^{T} \eta_\kappa d_{\kappa,t} + \mathbf{x}_{it}' \left[\boldsymbol{\beta}_1 + \boldsymbol{\varphi}_1 \sum_{\kappa=2}^{T} \eta_\kappa d_{\kappa,t} \right] + \left(\gamma_0 + \sum_{\kappa=2}^{T} \theta_\kappa d_{\kappa,t} + \mathbf{x}_{it}' \boldsymbol{\gamma}_1 \right) \varepsilon_{it}. \quad (2.3)$$

Two noteworthy observations are in order here. First, the discretized parameterization of the unknown $\mathrm{B}(t)$ and $\Gamma(t)$ is akin to a nonparametric local-constant estimation of these unknown functions of time with the bandwidth parameter being set to 0. Second, though it might appear at first that, when $\mathrm{B}(t)$ estimated with a series of time dummies, we obtain the time-varying slope coefficients on $\mathbf{x}_{it}$ by merely interacting the latter with time dummies and adding them as additional regressors, this is not quite the case because time dummies are restricted to have the same parameters $\{\eta_k\}$ both when entering additively as well as when interacting with $\mathbf{x}_{it}$. Thus, the location function is not a "fully saturated" specification with

[5] Under this identifying normalization, β_0, $\boldsymbol{\beta}_1$ and γ_0 are naturally interpretable as "reference" coefficients in time period $t = 1$.

$1+p+(T-1)(p+1)$ coefficients but, in fact, is a more parsimonious *nonlinear* (in parameters) function with only $1+2p+(T-1)$ coefficients.[6] This is important because, by avoiding a fully saturated specification that is equivalent to sample-splitting into cross-sections, we are able to accommodate time-invariant individual fixed effects in the model.

Incidentally, the nonlinearity of our model is also the reason why we do not use the Canay (2011) fixed-effects quantile regression estimator which provides an alternative to Machado & Santos Silva (2019) with the difference being that the former uses the check-function-based estimator as opposed to moment-based. Given that the L_1 optimization used in the check-function-based estimations is not as adept to handling nonlinearities in parameters and, more importantly, to the presence of many dummy variables (of which we have $T-1=62$ in our empirical application), we opt for the L_2 moment-based estimator.

Although the estimation of (2.2) can be done in one step via nonlinear method of moments, we adopt a multi-step procedure that is significantly easier to implement. This is possible because the moments implied by model (2.1) and its assumptions are sequential in nature. In other words, we can first estimate parameters of the location function and then those of the scale function in two separate steps. After that, based on the estimates of these parameters, the third step is taken to estimate unknown quantiles and, ultimately, recover time-varying quantile coefficients in (2.2). In what follows, we describe this procedure in detail.

2.1.1 *Estimation of the location and scale functions*

First, for ease of notation, define $\mathbf{d}_t = [d_{2,t}, \ldots, d_{T,t}]'$, $\boldsymbol{\eta} = [\eta_2, \ldots, \eta_T]'$ and $\boldsymbol{\theta} = [\theta_2, \ldots, \theta_T]'$. Under the assumption ***(ii)***, from (2.3) it follows that the conditional mean function of the log-yield is

$$\mathbb{E}\left[\log y_{it}|\mathbf{x}_{it}, \mathbf{d}_t\right] = \mu_i + \beta_0 + \sum_{\kappa=2}^{T} \eta_\kappa d_{\kappa,t} + \mathbf{x}_{it}'\left[\boldsymbol{\beta}_1 + \boldsymbol{\varphi}_1 \sum_{\kappa=2}^{T} \eta_\kappa d_{\kappa,t}\right], \tag{2.4}$$

[6]For some specificity, we have $T=63$ and $p=10$ in our empirical application.

which can be consistently estimated in the within-transformed form via nonlinear least squares after purging additive fixed effects.[7] Given the nonlinearity and high dimensionality of (2.4) in parameters, we estimate the slopes $[\boldsymbol{\eta}', \boldsymbol{\beta}_1', \boldsymbol{\varphi}_1']'$ via concentration by noticing that, conditional on $\boldsymbol{\eta}$, this mean regression is linear in $[\boldsymbol{\beta}_1', \boldsymbol{\varphi}_1']'$ yielding the profiled least-squares estimator for $[\boldsymbol{\beta}_1(\boldsymbol{\eta})', \boldsymbol{\varphi}_1(\boldsymbol{\eta})']'$. Specifically, letting the concentrated sum of (within-transformed) squared errors be

$$Q(\boldsymbol{\eta}) = \sum_i \sum_t \Bigg[\left(\log y_{it} - \overline{\log y}_i - \sum_\kappa \eta_\kappa \left(d_{\kappa,t} - \bar{d}_\kappa \right) \right) - (\mathbf{x}_{it} - \overline{\mathbf{x}}_i)' \boldsymbol{\beta}_1(\boldsymbol{\eta}) - \left(\mathbf{x}_{it} \sum_\kappa \eta_\kappa d_{\kappa,t} - \overline{\mathbf{x}_i \sum_\kappa \eta_\kappa d_\kappa} \right)' \boldsymbol{\varphi}_1(\boldsymbol{\eta}) \Bigg]^2, \tag{2.5}$$

with the "bar" denoting the cross-time averages of variables, we have the profiled estimators $[\boldsymbol{\beta}_1(\boldsymbol{\eta})', \boldsymbol{\varphi}_1(\boldsymbol{\eta})']' = \left(\sum_i \sum_t \mathbb{X}_{it} \mathbb{X}_{it}' \right)^{-1} \sum_i \sum_t \mathbb{X}_{it} y_{it}^*$, where $\mathbb{X}_{it} = \left[(\mathbf{x}_{it} - \overline{\mathbf{x}}_i)', \left(\mathbf{x}_{it} \sum_\kappa \eta_\kappa d_{\kappa,t} - \overline{\mathbf{x}_i \sum_\kappa \eta_\kappa d_\kappa} \right)' \right]'$ and $y_{it}^* = \log y_{it} - \overline{\log y}_i - \sum_\kappa \eta_\kappa \left(d_{\kappa,t} - \bar{d}_\kappa \right)$.

Thus, the nonlinear fixed-effects estimators of the slopes $[\boldsymbol{\eta}', \boldsymbol{\beta}_1', \boldsymbol{\varphi}_1']'$ in the location functions are

$$\widehat{\boldsymbol{\eta}} = \arg\min_{\boldsymbol{\eta}} Q(\boldsymbol{\eta}) \quad \text{and} \quad \widehat{\boldsymbol{\beta}}_1 = \boldsymbol{\beta}_1(\widehat{\boldsymbol{\eta}}), \; \widehat{\boldsymbol{\varphi}}_1 = \boldsymbol{\varphi}_1(\widehat{\boldsymbol{\eta}}). \tag{2.6}$$

Under the usual $\sum_{i=1}^n \mu_i = 0$ normalization, we can then recover the intercept β_0 and the fixed effects $\{\mu_i\}$:

$$\widehat{\beta}_0 = \frac{1}{nT} \sum_i \sum_t \left(\log y_{it} - \sum_\kappa \widehat{\eta}_\kappa d_{\kappa,t} - \mathbf{x}_{it}' \left[\widehat{\boldsymbol{\beta}}_1 + \widehat{\boldsymbol{\varphi}}_1 \sum_\kappa \widehat{\eta}_\kappa d_{\kappa,t} \right] \right), \tag{2.7}$$

$$\widehat{\mu}_i = \frac{1}{T} \sum_t \left(\log y_{it} - \widehat{\beta}_0 - \sum_\kappa \widehat{\eta}_\kappa d_{\kappa,t} - \mathbf{x}_{it}' \left[\widehat{\boldsymbol{\beta}}_1 + \widehat{\boldsymbol{\varphi}}_1 \sum_\kappa \widehat{\eta}_\kappa d_{\kappa,t} \right] \right) \quad \forall i. \tag{2.8}$$

Hence, the residual estimator is

$$\widehat{u}_{it} = \log y_{it} - \widehat{\mu}_i - \widehat{\beta}_0 - \sum_\kappa \widehat{\eta}_\kappa d_{\kappa,t} - \mathbf{x}_{it}' \widehat{\boldsymbol{\beta}}_1 + \widehat{\boldsymbol{\varphi}}_1 \sum_\kappa \widehat{\eta}_\kappa d_{\kappa,t}. \tag{2.9}$$

[7] Note that, although (2.4) is nonlinear, the presence of fixed effects does not give rise to the incidental parameter problem in this case because $\{\mu_i\}$ enters the model additively and is not inside the nonlinear mean function.

Next, consider the scale function. Based on the assumptions ***(ii)***–***(iii)***, we have an auxiliary conditional mean regression:

$$\mathbb{E}\left[|u_{it}|\big|\mathbf{x}_{it}, \mathbf{d}_t\right] = \gamma_0 + \sum_{\kappa} \theta_\kappa d_{\kappa,t} + \mathbf{x}'_{it}\boldsymbol{\gamma}_1, \tag{2.10}$$

from where the estimators of $[\boldsymbol{\theta}', \gamma_0, \boldsymbol{\gamma}'_1]$ are

$$\left[\widehat{\boldsymbol{\theta}}', \widehat{\gamma}_0, \widehat{\boldsymbol{\gamma}}'_1\right] = \Big(\sum_i \sum_t \mathcal{X}_{it}\mathcal{X}'_{it}\Big)^{-1} \sum_i \sum_t \mathcal{X}_{it}|\widehat{u}_{it}|, \tag{2.11}$$

with $\mathcal{X}_{it} = [1, \mathbf{d}'_t, \mathbf{x}'_{it}]'$ and $\widehat{u}_{it}$ estimated in (2.9).

2.1.2 *Estimation of quantiles*

For any given quantile index $0 < \tau < 1$, we first estimate the unconditional quantile of ε_{it}. From $u_{it} = \big(\gamma_0 + \sum_\kappa \theta_\kappa d_{\kappa,t} + \mathbf{x}'_{it}\boldsymbol{\gamma}_1\big)\varepsilon_{it}$, we have that

$$\mathbb{Q}_\tau\left[u_{it}|\mathbf{x}_{it}, \mathbf{d}_t\right] = \left(\gamma_0 + \sum_\kappa \theta_\kappa d_{\kappa,t} + \mathbf{x}'_{it}\boldsymbol{\gamma}_1\right) q_\tau\left(\varepsilon_{it}\right), \tag{2.12}$$

where $q_\tau = q_\tau\left(\varepsilon_{it}\right)$ is the τth unconditional quantile of ε_{it}. Hence, we estimate q_τ via a univariate quantile regression (with no intercept):

$$\widehat{q}_\tau = \arg\min_q \sum_i \sum_t \rho_\tau \left\{\widehat{u}_{it} - \left(\widehat{\gamma}_0 + \sum_\kappa \widehat{\theta}_\kappa d_{\kappa,t} + \mathbf{x}'_{it}\widehat{\boldsymbol{\gamma}}_1\right) q\right\}, \tag{2.13}$$

where $\rho_\tau\{\xi\} = \xi\left(\tau - \mathbb{I}\left\{\xi < 0\right\}\right)$ is the check function, $\widehat{u}_{it}$ is estimated in (2.9), and $\left[\widehat{\boldsymbol{\theta}}', \widehat{\gamma}_0, \widehat{\boldsymbol{\gamma}}'_1\right]'$ are estimated in (2.11).

With all parameters now estimated, we construct the estimator of the feasible analogue of the τth conditional quantile of the log-yield in (2.2) as

$$\widehat{\mathbb{Q}}_\tau\left[\log y_{it}|\mathbf{x}_{it}, \mathbf{d}_t\right]$$

$$
=\widehat{\mu}_i + \underbrace{\left[\widehat{\beta}_0 + \widehat{\gamma}_0\widehat{q}_\tau + \sum_\kappa \left(\widehat{\eta}_\kappa + \widehat{\theta}_\kappa\widehat{q}_\tau\right) d_{\kappa,t}\right]}_{\text{time-varying quantile interecept}} + \mathbf{x}_{it}^{\prime} \underbrace{\left[\widehat{\boldsymbol{\beta}}_1 + \widehat{\boldsymbol{\gamma}}_1\widehat{q}_\tau + \widehat{\boldsymbol{\varphi}}_1 \sum_\kappa \widehat{\eta}_\kappa d_{\kappa,t}\right]}_{\text{time-varying quantile slopes}}. \qquad (2.14)
$$

2.2 Bias-Corrected Bootstrap Inference

Due to a multi-step nature of our estimator, computation of the asymptotic variance of the parameter estimators is not as simple. Therefore, for hypothesis testing we rely on Efron's (1982) bias-corrected bootstrap percentile confidence intervals.

To approximate the distribution of the parameter estimators and secondary functions thereof, we use a wild residual block-bootstrap, which we adapt to allow for potential spatial cluster dependence in residuals across counties. That is,in addition to clustering of each cross-sectional unit (i.e., county) over time owing to the panel structure of the data, we also seek to allow for clustering across individual units that belong to the same geographic/climatic region. Here we use climate divisions defined by the U.S. National Oceanic and Atmospheric Administration as the geographic scope for spatial clustering because by construction counties within a climate division share some common climate characteristics.[8] Such a two-way clustering allows an unrestricted dependence due to unit-specific time-invariant random unobservables as well as regional weather shocks affecting multiple units at once.[9] Generally, in the case of a two-way clustering, one can draw bootstrap disturbances based on either one of the cluster dimensions or their intersection. MacKinnon et al. (2017) show that the three designs are asymptotically valid and that a particular choice may matter little in finite samples. In our case, county-specific panel clusters are actually sub-clusters of larger multi-county climate-division-based clusters because of time-invariance of the latter. We therefore

[8]Each of the contiguous U.S. state is divided into up to ten climate divisions. We refer readers to U.S. National Oceanic and Atmospheric Administration for a map of climate divisions available at https://www.ncdc.noaa.gov/monitoring-references/maps/us-climate-divisions.php (accessed April 6, 2020). Building off Bester et al.'s (2011) intuition, a particular choice of spatial groups of counties may be of secondary importance so long as cluster-averages are approximately independent in errors, which is reasonable to expect in our application because climate divisions are large enough and spatial dependence in errors is via highly localized weather shocks. In other words, once we control for county fixed effects, time indices, and the key weather variables, it is reasonable to believe that the average error terms are approximately independent across climate divisions.

[9]Furthermore, unlike earlier studies that utilize spatial error models (e.g., Schlenker & Roberts, 2009; Miao et al., 2016), we do not need to specify a spatial weighting matrix the choice of which creates another source of potential misspecification of the standard errors. Our treatment of spatial effects in unobservables is, therefore, less restrictive thereby robustifying our statistical inference.

opt to design bootstrap sampling based on climate divisions thereby drawing panels of bootstrap residuals within a given division jointly which preserves both the intra-division and within-county patterns of correlation. The bootstrap algorithm is described in Appendix A.

With the bootstrap distribution in hand, we can then construct bias-corrected confidence intervals. To make matters concrete, let the (potentially, observation- and quantile-specific) estimand of interest be $\mathcal{E}$ with the corresponding point estimate denoted by $\widehat{\mathcal{E}}$. We use the empirical distribution of M ($M = 500$ in this study) bootstrap replicas $\{\widehat{\mathcal{E}}^1, \ldots, \widehat{\mathcal{E}}^M\}$ to estimate $(1-a) \times 100\%$ confidence bounds for $\mathcal{E}$ as intervals between the $[a_1 \times 100]$th and $[(1-a_2) \times 100]$th percentiles of the bootstrap distribution, where $a_1 = \Phi\left(2\widehat{z}_0 + \Phi^{-1}(\alpha/2)\right)$ and $a_2 = \Phi\left(2\widehat{z}_0 + \Phi^{-1}(1-\alpha/2)\right)$ with $\Phi(\cdot)$ being the standard normal cdf along with its quantile function $\Phi^{-1}(\cdot)$, and

$$\widehat{z}_0 = \Phi^{-1}\left(\#\{\widehat{\mathcal{E}}^m < \widehat{\mathcal{E}}\}/M\right) \tag{2.15}$$

is a bias-correction factor measuring median bias, with $\#\{\mathcal{A}\}$ being a count function that returns the number of times condition $\mathcal{A}$ is true.

2.3 Model Specification Testing

We also conduct specification tests. With the time-invariant fixed-coefficient specifications of the yield–climate relationship remaining dominant in the literature, the attempts to allow for temporal effects in the regression have mainly been limited to the inclusion of additive time trends which, while allowing for a *neutral* change in the log-yield, still assumes time-invariant marginal effects of the weather variables (e.g., Schlenker & Roberts, 2009; Chen et al., 2016; Zhang et al., 2017). Such specifications are arguably more restrictive than ours that features flexible *non-neutral* time indices. We test our model against two versions of such an alternative specification—one with a neutrally additive linear time trend and the other with both linear and quadratic time trends—both of which assume that the effects of climate on crop yields are time-invariant.

We use a nonlinear version of the conditional quantile encompassing test by Kuan &

Lin (2010) that is capable of discriminating between *non*-nested specifications of quantile model. More specifically, we are interested in testing our specification in (2.1) against the location-scale specifications with the linear time trend, i.e.,

$$\log y_{it} = \mu_i + \beta_0 + \delta_1 t + \mathbf{x}_{it}'\boldsymbol{\beta}_1 + (\gamma_0 + \lambda_1 t + \mathbf{x}_{it}'\boldsymbol{\gamma}_1)\,\varepsilon_{it}, \tag{2.16}$$

and with the quadratic time trend:

$$\log y_{it} = \mu_i + \beta_0 + \delta_1 t + \delta_2 t^2 + \mathbf{x}_{it}'\boldsymbol{\beta}_1 + \left(\gamma_0 + \lambda_1 t + \lambda_2 t^2 + \mathbf{x}_{it}'\boldsymbol{\gamma}_1\right)\varepsilon_{it}. \tag{2.17}$$

In terms of the implied quantile functions of the log-yield, we are to test H_0 of our time-varying specification in (2.2) against the following two fixed-slope alternatives:

$$\mathrm{H}_1(i):\ \mathbb{Q}_\tau\left[\log y_{it}|\mathbf{x}_{it},t\right] = \mu_i + \underbrace{\left[\beta_0 + \gamma_0 q_\tau + (\delta_1 + \lambda_1 q_\tau)\,t\right]}_{\text{time-varying quantile intercept}} + \mathbf{x}_{it}' \underbrace{\left[\boldsymbol{\beta}_1 + \boldsymbol{\gamma}_1 q_\tau\right]}_{\text{fixed quantile slopes}}, \tag{2.18}$$

$$\mathrm{H}_1(ii):\ \mathbb{Q}_\tau\left[\log y_{it}|\mathbf{x}_{it},t\right] = \mu_i + \underbrace{\left[\beta_0 + \gamma_0 q_\tau + (\delta_1 + \lambda_1 q_\tau)\,t + (\delta_2 + \lambda_2 q_\tau)\,t^2\right]}_{\text{time-varying quantile intercept}} + \mathbf{x}_{it}' \underbrace{\left[\boldsymbol{\beta}_1 + \boldsymbol{\gamma}_1 q_\tau\right]}_{\text{fixed quantile slopes}}. \tag{2.19}$$

The test is essentially based on the moment restrictions for the variables that appear in the alternative specifications but are omitted from the model under the null. In our case, these are the time trend variables. Thus, letting $\widetilde{\boldsymbol{\Theta}}$ collectively denote the intercept and slope parameter estimators under H_0, the test statistic for a given quantile index $\tau \in (0,1)$ is given by

$$\Psi_\tau = \frac{1}{\tau(1-\tau)}\widetilde{\boldsymbol{\psi}}(\widetilde{\boldsymbol{\Theta}})'\mathbf{V}_n^{-1}\widetilde{\boldsymbol{\psi}}(\widetilde{\boldsymbol{\Theta}}), \tag{2.20}$$

where

$$\widetilde{\boldsymbol{\psi}}(\widetilde{\boldsymbol{\Theta}}) = \frac{1}{\sqrt{nT}}\sum_i\sum_t \left(\mathbf{z}_{it} - \mathbf{M}_1\mathbf{M}_2^{-1}\widetilde{\mathcal{X}}_{it}\right)\left[\tau - \mathbb{1}\left\{\widetilde{v}_{it}(\widetilde{\boldsymbol{\Theta}}) < 0\right\}\right] \tag{2.21}$$

$$\mathbf{V}_n = \frac{1}{\sqrt{nT}}\sum_i\sum_t \left(\mathbf{z}_{it} - \mathbf{M}_1\mathbf{M}_2^{-1}\widetilde{\mathcal{X}}_{it}\right)\left(\mathbf{z}_{it} - \mathbf{M}_1\mathbf{M}_2^{-1}\widetilde{\mathcal{X}}_{it}\right)', \tag{2.22}$$

with $\mathbf{z}_{it}$ being a vector of "additional" variables under H_1: $\mathbf{z}_{it} = t$ in case of the alternative in (2.18) and $\mathbf{z}_{it} = (t, t^2)'$ in case of the alternative in (2.19). Further, $\widetilde{\mathcal{X}}_{it} = \frac{\partial Q_\tau[y_{it}|\cdot]}{\partial \mathbf{\Theta}}\Big|_{\widetilde{\mathbf{\Theta}}}$, $\mathbf{M}_1 = \frac{1}{nT}\sum_i \sum_t \mathbf{z}_{it}\widetilde{\mathcal{X}}'_{it}$ and $\mathbf{M}_2 = \frac{1}{nT}\sum_i \sum_t \widetilde{\mathcal{X}}_{it}\widetilde{\mathcal{X}}'_{it}$.

The test statistics in (2.20) is asymptotically χ^2-distributed under H_0, our preferred model. The test is one-sided and the Ψ_τ statistic in (2.20) is $\chi^2_{\dim(\mathbf{z})}$ under the null.

3 Data

The county-level corn and soybean yields are derived by using crop production divided by the harvested acreage in a county (Schlenker & Roberts, 2009). The county-level crop production and harvested acreage data are obtained from the National Agricultural Statistics Service (NASS) of the U.S. Department of Agriculture (USDA).[10] We focus on the rainfed counties (i.e., counties east of the 100th Meridian) because these counties account for about 93% of corn and 99% of soybeans production in the United States (Burke & Emerick, 2016). The temporal range of the yield data is between 1948 and 2010, to be consistent with historical climate data available to us. Table 1 presents summary statistics for the corn and soybean datasets used in this study, from where we can see that the corn yield in our sample varies from 0.04 to 212 bushel/acre with the corresponding inter-quartile range of 47.5–103.3 bushel/acre. For the soybean yield, the minimum and maximum yields are 0.34 and 249 bushel/acre, respectively; and the inter-quartile range is between 20.2 and 34 bushel/acre.

Besides the weather variables that are commonly considered in the literature such as temperature and precipitation, in our model we control for multiple other weather variables to further mitigate potential omitted variable bias. These additional covariates include wind speed, specific humidity, long- and short-wave radiation, as well as surface pressure. The potential for omitted variable bias (even with the use of fixed-effects models) has been well recognized in the climate econometrics literature, and one remedy for it is to include additional time-varying weather variables (e.g., Zhang et al., 2017; Mendelsohn & Massetti,

[10]NASS also directly reports county-level crop yields for corn and soybeans. We find negligible difference between the NASS-reported yield data and the yield series derived from the production and harvested acreage data.

2017; Blanc & Schlenker, 2017) which is the route we pursue in our paper. Therefore, our climate data contain eight variables: maximum temperature, minimum temperature, precipitation, wind speed, humidity, long-wave radiation, short-wave radiation, and surface pressure.

To ensure consistency among these variables, all historical climate data are obtained from the Terrestrial Hydrology Research Group (THRG) at Princeton University, which was initially developed by Sheffield et al. (2006) and has been used in many climate studies.[11] The THRG dataset contains daily data for all aforementioned weather variables at the 0.25 degree longitude and latitude resolution globally. We obtain the most recently updated version of the dataset that contains data from 1948 to 2010. The THRG data are reanalysis data that are generated by combining observed climate data and physics-based climate models. The advantages of such reanalysis data lie in the availability of more weather variables and a high resolution that mitigate the omitted variable bias, whereas a disadvantage is the existence of outliers and larger measurement error that may cause the attenuation bias (Blanc & Schlenker, 2017). Nevertheless, this kind of data are widely used in studies about social or economic impacts of climate change (e.g., Guiteras, 2010; Hsiang et al., 2011; Schlenker & Lobell, 2010).[12]

Since planting of corn and soybeans in the rainfed U.S. mainly occurs in March and harvesting in September (National Agricultural Statistics Service., 2010), we define the growing season for corn and soybeans as March to August. Such a definition of growing season for U.S. corn and soybeans is widely used in the literature (e.g., Schlenker & Roberts, 2009; Miao et al., 2016). Thus, the measurement of weather variables in our analysis is restricted to the defined growing season. Daily maximum and minimum temperature, together with a sinusoidal curve, are used to derive the daily distribution of temperature, on which the calculation of growing degree days (GDD) in each day is based (Schlenker & Roberts, 2009; Snyder, 1985). The total GDD over the entire growing season is simply the sum of daily GDD over the growing season. Schlenker & Roberts (2009) find that temperatures higher

[11] The weblink is http://hydrology.princeton.edu/data.pgf.php (accessed March 18, 2020).

[12] Auffhammer et al. (2013) provide a comprehensive review of issues pertaining to various types of climate data being used in climate change studies.

than 29°C are harmful for corn and 30°C for soybeans. We therefore set the upper threshold of their respective GDD calculation at these two values, with the lower threshold at 8°C. We label these temperature variables as $\mathrm{GDD}_{8-29^{\circ}\mathrm{C}}$ for corn and $\mathrm{GDD}_{8-30^{\circ}\mathrm{C}}$ for soybeans. Following Schlenker et al. (2006) and Chen et al. (2016), we also include GDD above the upper thresholds, respectively denoted by $\mathrm{GDD}_{29^{\circ}\mathrm{C}+}$ and $\mathrm{GDD}_{30^{\circ}\mathrm{C}+}$, to reflect the impact of overheat on crop yields. The precipitation variable is measured by using accumulated precipitation over the growing season for each year. The remaining variables (i.e., wind speed, humidity, long- and short-wave radiation, and surface pressure) are measured as simple averages of daily values over the growing season.

Because the climate data are at the 0.25-degree-grid level whereas the crop yield data are at the county level, we need to aggregate the grid-level climate data to the county level to match with the crop yield data. We employ two widely used approaches to do so. Following Zhang et al. (2017), the first approach is to average weather variables across the grids located within a 100-kilometer radius of a given county centroid using the inverse of the distance between each grid centroid and the county centroid as a weight. The second approach à la Chen et al. (2016) aggregates weather variables using their simple averages over the grids lying within the county's boundary. For counties that do not have any grids within their boundaries, we use the simple average of weather variables from four grids that are closest to the county centroid. We find negligible differences in the climate data constructed using either of these two approaches. Therefore, in our analysis, we focus on the data obtained using the first approach. Summary statistics of the weather variables for both corn and soybeans are reported in Table 1. Table B.1 in Appendix B also reports the correlation coefficients between these weather variables. The variables are generally correlated with each other, which lends support to including additional weather variables in regressions to avoid omitted variable bias.

Climate data used for projecting future climate change effects on crop yields are obtained from the Multivariate Adaptive Constructed Analogs (MACA) dataset.[13] The MACA dataset contains information on all weather variables from our historical dataset except the

[13]The weblink is https://climate.northwestknowledge.net/MACA/index.php (accessed July 25, 2018).

long-wave radiation and surface pressure. We use data for the 2040–2059 and 2080–2099 periods to respectively represent the medium- and long-term future climate conditions. Among the 20 global climate models available in the MACA dataset, we choose the predicted climate data generated by the HadGEM2-ES365 and NorESM1-M models. These two models are selected because they are widely used in climate studies and provide good contrasts in future climate predictions: the predicted temperature increase in the HadGEM2-ES365 model is larger than that in the NorESM1-M model (Warszawski et al., 2014; Miao et al., 2016). For each of the two models, we obtain the predicted climate data under two warming scenarios, namely RCP4.5 and RCP8.5. To be consistent with the historical climate data used in the analysis, we obtain the daily weather variables with the 0.25-degree resolution. The future $\text{GDD}_{8-29^\circ\text{C}}$, $\text{GDD}_{8-30^\circ\text{C}}$, $\text{GDD}_{29^\circ\text{C}+}$, $\text{GDD}_{30^\circ\text{C}+}$, precipitation, and other weather variables are constructed exactly as their historical counterparts. Tables B.2–B.5 in Appendix B provide summary statistics of future climate data for both the corn- and soybean-producing counties predicted by the two climate model. From these table, we see that in the long term climate will become warmer compared with the medium term, regardless of the RCP scenarios considered. For instance, take the HadGEM2-ES365 climate predictions for corn-producing counties: the median overheat $\text{GDD}_{29^\circ\text{C}+}$ in the long term will be about 33% (respectively, 80%) higher than that in the medium term under the warming scenario of RCP4.5 (respectively, RCP8.5). Under RCP4.5, the precipitation will slightly decrease in the long term when compared with the medium term. Under RCP8.5, however, the precipitation is predicted to increase approximately by 8% at the median. The data do not show significant differences in other weather variables across time horizons or warming scenarios.

4 Empirical Results

This section reports the results based on our time-varying-coefficient quantile fixed-effects model in (2.1)–(2.2). Specifically, vector $\mathbf{x}_{it}$ includes the county-level weather variables discussed in Section 3 and summarized in Table 1. To capture potential nonlinearities in the effects of temperature and precipitation, $\mathbf{x}_{it}$ also includes quadratic terms of $\text{GDD}_{8-29^\circ\text{C}}$ for corn (or $GDD_{8-30^\circ C}$ for soybeans) and precipitation. Following Schlenker et al. (2006), the overheat measure $GDD_{29^\circ C+}$ (or $GDD_{30^\circ C+}$) is included after taking the square root thereof to both scale the variable as well as accommodate diminishing effects. To sufficiently capture potential distributional heterogeneity across the log-yield distribution, we estimate our model for the 0.25^{th}, 0.50^{th}, and 0.75^{th} inter-quartile quantiles as well as the 0.90^{th} conditional yield quantile. The 0.25^{th} and 0.90^{th} conditional yield quantiles are of particular interest because they provide evidence regarding the impact of climate change on unproductive and highly productive crop-growing areas in the total crop production.

To empirically assess how the adoption of a more restrictive fixed-coefficient modeling of the climate–yield relationship customarily employed in the literature may affect the estimates and, subsequently, the conclusions about the climate change effects on corn and soybean yields, we also estimate the quantile model where, following the wide practice in the literature, all slope coefficients are *a priori* assumed to be constant over time. Specifically, we consider two alternative quantile specifications in (2.18)–(2.19) à la Schlenker & Roberts (2009), Chen et al. (2016) and Zhang et al. (2017) that allow for neutral temporal shifts in the climate-yield relationship via additive—linear or quadratic—time trends but still assume time-invariant marginal effects (i.e., fixed slope coefficients) of the weather variables. These popular specifications are more restrictive than ours, which features flexible *non*-neutral time indices. Note that these fixed-slope models match our time-varying-coefficient model in all remaining respects in order to ensure the maximal comparability. We formally test our model against these alternatives using a nonlinear version of the Kuan & Lin (2010) test described in Section 2.3. In all cases, for both the corn and soybean log-yields, we fail to reject the null of our non-neutral specification with p-values of 0.8 or higher (see Table 2). Thus, the data provide strong support to our more flexible time-varying-coefficient modeling of the climate–yield relationship for both crops.

We next discuss our regression results, which we contrast with those from the fixed-slope specification with a neutrally additive linear time trend discussed above (see eqs. (2.16) and (2.18)). We use this alternative model for comparison primarily because it continues to be a popular empirical specification in the literature as well as because the other alternative specification with additive quadratic trends (see eqs. (2.17) and (2.19)) yields quite similar results (the quadratic time trends are generally insignificant). Due to the limit of space, we only include results for corn yield in the main text whereas the results for soybean yield are presented in Appendix C and the results for fixed-slope specifications in Appendix D. The inference on point estimates of all time-varying or fixed coefficients as well as other functional estimates derived from them is conducted using bias-corrected 95% spatial-block bootstrap percentile confidence intervals as described in Section 2.2.

4.1 Climate Effects across Quantiles

Table 3 reports time-varying coefficient estimates for the corn yield at the 0.25^{th}, 0.50^{th}, 0.75^{th}, and 0.90^{th} quantiles of its log-yield distributions. The left panel in the table summarizes slope coefficient estimates for each regressor. Recall that, because we have 63 years of data and the coefficients are time-varying, we have 63 year-specific point estimates of the time-varying coefficient for each variable included in the model, whose minimum, maximum, and the first three quartile values are reported in the left-hand-side "*All Estimates*" panel. The difference between this and the "*Statistically Significant Estimates*" panel on the right is that the latter presents summary statistics only for the statistically significant coefficient point estimates. The very last column in Table 3, labeled "$\neq 0$ (%)", reports the share of such statistically significant year-specific estimates for each time-varying slope coefficient. Table C.1 reports analogous results for the soybean yield.

Table 3 shows that in most cases the coefficients of a linear $\text{GDD}_{8-29^\circ\text{C}}$ term are positive whereas the sign of the quadratic term coefficients is negative. This suggests an inverse-U-shaped relationship between the log-yield and $\text{GDD}_{8-29^\circ\text{C}}$ across all considered quantiles. That is, *ceteris paribus*, while higher $\text{GDD}_{8-29^\circ\text{C}}$ is generally beneficial for corn yields, the effect is diminishing and, beyond some point, higher $\text{GDD}_{8-29^\circ\text{C}}$ may harm the yields. The last column of Table 3 shows that at least 84% (respectively, 52%) of the coefficients associated with the linear term (respectively, the quadratic term) of $\text{GDD}_{8-29^\circ\text{C}}$ are statistically significant across all estimated yield quantiles. Note that the share of statistically significant coefficients of the linear term (respectively, quadratic term) decreases by about 15 (respectively, 30) percentage points as we move from the 0.25^{th} to the 0.90^{th} log-yield quantile, which indicates that high-yielding counties are less sensitive to $\text{GDD}_{8-29°\text{C}}$.

Figure 1 plots the marginal-effect functions of $\text{GDD}_{8-29°\text{C}}$ for the corn yield; recall that the quantile-specific time-varying marginal effects from model (2.2) are $\boldsymbol{\beta}_1 + \boldsymbol{\varphi}_1\text{B}(t) + \boldsymbol{\gamma}_1 q_\tau$. The analogous results for soybean yields are presented in Figure C.1. We tabulate estimated year-specific marginal-effect functions (each plotted as a dashed black line) by decades. The solid pink lines in Figures 1 and C.1 correspond to the marginal effect estimate from the fixed-coefficient model that assumes time-invariance of slopes.[14] Figure 1 shows that, as we move from the 0.25^{th} to the 0.90^{th} quantile, the bundles of dashed black lines shift closer to the zero line, especially in the later three decades of our sample period. This suggests that the marginal effect of $\text{GDD}_{8-29°\text{C}}$ is less varying and smaller in absolute value for higher corn yield quantiles.

The coefficients of total $\text{GDD}_{29°\text{C}+}$ ("overheat GDD" hereafter) measure the quantile impact of overheat temperatures on crop yields. Table 3 shows that the time-varying coefficients of overheat GDD are all expectedly negative, with the share of statistically significant estimates being 100% for all yield quantiles. The median significant coefficient over the entire sample period for the four yield quantiles is respectively estimated at –9.24, –7.89, –6.76, and –5.87, implying a sizable adverse effect of overheat temperatures across the entire yield distribution but with larger magnitudes for its left tail. For instance, an additional overheat growing degree day in a median-yield corn-producing area is estimated to decrease corn yields by around 7.89% at the median. The corresponding figure for the 0.90^{th} quantile area is a more modest 5.87%. These results suggest that the high-yielding counties are less sensitive to the yield-loss damage from 29°C+ overheat temperatures. This finding can also be discerned from Figure 2 that depicts the yearly marginal effect estimates of overheat GDD. As we move from lower to upper yield quantiles, the time-varying-coefficient estimates move closer to the zero line from below, indicating that the marginal effects become less negative.

[14] For parameter estimates from the fixed-coefficient model for both the corn and soybeans, see Tables D.1 – D.4 in the Appendix.

Marginal effect functions of precipitation for corn yields display a pattern similar to that of $\text{GDD}_{8-29^\circ\text{C}}$. Specifically, from the results presented in Table 3 we see that the coefficients on the quadratic term of precipitation are consistently negative across different quantiles, implying an inverse-U-shaped relationship between total growing-season precipitation and corn yields. Similar to the marginal effects of $\text{GDD}_{8-29^\circ\text{C}}$, the share of statistically significant point estimates decreases as one moves along the yield distribution from the 0.25^{th} to the 0.90^{th} quantile, although the lowest share is still higher than 80%. This indicates that, for high corn-yielding counties, the inverse-U-shaped relationship between yields and precipitation is less significant. Figure 3 shows that, as we move from lower to higher quantiles, magnitudes of the marginal effects of precipitation decrease (i.e., both the intercepts and slopes of dashed black lines get smaller in absolute value), particularly in the most recent decades, thereby indicating that higher-yielding areas tend to be less sensitive to precipitation, *ceteris paribus*.

In the case of soybean yields, we observe similar patterns of the climate effects like those for corn. For instance, there is an inverse-U-shaped relationship between soybean yields and within-county $\text{GDD}_{8-30^\circ\text{C}}$; an analogous relation is also estimated for within-county precipitation (see Table C.1). Figure C.1 suggests that, in a given decade, the marginal-effect functions of $\text{GDD}_{8-30^\circ\text{C}}$ (dashed black lines) for upper soybean yield quantiles have smaller intercepts and flatter slopes than do those for lower quantiles. This finding indicates that high-yielding counties are less sensitive to $\text{GDD}_{8-30^\circ\text{C}}$. Overheat GDD has negative and statistically significant impacts on soybean yields across all quantiles. Moreover, as can be seen in Figure C.2, the negative marginal effect estimates of overheat GDD lie closer to zero for upper yield quantiles than those for lower quantiles. Moreover, the marginal effects of total precipitation on soybean yields are smaller in absolute values for higher quantiles (see Figure C.3).

4.2 Sensitivity to Climate Variation across Decades

Because our model accommodates temporal changes in the relationship between crop yields and weather variables, with the 63-year sample we can examine how marginal effects of weather variables on corn and soybean yields have evolved over time. Figures 1 to 3 depict such changes in the estimated marginal effects over the course of our sample period for normal GDD, overheat GDD, and precipitation for corn yields. For soybean yields, the corresponding figures are Figures C.1 to C.3.

Consider the sensitivity of corn yield to normal GDD, i.e., $\mathrm{GDD}_{8-29^{\circ}\mathrm{C}}$. From Figure 1, it is evident that, for each of the four estimated corn yield quantiles, the plotted dashed black lines corresponding to its year-specific marginal-effect functions have become flatter with time, especially in later decades. For instance, the marginal-effect of normal GDD on the 0.90^{th} corn yield quantile in the 1950s is about –0.07% when evaluated at $\mathrm{GDD}_{8-29^{\circ}\mathrm{C}} = 2{,}000$. However, in the 2000s, the effect becomes about –0.04% (see the last row in Figure 1). A similar temporal pattern is exhibited by sensitivity of corn yields to precipitation (see Figure 3), with its being most apparent for upper quantiles. These findings suggest that, with time, perhaps advances in seed technology and farm management practices have made corn yields less sensitive to total $\mathrm{GDD}_{8-29^{\circ}\mathrm{C}}$ and precipitation realizations within the county, *ceteris paribus*. These advances, however, do not seem to have benefited low-yielding areas much. For soybeans, the marginal-effect functions of $\mathrm{GDD}_{8-30^{\circ}\mathrm{C}}$ and precipitation become flatter across the six decade-windows and all yield quantiles as well (see Figures C.1 and C.3).

Figure 2 plots the yearly estimates of marginal effects of overheat GDD on corn yields over 1948–2010 across different yield quantiles. The figure shows that, the negative marginal effects have displayed a clear upward trend for both corn and soybean yields, indicating that the magnitude of a negative marginal effect has been decreasing across all considered yield quantiles. Similar to our time-varying-coefficient model, the more restrictive fixed-coefficient model also points to the lower sensitivity of yields to overheat GDD at higher quantiles of corn yield, evidenced by the horizontal dashed pink line approaching the zero line as the yield quantile goes up. The fixed-coefficient model is generally, however, unable to detect a decline in the effect size of overheat temperatures in the recent decades. That is, a fixed-coefficient model tends to overestimate the negative impact of overheat GDD on corn yields in 1990–2010, with overestimation being particularly large (more than 100%) for lower yield quantiles. Although for soybeans, such an overestimation is not as pronounced.

4.3 Projections of Future Climate Change Impacts

We use the estimated reduced-form relationship between the log-yield and weather variables to evaluate potential effects of the projected climate change on U.S. corn and soybean yields in the future. For this purpose, quantile regression offers yet another advantage over conditional-mean models whereby, owing to a "monotone equivariance property" of quantiles, our estimates of projected changes in the level of crop yields are immune to transformation biases that are typical in conditional-mean analyses.

Specifically, rightly recognizing that log-differences provide poor approximations to non-negligible percentage changes just like we do in this paper, many existing studies (e.g., Miao et al., 2016; Zhang et al., 2017) compute future projections using the proper definition of percentage change in the *level* of predicted outcome variable (e.g., crop acreage or yields). However, they usually do so by exponentiating the predicted *logarithm* of an agricultural outcome from their estimated conditional-mean regressions while ignoring Jensen's inequality. Consequently, such average projections are likely biased. To see this, note that most studies estimate a conventional fixed-coefficient conditional-mean regression in logs à la $\log y = \mathbf{w}'\boldsymbol{\beta} + \epsilon$ assuming that $\mathbb{E}[\epsilon|\mathbf{w}] = 0$, from where it trivially follows that $\mathbb{E}[y|\mathbf{w}] = \exp\{\mathbf{w}'\boldsymbol{\beta}\}\mathbb{E}[\exp\{\epsilon\}|\mathbf{w}]$. Thus, the percentage change in the average yield from time t to time t' equals $[\exp((\mathbf{w}_{t'} - \mathbf{w}_t)'\boldsymbol{\beta})r(\mathbf{w}_{t'})/r(\mathbf{w}_t)] - 1$, where $r(\mathbf{w}) \equiv \mathbb{E}[\exp\{\epsilon\}|\mathbf{w}]$. Nonetheless, the level-of-yield decline projections are oftentimes computed simply as $\exp\{(\mathbf{w}_{t'} - \mathbf{w}_t)'\boldsymbol{\beta}\} - 1$ which, due to omission of the $r(\mathbf{w})$ terms, will be biased and need not have the same magnitude or even sign as the true quantity unless $\exp\{\epsilon\}$ is mean-independent of $\mathbf{w}$ which is unlikely to be true in practice, say, if ϵ is heteroskedastic. In the case of quantile estimation, we however do *not* face such a problem owing to the equivariance of quantiles to monotone transformations according to $\mathbb{Q}_\tau[y|\mathbf{w}] = \mathbb{Q}_\tau[\exp\{\log y\}|\mathbf{w}] = \exp\{\mathbb{Q}_\tau[\log y|\mathbf{w}]\}$ (e.g., see Koenker, 2005).

We predict future crop yield quantiles using climatic forecasts from two popular global climate models—HadGEM2-ES365 and NorESM1-M, each considered under a mild global warming scenario (RCP4.5) and a severe warming scenario (RCP8.5)—which we then compare to the crop yields predicted using historic climate data from the most recent ten years (i.e., 2001–2010) in our sample. To smooth yearly weather fluctuations in the historic data, we use averages of the 2001–2010 weather variables as a "present" benchmark for future climate forecasts. When predicting future crop yields we also fix time-varying coefficients at their 2001–2010 average levels representative of the most recently available technology, effectively assuming no technology-driven improvements in the crop productivity in the future. By doing so, we seek to avoid unnecessarily excessive extrapolation into the future, and hence, our estimates are likely to be on a more conservative end.[15] Also, since the future climate datasets do not include long-wave radiation or surface pressure, we assume that these two variables remain constant at their 2001–2010 average values.[16]

The future yield change projection (in percent) for a specific future year, h, in a given county over a medium-term $h \in \{2040, 2041, \ldots, 2059\}$ or a long-term $h \in \{2080, 2081, \ldots, 2099\}$ horizon is estimated for each given quantile index τ as

$$\%\Delta\mathbb{Q}_\tau[y_{ih}|\cdot] = \exp\left\{\left(\mathbf{x}_{ih} - \overline{\mathbf{x}}_i\right)'\overline{\boldsymbol{\beta}}_\tau\right\} - 1, \tag{4.1}$$

where $\overline{\mathbf{x}}_i = \frac{1}{10}\sum_{t=2001}^{2010}\mathbf{x}_{it}$ and $\overline{\boldsymbol{\beta}}_\tau = \frac{1}{10}\sum_{t=2001}^{2010}\boldsymbol{\beta}_\tau(t)$, with $\boldsymbol{\beta}_\tau(t) = \boldsymbol{\beta}_1 + \boldsymbol{\gamma}_1 q_\tau + \boldsymbol{\varphi}_1\mathrm{B}(t)$ being the time-varying quantile slope vector from (2.2). The county-level yield projections are then aggregated via acreage-weighted averages with the weights constructed using the average 2001–2010 county-level acreage for the crop in question. Tables 4 and C.2 summarize these results based on the estimates of time-varying coefficients whereas Tables D.5–D.8 in

[15] Also note that we would be unable to extrapolate time-varying quantile coefficients in our model even if we wanted to because we employ (nonparametric) discretization when estimating unobservable time indices. Unlike the continuous treatment of time (via trends), a dummy-based discrete modeling of time possesses no out-of-sample prediction power. This is the cost of making fewer assumptions than in a time-trend-based specification.

[16] This should not be considered as a major limitation of the prediction because except temperature and precipitation, other predicted weather variables only differ slightly from their historical values (see Tables B.2 to B.5).

the Appendix report the results based on the fixed-coefficient estimates.

Table 4 shows that the estimated average decline in corn yields due to the future climate change can be up to 53%, depending on the time horizon, global climate projections, and yield quantiles. Overall, the negative impacts of future climate change on corn yields are of larger magnitudes for lower quantiles. For instance, under the long-term (2080–2099) RCP8.5 scenario, corn yield reductions projected using the HadGEM2-ES365 future climate data are 49.7%, 39.3%, 28.7%, and 18.9% for the 0.25^{th}, 0.50^{th}, 0.75^{th}, and the 0.90^{th} quantiles, respectively. This indicates that future climate change has the potential to make corn yields even more negatively skewed. Although our data are for the corn production in the United States, which employs the most advanced agricultural technologies and management practices, this finding also sheds light on the distributional heterogeneity of the climate change effects on agriculture in the world more generally: less productive regions (read, developing countries) are expected to be hit by climate change the most, whereas more productive regions (read, developed countries) may be more immune to negative climate change effects.

Contrasting projections for corn yield decline attributed to climate change based on the time-varying-coefficient model (see Table 4) to those based on the fixed-coefficient model (see Table D.5 in the Appendix), we find that the results in Table D.5 are much larger in the absolute value.[17] For instance, based on the NorESM1-M forecasts under the warming scenario RCP4.5, our time-varying-coefficient model predicts the corn yield decline at the 0.25^{th} quantile to be 14.9% over 2040–2049 (see the third panel in Table 4) whereas the fixed-coefficient model predicts the decline to be two times larger at 29.9% (see the third panel in Table D.5). This contrast is most obvious in Figures 4–5 that plot the average corn yield change projections in six-year rolling windows. From the two figures, it is obvious that the predictions based on the fixed-coefficient model (dashed pink lines) lie significantly below their counterparts from the preferred model (solid lines with markers) thereby generating grossly over-estimated climate-change-driven yield declines in the future. On many occasions, corn yield reduction projections from the fixed-coefficient model are more than twice as large

[17]To make models comparable, we only examine the impact of the impact of weather variables, and time trend variables are excluded in the prediction. This is because of the assumption that the "technology" stays unchanged.

as the predictions from the time-varying-coefficient model.

In the case of soybean yields, we generally document similar findings about future yield declines as those for corn. Overall, soybean yield reduction attributed to climate change ranges between 12.1% and 57.9%, although the magnitudes under various scenarios are typically larger than those of corn, especially at lower yield quantiles (Table C.2). We also find that differences between soybean yield decline projections from the fixed-coefficient and those from the time-varying-coefficient models are more muted than the analogous differences in the case of corn yield (Figures C.4 and C.5).

Figure 6 further presents contrasting projections for corn yield decline based on our time-varying-coefficient model and those based on a fixed-coefficient conditional *mean* model. We present this comparison because the latter model is widely used in the existing studies to examine the impact of climate change on agriculture. From the figure we can see that, depending on the future warming scenario and time horizon, the projections based on the fixed-coefficient conditional mean model range between -30% and -70%, a range close to the findings in Schlenker & Roberts (2009). However, these projections are well below the projections based on our time-varying coefficients conditional quantile model, which underscores the importance of accounting for the distributional and temporal heterogeneity in examining the climate-agriculture relationship.

The four maps in Figure 7 present geographical configurations of future climate effects on corn yields across counties. These maps summarize the projections based on our time-varying-coefficient model for the median quantile ($\tau = 0.5$). The first (respectively, second) column depicts projected county-specific median yield reductions attributed to the climate change in the medium (respectively, long) term. Clearly, the projected corn yield declines in the long term are much higher than those in the medium term. The maps indicate that, under the future climate scenario predicted by the HadGEM2-ES365 model, the largest reduction in corn yields is to occur in the southern part of the Midwest region (e.g., Illinois, Indiana, and Missouri) and in some southern states (see the top row of maps in the figure). Based on climate predictions from the NorESM1-M model, however, the largest reduction is to occur in the Great Plains region (see the bottom row of maps in the figure). The same impact pattern holds for the projected reduction in soybean yields (see Figure C.6 in the Appendix). Not only do these findings signify acute heterogeneity of climate impacts across regions, but they also show that predictions based on future climate data generated by different global climate models may differ significantly.

We also examine the geographical configurations of the differences in the projected corn yield reductions between the time-varying-coefficient and the fixed-coefficient models. Figure 8 includes four such maps for the median corn yield quantile. Here we see that the overestimation by the fixed-coefficient model mainly occurs in the southeastern states, and it is more significant in the long term than in the medium term. For median soybean yields (Figure C.7 in the Appendix), the overestimation takes places predominantly in the southern Great Plains and some southeastern states. Similar to the corn yield decline predictions, it is more severe in the long term.

4.4 Robustness

Here we probe the robustness of our estimation results to different variable specifications and to estimation techniques. So far, we have employed a GDD-based measure of temperature to capture the non-linear impact of the latter on crop yields. An alternative approach to GDD, originally proposed by Schlenker & Roberts (2009) and also widely used in the literature such as Chen et al. (2016) and Zhang et al. (2017), is to measure the exposure time within a certain temperature range during growing season. We follow Schlenker & Roberts (2009) to calculate the time exposure within each 5°C interval starting from 0°C and up to $35-40$°C and 40°C+. The results are presented in Appendix E. Figures E.1 and E.2 show that the temperature between 10°C and 30°C is typically beneficial to corn and soybean yields. Temperature above 30°C, however, is highly detrimental to crop yields. These findings are consistent with the existing literature. Two obvious features of these two figures are: *i*) within a given decade, as we move from lower yield quantiles to higher yield quantiles, the negative impact of temperature above 30° becomes smaller (i.e., the black dashed lines approach the zero line from below); and *ii*) for a given yield quantile, as we move from earlier decades to later decades, the negative impact of temperature above 30° becomes smaller as well. This finding is consistent what we have in Figures 1, 2, C.1, and C.2. In Appendix E we also presented the predictions of the impact of future climate change on crop yields based on estimates using this alternative approach to measuring temperature (see Figures E.3 to E.6). The results are consistent with those from our main model discussed in Section 4.3.

As another robustness check, we also weight our regressions by the harvested acreage of a crop to facilitate a more representative acre-based interpretation of our results. In doing so, we account for the variation in the size of each unit of analysis (county) because the county-level panel is essentially grouped data. The results from weighted regressions are presented in Appendix F. Specifically, Tables F.1 and F.2 are the counterparts of Tables 3 and C.1 of our main results. A comparison between Table F.1 and Table 3 shows that the coefficients for corn yield models are close and the results are robust to the weighting. The same conclusion can be drawn for soybean yield models. Appendix F also include the counterparts of Figures 1 to 5 and Figures C.1 to C.5. We can see that results from weighted regressions have similar patterns and magnitude with those from our main results, indicating that our results are robust to the weighting.

5 Conclusions

Applying a panel-data quantile regression with time-varying coefficients to study responses of crop yields to weather variables, we find that the sensitivity of U.S. corn and soybean yields to climate variation exhibits a clear distributional heterogeneity and that the yields have gradually become less responsive to GDD, overheat GDD, and precipitation over the past six decades. Specifically, we find that the direct marginal effect of normal GDD (namely, $\text{GDD}_{8-29^\circ\text{C}}$ for corn and $\text{GDD}_{8-30^\circ\text{C}}$ for soybeans) and that of precipitation are smaller at upper yield quantiles than at lower quantiles. We also find a sizable adverse effect of overheat GDD across the entire yield distribution, with larger magnitudes at lower yield quantiles. For both corn and soybean yields, the marginal effects of overheat GDD across all four considered quantiles had been decreasing over our sample period, 1948-2010.

Based on future climate data generated by two global climate models (HadGEM2-ES365 and NorESM1-M) under two warming scenarios (RCP4.5 and RCP8.5) and two temporal frameworks (2040–2059 for medium-term and 2080–2099 for long-term), our time-varying-coefficient model predicts that the corn yield declines attributed to future climate change can be up to 53%, depending on yield quantiles, global climate models, warming scenarios, and time horizons. For soybean yields, such a decline can be up to 57.9%. The results show that the negative impacts of future climate change on corn yields are of much larger magnitudes for yields at lower quantiles. This finding sheds light on the distributional heterogeneity of climate change effects on agriculture: crop yields in less productive regions such as developing countries may be hit by future climate change the most, whereas yields in more productive regions may suffer less from climate change. This indicates that, to mitigate climate change effects on agriculture, resources ought to be tilted toward low-yielding regions.

Contrasting our results with those based on the fixed-coefficient model with additive time trends, we find that the fixed-coefficient model tends to significantly overestimate the responsiveness of crop yields to climate variation and, therefore, overestimates the negative impact of future climate change on crop yields. On many occasions, the corn yield decline projections from the fixed-coefficient model are about twice as large as the predictions from our time-varying-coefficient model. Although for soybeans, such an overestimation is not as pronounced. Therefore, establishing damage functions for the integrated policy assessment models based on fixed-coefficient models should proceed with caution.[18]

To conclude, robust impact measurement is key for designing well-grounded economic policies. Overall, by applying a novel approach, our study reveals a non-negligible distributional heterogeneity of climate change effects on agriculture and underscores the importance of considering flexible time-varying-coefficient models when studying the climate-yield relationship over a relatively long time horizon. Although we focus on the relationship between climate and yields, our econometric approach can be readily applied to examining the effects of climate change on other aspects of agricultural or non-agricultural sectors such as land

[18]For instance, see Moore & Diaz (2015) for a discussion of the integrated policy assessment models.

values, farm returns, firm productivity, and even health outcomes. Future research along the line in this article may benefit from the increasing availability of sub-county-level or even field-level data to further explore the distributional heterogeneity of climate change effects. Since the present study is more focused on quantifying the climate effect heterogeneity instead of exploring the sources of this heterogeneity, it does not shed much insight into the drivers of the heterogeneity. Future research is in order to identify drivers of the heterogeneity such as technology advances, management, and natural resource endowment and to quantify their roles in determining adaptation to climate change in agriculture.

References

Antle, J. M. & Stöckle, C. O. (2017). Climate impacts on agriculture: insights from agronomic-economic analysis. *Review of Environmental Economics and Policy*, *11*(2), 299–318.

Auffhammer, M., Hsiang, S., Schlenker, W., & Sobel, A. (2013). Using weather data and climate model output in economic analyses of climate change. *Review of Environmental Economics and Policy*, *7*(2), 181–198.

Baltagi, B. H. & Griffin, J. M. (1988). A general index of technical change. *Journal of Political Economy*, *96*(1), 20–41.

Bester, C. A., Conley, T. G., & Hansen, C. B. (2011). Inference with dependent data using cluster covariance estimators. *Journal of Econometrics*, *165*, 137–151.

Blanc, E. & Schlenker, W. (2017). The use of panel models in assessments of climate impacts on agriculture. *Review of Environmental Economics and Policy*, *11*(2), 258–279.

Burke, M. & Emerick, K. (2016). Adaptation to climate change: Evidence from us agriculture. *American Economic Journal: Economic Policy*, *8*(3), 106–140.

Canay, I. A. (2011). A simple approach to quantile regression for panel data. *Econometrics Journal*, *14*, 368–386.

Chen, S., Chen, X., & Xu, J. (2016). Impacts of climate change on agriculture: evidence from china. *Journal of Environmental Economics and Management*, *76*, 105–124.

Deschênes, O. & Greenstone, M. (2007). The economic impacts of climate change: Evidence from agricultural output and random fluctuations in weather. *The American Economic Review*, *97*(1), 354–385.

Efron, B. (1982). *The Jackknife, the Bootstrap, and Other Resampling Plans.* Society for Industrial and Applied Mathematics.

Galvão, A. F. & Kato, K. (2018). Quantile regression methods for longitudinal data. In R. Koenker, V. Chernozhukov, X. He, & L. Peng (Eds.), *Handbook of Quantile Regression,* chapter 19, (pp. 363–380). Chapman-Hall/CRC, Boca Raton (FL).

Guiteras, R. (2010). The impact of climate change on indian agriculture. University of Maryland Working Paper.

Hsiang, S. (2016). Climate econometrics. *Annual Review of Resource Economics*, *8*, 43–75.

Hsiang, S. M., Meng, K. C., & Cane, M. A. (2011). Civil conflicts are associated with the global climate. *Nature*, *476*, 438–441.

Koenker, R. (2004). Quantile regression for longitudinal data. *Journal of Multivariate Analysis*, *91*, 74–89.

Koenker, R. (2005). *Quantile Regression.* New York: Cambridge University Press.

Koenker, R. & Bassett, G. (1982). Robust test for heteroskedasticity based on regression quantiles. *Econometrica*, *50*, 43–61.

Koenker, R. & Hallock, K. F. (2001). Quantile regression. *Journal of Economic Perspectives*, *15*, 143–156.

Kuan, C. & Lin, H. (2010). An encompassing test for non-nested quantile regression models. *Economics Letters*, *107*, 257–260.

Lobell, D. B., Roberts, M. J., Schlenker, W., Braun, N., Little, B. B., Rejesus, R. M., & Hammer, G. L. (2014). Greater sensitivity to drought accompanies maize yield increase in the u.s. midwest. *Science*, *344*(6183), 516–519.

Machado, J. A. F. & Santos Silva, J. M. C. (2019). Quantiles via moments. *Journal of Econometrics*, *213*(1), 145–173.

MacKinnon, J. G., Nielson, M. Ø., & Webb, M. D. (2017). Bootstrap and asymptotic inference with multiway clustering. Queen's Economics Department Working Paper No. 1386, Queen's University.

Mendelsohn, R., Dinar, A., & Sanghi, A. (2001). The effect of development on the climate sensitivity of agriculture. *Environment and Development Economics*, *6*(1), 85–101.

Mendelsohn, R., Nordhaus, D., & Shaw, D. (1994). The impact of global warming on agriculture: A ricardian analysis. *American Economic Review*, *84*(4), 753–771.

Mendelsohn, R. O. & Massetti, E. (2017). The use of cross-sectional analysis to measure climate impacts on agriculture: theory and evidence. *Review of Environmental Economics and Policy*, *11*(2), 280–298.

Miao, R., Khanna, M., & Huang, H. (2016). Responsiveness of crop yield and acreage to prices and climate. *American Journal of Agricultural Economics*, *98*(1), 191–211.

Moore, F. C. & Diaz, D. B. (2015). Temperature impacts on economic growth warrant stringent mitigation policy. *Nature Climate Change*, *5*, 127—-131.

National Agricultural Statistics Service. (2010). Field crops usual planting and harvesting dates. Agricultural Handbook Number 628. U.S. Department of Agriculture, October.

National Research Council (1983). *Changing Climate: Report of the Carbon Dioxide Assessment Committee*. Washington, DC: National Academies Press.

Schlenker, W., Hanemann, M. W., & Fisher, A. C. (2005). Will u.s. agriculture really benefit from global warming? accounting for irrigation in the hedonic approach. *The American Economic Review*, *95*(1), 395–406.

Schlenker, W., Hanemann, M. W., & Fisher, A. C. (2006). The impact of global warming on u.s. agriculture: an econometric analysis of optimal growing conditions. *Review of Economics and Statistics*, *88*(1), 113–125.

Schlenker, W. & Lobell, D. B. (2010). Robust negative impacts of climate change on african agriculture. *Environmental Research Letters*, *5*(1), 1–8.

Schlenker, W. & Roberts, M. (2009). Nonlinear temperature effects indicate severe damages to u.s. crop yields under climate change. *Proceedings of the National Academy of Sciences of the United States of America*, *106*(37), 15594–15598.

Sheffield, J., Goteti, G., & Wood, E. F. (2006). Development of a 50-yr high-resolution global dataset of meteorological forcings for land surface modeling. *Journal of Climate*, *19*(13), 3088–3111.

Snyder, R. L. (1985). Hand calculating degree days. *Agricultural and Forest Meterology*, *35*(1–4), 353–358.

Warszawski, L., Frieler, K., Huber, V., Piontek, F., Serdeczny, O., & Schewe, J. (2014). The inter-sectoral impact model intercomparison project (isi-mip): Project framework. *Proceedings of the National Academy of Sciences of the United States of America*, *111*(9), 3228–3232.

Yu, T. & Babcock, B. A. (2010). Are u.s. corn and soybeans becoming more drought tolerant? *American Journal of Agricultural Economics*, *92*(5), 1310–1323.

Zhang, P., Zhang, J., & Chen, M. (2017). Economic impacts of climate change on agriculture: The importance of additional climatic variables other than temperature and precipitation. *Journal of Environmental Economics and Management*, *83*, 8–31.

Table 1. Summary Statistics of Historical Yield and Climate Data (1948–2010)

	Corn							*Soybeans*						
Variable	Mean	Min	1st Qu.	Median	3rd Qu.	Max	Std.	Mean	Min	1st Qu.	Median	3rd Qu.	Max	Std.
Yield (bushel/acre)	78.10	0.04	47.46	74.00	103.33	211.98	38.04	27.71	0.34	20.20	26.17	34.00	249.39	9.95
Total $GDD_{8-29^{\circ}C}$	2,004	817	1,665	2,001	2,324	3,286	424							
Total $GDD_{29^{\circ}C+}$	51.97	0.00	13.63	36.88	77.42	525.75	49.20							
Total $GDD_{8-30^{\circ}C}$								2,021	817	1,673	2,017	2,348	3,346	435
Total $GDD_{30^{\circ}C+}$								34.99	0.00	7.74	23.86	52.93	311.65	34.56
Total Precipitation (mm)	592	97	489	582	684	1382	151	595	115	493	582	684	1369	149
Ave. Wind Speed (m/s)	3.11	2.07	2.74	3.1	3.45	5.46	0.47	3.13	2.07	2.78	3.13	3.45	5.29	0.45
Ave. Humidity (kg/kg)	0.012	0.006	0.01	0.012	0.013	0.018	0.002	0.012	0.006	0.010	0.012	0.013	0.018	0.002
Ave. Long-Wave Radiation (W/m^2)	352	301	339	352	365	437	18	352	303	339	352	365	434	17
Ave. Short-Wave Radiation (W/m^2)	233	189	222	231	243	288	14	233	190	222	231	243	284	14
Ave. Surface Pressure (kPa)	98.61	93.27	97.5	98.72	99.77	102.08	1.67	98.75	93.35	97.69	98.88	99.87	102.05	1.63

Note: The numbers of observations for the corn and soybean datasets are 118,134 and 91,977, respectively. All weather variables are measured within the growing season (March to August). Average weather variables are simple averages of their daily values across the growing season.

Table 2. Model Specification Test Results

	Yield Quantiles			
	0.25th	0.50th	0.75th	0.90th
	Corn Yields			
H_0: Our Specification *v.* H_1: Neutral Linear Trend	0.9464	0.8974	0.8665	0.9950
H_0: Our Specification *v.* H_1: Neutral Quadratic Trend	0.9858	0.9856	0.9005	0.8684
	Soybean Yields			
H_0: Our Specification *v.* H_1: Neutral Linear Trend	0.9478	0.7958	0.8959	0.9941
H_0: Our Specification *v.* H_1: Neutral Quadratic Trend	0.9967	0.8291	0.9477	0.9817

Note: Reported are the p-values for the Ψ_τ test statistic.

Table 3. Time-Varying Quantile Slope Coefficient Estimates for the Corn Yield

Variable	*All Estimates* Min	1st Qu.	Median	3rd Qu.	Max	*Statistically Significant Estimates* Min	1st Qu.	Median	3rd Qu.	Max	$\neq 0$ (%)
The 0.25th Yield Quantile											
Total $GDD_{8-29°C}$	0.0433	0.0986	0.1402	0.203	0.2931	0.0654	0.1011	0.1437	0.2038	0.2931	98.4
Total $GDD_{8-29°C}$ sq. ($\times 10^{-3}$)	–0.0564	–0.0364	–0.0224	–0.0132	–0.0009	–0.0564	–0.0394	–0.0272	–0.017	–0.0115	84.1
Total $GDD_{29°C+}$ (square root)	–13.2564	–10.8901	–9.2392	–8.1473	–6.6947	–13.2564	–10.8901	–9.2392	–8.1473	–6.6947	100
Total Precipitation	0.0913	0.1256	0.1514	0.1903	0.2461	0.0913	0.1256	0.1514	0.1903	0.2461	100
Total Precipitation sq. ($\times 10^{-3}$)	–0.2177	–0.1575	–0.1154	–0.0876	–0.0506	–0.2177	–0.1575	–0.1154	–0.0876	–0.0506	100
Average Wind Speed	–6.5986	–5.9685	–5.5289	–5.2381	–4.8513	–6.4674	–5.9685	–5.6526	–5.3422	–5.1278	81
Average Humidity ($\times 10^{3}$)	–4.9245	–4.0543	–3.4471	–3.0455	–2.5113	–4.9245	–4.0888	–3.5794	–3.1571	–2.7366	93.7
Average Long-Wave Radiation	0.1447	0.2062	0.2524	0.3224	0.4226	0.2454	0.2767	0.3181	0.3757	0.4226	55.6
Average Short-Wave Radiation	–1.394	–0.7852	–0.3605	–0.0795	0.2942	–1.394	–0.995	–0.5896	–0.3198	0.2942	73
Average Surface Pressure	3.0819	3.6667	4.1063	4.7709	5.7235	3.0819	3.6667	4.1063	4.7709	5.7235	100
The 0.50th Yield Quantile											
Total $GDD_{8-29°C}$	0.0255	0.0808	0.1223	0.1852	0.2753	0.0488	0.0871	0.1294	0.1867	0.2753	96.8
Total $GDD_{8-29°C}$ sq. ($\times 10^{-3}$)	–0.0521	–0.0321	–0.0181	–0.0088	0.0035	–0.0521	–0.0398	–0.0267	–0.0177	–0.011	69.8
Total $GDD_{29°C+}$ (square root)	–11.9087	–9.5424	–7.8915	–6.7996	–5.347	–11.9087	–9.5424	–7.8915	–6.7996	–5.347	100
Total Precipitation	0.0612	0.0954	0.1212	0.1601	0.2159	0.0612	0.0954	0.1212	0.1601	0.2159	100
Total Precipitation sq. ($\times 10^{-3}$)	–0.1958	–0.1355	–0.0935	–0.0657	–0.0287	–0.1958	–0.136	–0.0958	–0.0674	–0.0435	98.4
Average Wind Speed	–6.2351	–5.605	–5.1654	–4.8746	–4.4879	–6.0061	–5.5862	–5.2891	–4.9871	–4.8274	74.6
Average Humidity ($\times 10^{3}$)	–4.836	–3.9658	–3.3586	–2.957	–2.4228	–4.836	–4.0395	–3.543	–3.097	–2.7142	88.9
Average Long-Wave Radiation	0.0439	0.1054	0.1516	0.2215	0.3217	0.2135	0.2224	0.243	0.2677	0.2888	19
Average Short-Wave Radiation	–1.325	–0.7162	–0.2914	–0.0105	0.3633	–1.325	–0.9397	–0.5437	–0.2578	0.3633	71.4
Average Surface Pressure	2.6499	3.2347	3.6743	4.3389	5.2915	2.6499	3.2347	3.6743	4.3389	5.2915	100

Notes: The left panel summarizes all point estimates, whereas the right panel summarizes only statistically significant point estimates of time-varying slope coefficients. The last column reports the share of sample period for which time-varying slope coefficients are statistically significant. Statistical significance is assessed using two-sided 95% bias-corrected percentile confidence intervals. The reported estimates are measured in % of yield per unit in the corresponding regressor.

Table 3. Time-Varying Quantile Slope Coefficient Estimates for the Corn Yield (cont.)

Variable	*All Estimates*					*Statistically Significant Estimates*					
	Min	1st Qu.	Median	3rd Qu.	Max	Min	1st Qu.	Median	3rd Qu.	Max	$\neq 0$ (%)
The 0.75th Yield Quantile											
Total $GDD_{8-29°C}$	0.0105	0.0658	0.1074	0.1703	0.2603	0.0418	0.0807	0.1279	0.1799	0.2603	87.3
Total $GDD_{8-29°C}$ sq. ($\times 10^{-3}$)	–0.0485	–0.0284	–0.0145	–0.0052	0.0071	–0.0485	–0.039	–0.0272	–0.0192	–0.0114	57.1
Total $GDD_{29°C+}$ (square root)	–10.7813	–8.415	–6.7641	–5.6722	–4.2196	–10.7813	–8.415	–6.7641	–5.6722	–4.2196	100
Total Precipitation	0.0359	0.0702	0.096	0.1349	0.1907	0.0497	0.0718	0.0981	0.1354	0.1907	98.4
Total Precipitation sq. ($\times 10^{-3}$)	–0.1774	–0.1171	–0.0751	–0.0473	–0.0103	–0.1774	–0.1195	–0.0843	–0.055	–0.0274	93.7
Average Wind Speed	–5.931	–5.3009	–4.8614	–4.5706	–4.1838	–5.5789	–5.2622	–5.0156	–4.8419	–4.6629	49.2
Average Humidity ($\times 10^{3}$)	–4.762	–3.8917	–3.2846	–2.883	–2.3487	–4.762	–3.9849	–3.4825	–3.0267	–2.6771	87.3
Average Long-Wave Radiation	–0.0405	0.021	0.0673	0.1372	0.2374						0
Average Short-Wave Radiation	–1.2672	–0.6584	–0.2337	0.0473	0.421	–1.2672	–0.8932	–0.4948	–0.2222	0.421	69.8
Average Surface Pressure	2.2886	2.8733	3.3129	3.9775	4.9301	2.2886	2.8733	3.3129	3.9775	4.9301	100
The 0.90th Yield Quantile											
Total $GDD_{8-29°C}$	–0.0013	0.054	0.0956	0.1584	0.2485	0.0464	0.0711	0.1171	0.1721	0.2485	84.1
Total $GDD_{8-29°C}$ sq. ($\times 10^{-3}$)	–0.0456	–0.0256	–0.0116	–0.0024	0.0099	–0.0456	–0.0365	–0.0252	–0.0167	–0.0115	52.4
Total $GDD_{29°C+}$ (square root)	–9.8896	–7.5233	–5.8724	–4.7804	–3.3279	–9.8896	–7.5233	–5.8724	–4.7804	–3.3279	100
Total Precipitation	0.016	0.0502	0.076	0.1149	0.1707	0.0347	0.059	0.087	0.1184	0.1707	90.5
Total Precipitation sq. ($\times 10^{-3}$)	–0.1629	–0.1026	–0.0606	–0.0328	0.0042	–0.1629	–0.1118	–0.0749	–0.0442	–0.0277	84.1
Average Wind Speed	–5.6905	–5.0604	–4.6209	–4.3301	–3.9433	–5.2351	–5.0097	–4.7807	–4.6702	–4.4972	39.7
Average Humidity ($\times 10^{3}$)	–4.7034	–3.8332	–3.226	–2.8244	–2.2902	–4.7034	–3.9264	–3.424	–2.9682	–2.6185	87.3
Average Long-Wave Radiation	–0.1072	–0.0457	0.0006	0.0705	0.1707						0
Average Short-Wave Radiation	–1.2215	–0.6127	–0.188	0.093	0.4667	–1.2215	–0.8225	–0.4171	–0.1473	0.4667	73
Average Surface Pressure	2.0027	2.5875	3.0271	3.6917	4.6443	2.0027	2.5875	3.0271	3.6917	4.6443	100

Notes: The left panel summarizes all point estimates, whereas the right panel summarizes only statistically significant point estimates of time-varying slope coefficients. The last column reports the share of sample period for which time-varying slope coefficients are statistically significant. Statistical significance is assessed using two-sided 95% bias-corrected percentile confidence intervals. The reported estimates are measured in % of yield per unit in the corresponding regressor.

Table 4. Corn Yield Change Predictions Based on Various Climate Forecasts (%)

	RCP4.5 Scenario				*RCP8.5 Scenario*			
Horizon	0.25th Quant.	0.50th Quant.	0.75th Quant.	0.90th Quant.	0.25th Quant.	0.50th Quant.	0.75th Quant.	0.90th Quant.
Based on HadGEM2-ES365 Forecasts								
2040–2049	–17.8	–12.2	–7.1	–2.8	–32.3	–24.3	–16.7	–10
	(–23.6, –11.4)	(–18.1, –4)	(–13.4, 1.6)	(–9.3, 6.1)	(–38.6, –24)	(–31.4, –14.8)	(–24.5, –6.2)	(–18.5, 1.3)
2050–2059	–27.4	–20	–13	–6.9	–33.1	–24.7	–16.8	–9.9
	(–34.1, –20.4)	(–26.7, –11.1)	(–20.5, –3.2)	(–15, 3.7)	(–39.7, –24.8)	(–32, –15.1)	(–24.9, –6.1)	(–18.7, 1.9)
2040–2059	–22.6	–16.1	–10	–4.9	–32.7	–24.5	–16.7	–9.9
	(–28.8, –16.1)	(–22.4, –7.7)	(–16.7, –0.9)	(–12.1, 4.9)	(–39.5, –25.3)	(–31.6, –14.9)	(–24.8, –6.1)	(–18.7, 1.6)
2080–2089	–32	–23.4	–15.3	–8.1	–46.5	–36.3	–26.1	–16.8
	(–39.3, –24.8)	(–30.8, –14.6)	(–23.3, –5.2)	(–16.9, 3.1)	(–53.7, –38)	(–44.7, –26.2)	(–35.9, –14.2)	(–27.7, –3.3)
2090–2099	–29.8	–21.4	–13.4	–6.5	–53	–42.3	–31.3	–21
	(–37, –22.2)	(–28.8, –12.2)	(–21.4, –3.4)	(–15.3, 4.5)	(–59.9, –44.6)	(–50.7, –31.8)	(–41.4, –18.6)	(–32.8, –6.2)
2080–2099	–30.9	–22.4	–14.4	–7.3	–49.7	–39.3	–28.7	–18.9
	(–38.2, –23.6)	(–29.7, –13.5)	(–22.4, –4.5)	(–16.1, 3.6)	(–57.6, –41.5)	(–47.7, –29)	(–38.6, –16.4)	(–30.4, –4.7)
Based on NorESM1-M Forecasts								
2040–2049	–14.9	–9.8	–5.2	–1.3	–20.3	–13.5	–7.3	–2
	(–20.8, –8.2)	(–15.8, –1.7)	(–11.4, 3.3)	(–7.9, 7.6)	(–26.8, –12.8)	(–20.1, –4.7)	(–14.4, 2.4)	(–9.5, 8.3)
2050–2059	–19.2	–12.9	–7.1	–2.1	–24.5	–17	–10	–4
	(–25.4, –11.9)	(–19.4, –4)	(–13.9, 2.3)	(–9.3, 7.7)	(–31.1, –17.3)	(–23.7, –8.4)	(–17.2, –0.6)	(–11.7, 6.2)
2040–2059	–17	–11.3	–6.1	–1.7	–22.4	–15.3	–8.7	–3
	(–23.1, –10.1)	(–17.6, –2.8)	(–12.7, 2.9)	(–8.6, 7.7)	(–29, –15.1)	(–21.8, –6.4)	(–15.7, 1)	(–10.6, 7.4)
2080–2089	–17	–10.8	–5.1	–0.3	–34.6	–24.8	–15.3	–7
	(–23.2, –9.9)	(–17.1, –2.8)	(–11.7, 3.4)	(–7.2, 8.8)	(–42, –26.2)	(–32.7, –14.8)	(–23.9, –3.9)	(–16.4, 5.8)
2090–2099	–25	–17.2	–9.8	–3.5	–46.6	–35.9	–25.2	–15.3
	(–31.7, –17.5)	(–24, –8.4)	(–17.3, –0.1)	(–11.5, 7.3)	(–54.2, –38.4)	(–44.6, –25.5)	(–35, –12.9)	(–26.5, –1.4)
2080–2099	–21	–14	–7.5	–1.9	–40.6	–30.3	–20.2	–11.2
	(–27.6, –13.7)	(–20.5, –5.6)	(–14.5, 1.6)	(–9.4, 8)	(–48.2, –32.6)	(–38.6, –20.1)	(–29.6, –8.6)	(–21.4, 2)

Notes: Reported are the aggregate averages of point estimates of county-level yield declines predicted using future climate forecasts and using the estimated average 2001–2010 time-varying coefficients representative of the most recently available technology. The average is weighted by the average 2001-2010 county-level acreage for the crop in question. Two-sided 95% bias-corrected percentile confidence intervals are in parentheses. The reported estimates are measured in % of yield.

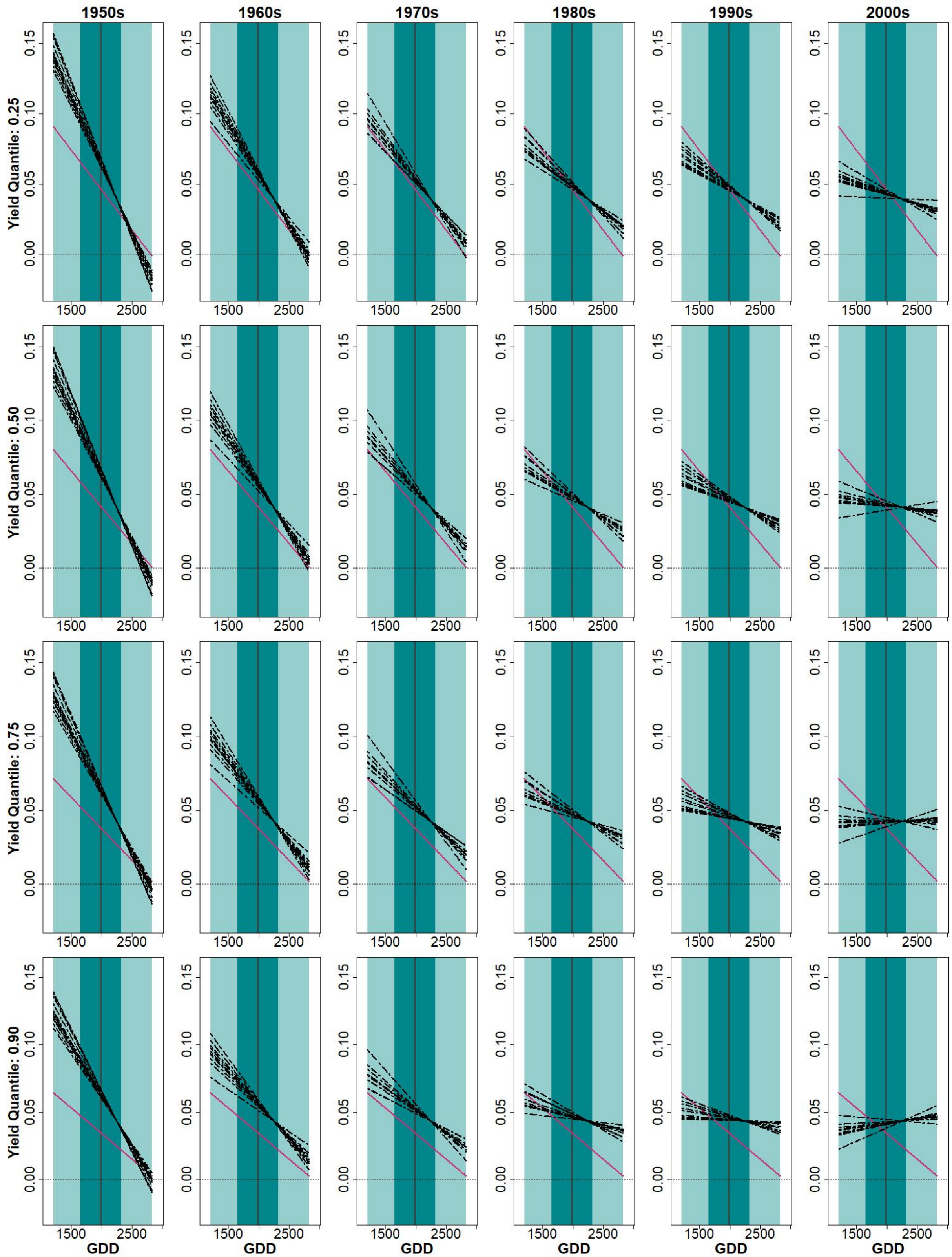

Figure 1. Marginal-Effect Function Estimates of Total $GDD_{8-29^\circ C}$ for the Corn Yield (in %)

Notes: This figure plots the marginal effect of total $GDD_{8-29^\circ C}$ in each year over the six decades in our sample. These marginal effects are linear functions of $GDD_{8-29^\circ C}$ because the estimated quantile function assumes a quadratic relationship between crop yield and $GDD_{8-29^\circ C}$. Each dashed black line corresponds to the estimates from our time-varying coefficient model in a specific year. A solid pink line corresponds to the estimates from a fixed-coefficient conditional yield quantile model. Dark (respectively, light) shaded areas illustrate the inter-quartile (respectively, middle 95%) ranges of total $GDD_{8-29^\circ C}$ in each decade.

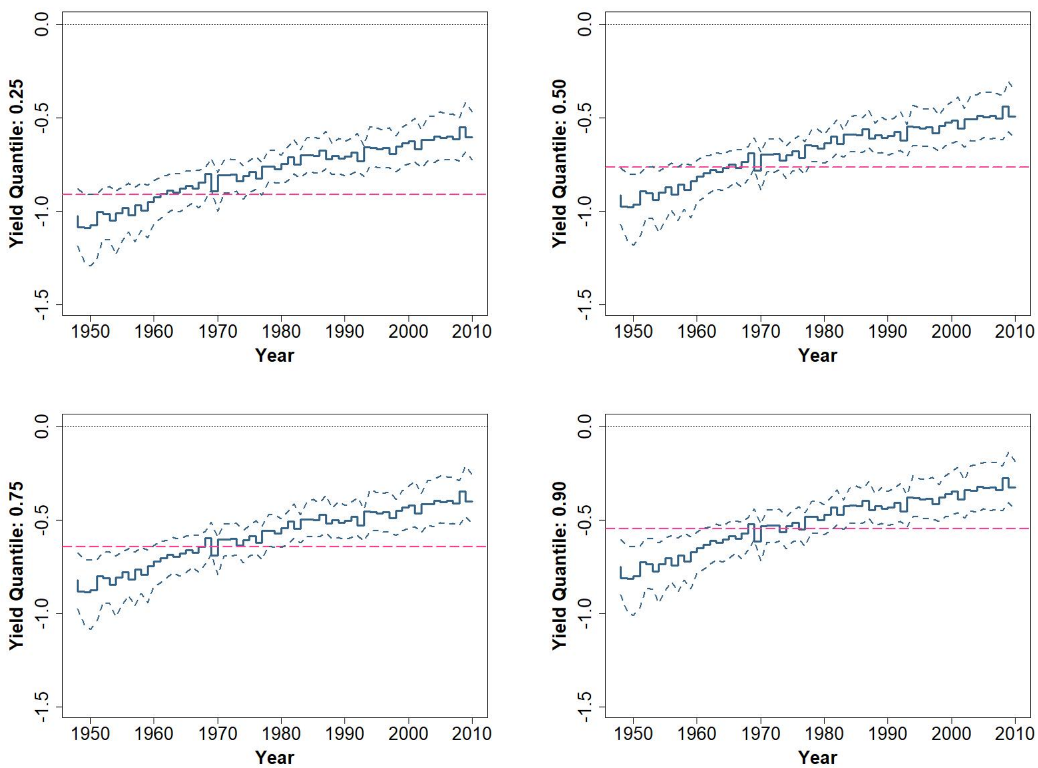

Figure 2. Marginal Effect Estimates of Total $GDD_{29^{\circ}C+}$ for the Corn Yield with Two-Sided 95% Confidence Intervals (in % per GDD)

Notes: This figure depicts the marginal effect estimates of total $GDD_{29^{\circ}C+}$ in each year of the sample. The marginal effect depends on the value of total $GDD_{29^{\circ}C+}$ because the variable enters regression in its square root value. The estimates presented in the figure are evaluated at the median $GDD_{29^{\circ}C+}$ in a year across the counties in the sample. Horizontal dashed pink lines correspond to the same estimates but from a fixed-coefficient model.

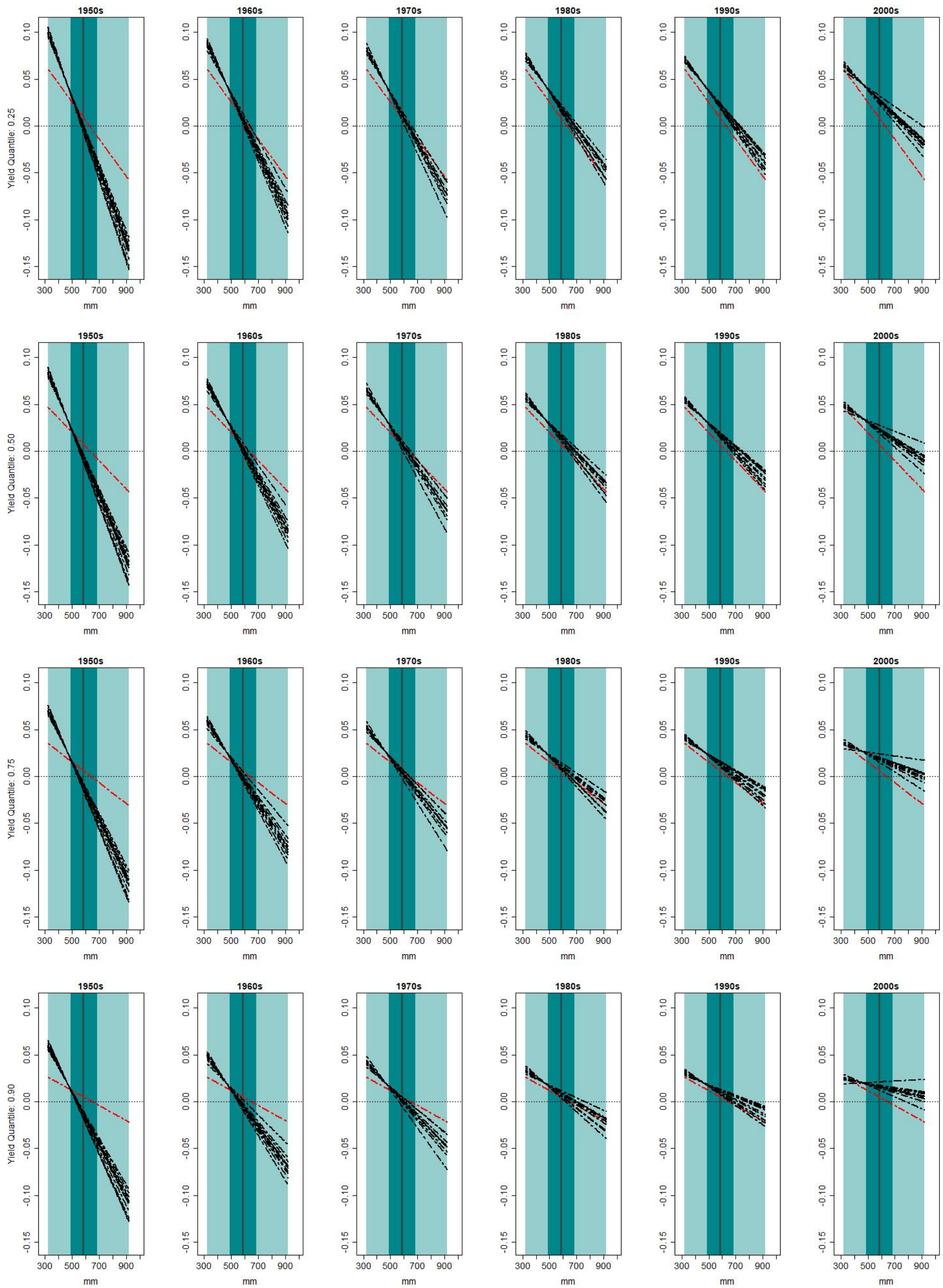

Figure 3. Marginal-Effect Function Estimates of Total Precipitation for the Corn Yield (in %)
Notes: This figure plots the marginal effect of total precipitation in each year over the six decades in our sample. These marginal effects are linear functions of precipitation because the estimated quantile function assumes a quadratic relationship between crop yield and precipitation. Each dashed black line corresponds to the estimates from our time-varying coefficient model in a specific year. A dashed red line corresponds to the estimates from a fixed-coefficient conditional yield quantile model. Dark (light) shaded areas illustrate the inter-quartile (middle 95%) ranges of total precipitation in each decade.

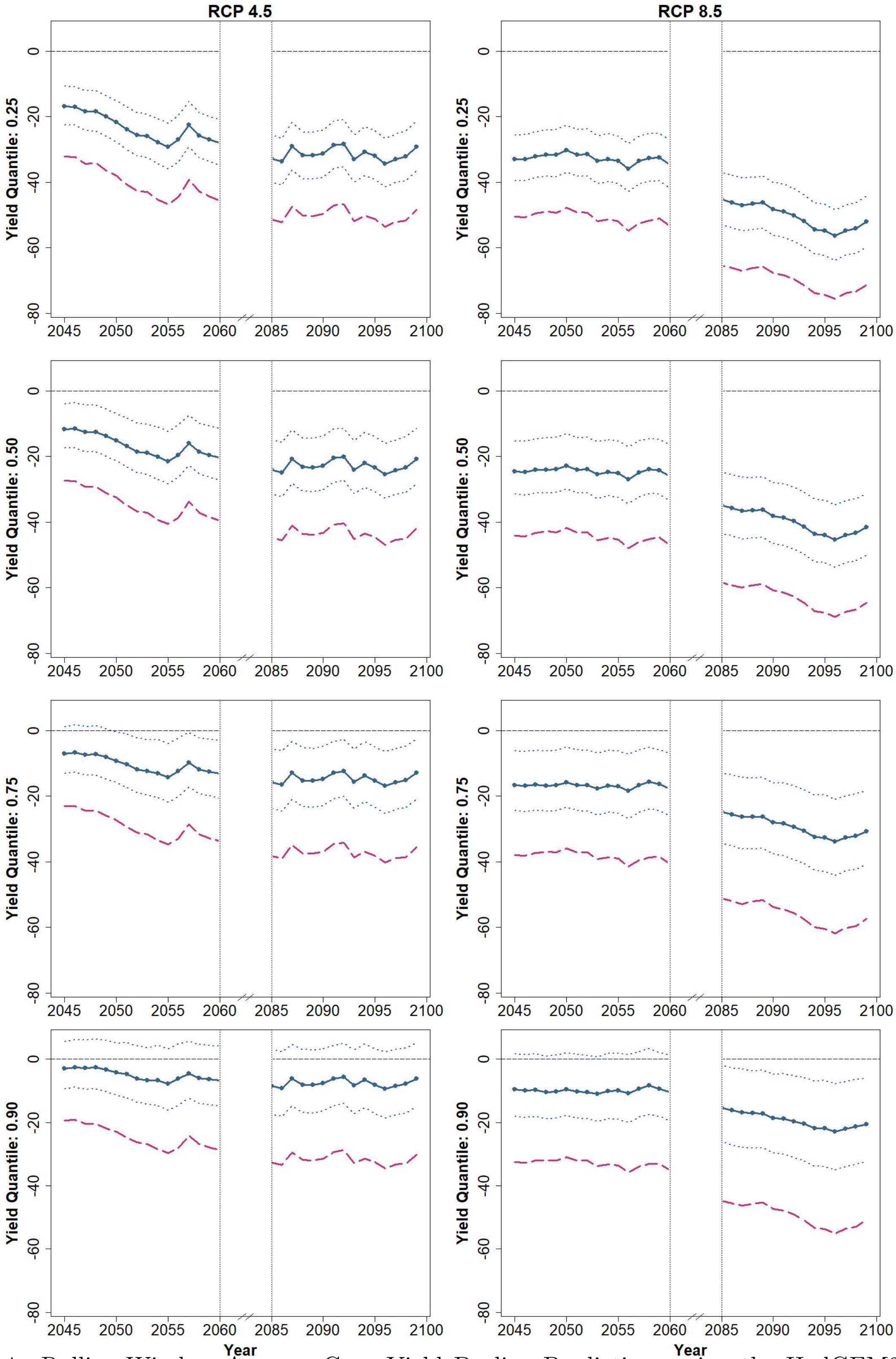

Figure 4. Rolling-Window Average Corn Yield Decline Predictions using the HadGEM2-ES365 Forecasts with Two-Sided 95% Confidence Intervals (in %)

Notes: This figure plots projections of corn yield decline due to future climate change. To smooth out the annual variation of future weather, we present six-year rolling-window average of the projected yield decline. Solid blue lines correspond to the estimates from our time-varying coefficient model. The dotted blue lines depict the 95% confidence intervals. Dashed pink lines correspond to the estimates from a fixed-coefficient model.

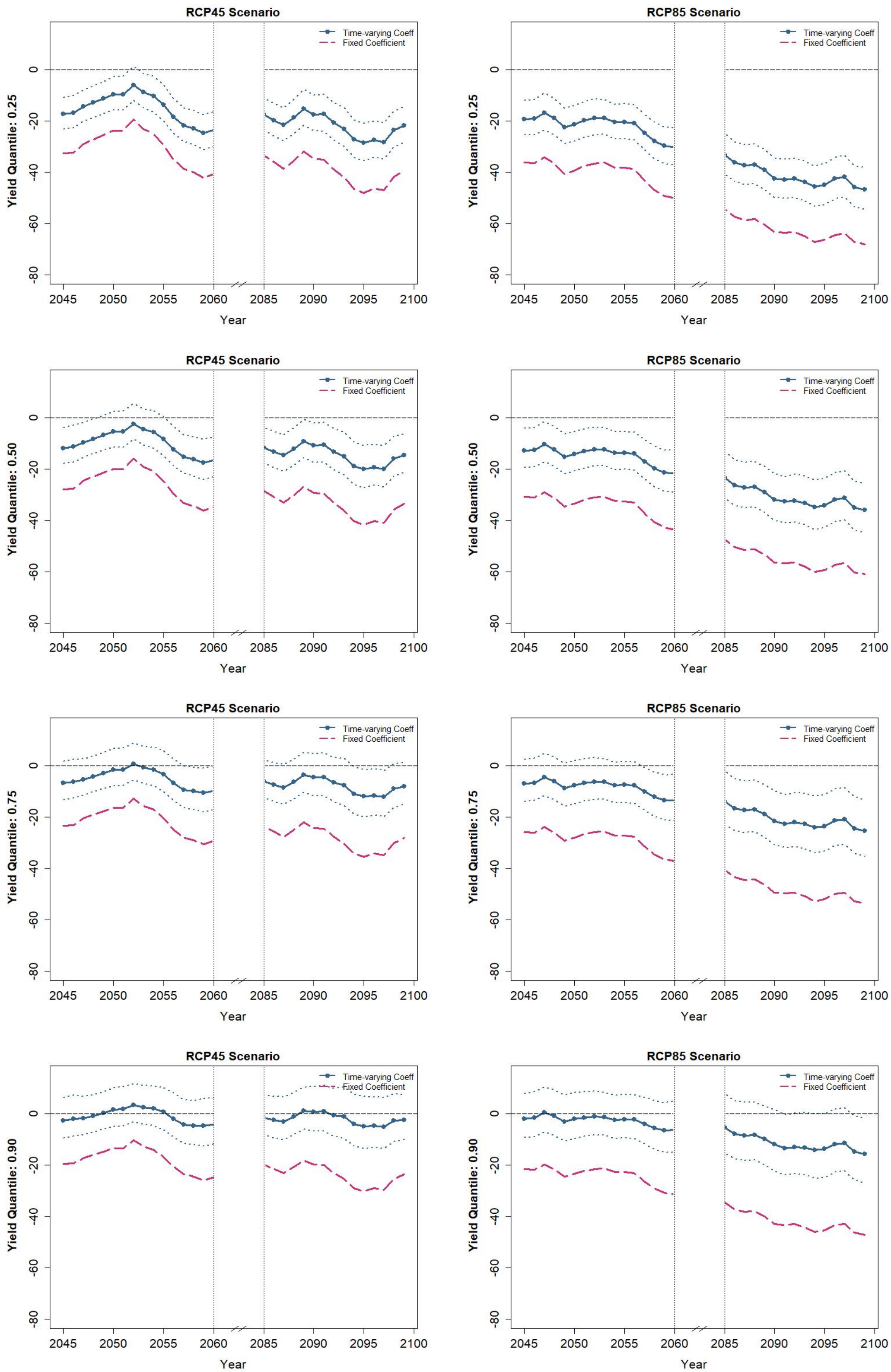

Figure 5. Rolling-Window Average Corn Yield Decline Predictions using the NorESM1-M Forecasts with Two-Sided 95% Confidence Intervals (in %)

Notes: This figure plots projections of corn yield decline due to future climate change. To smooth out the annual variation of future weather, we present six-year rolling-window average of the projected yield decline. Solid blue lines correspond to the estimates from our time-varying coefficient model. The dotted blue lines depict the 95% confidence intervals. Dashed pink lines correspond to the estimates from a fixed-coefficient model.

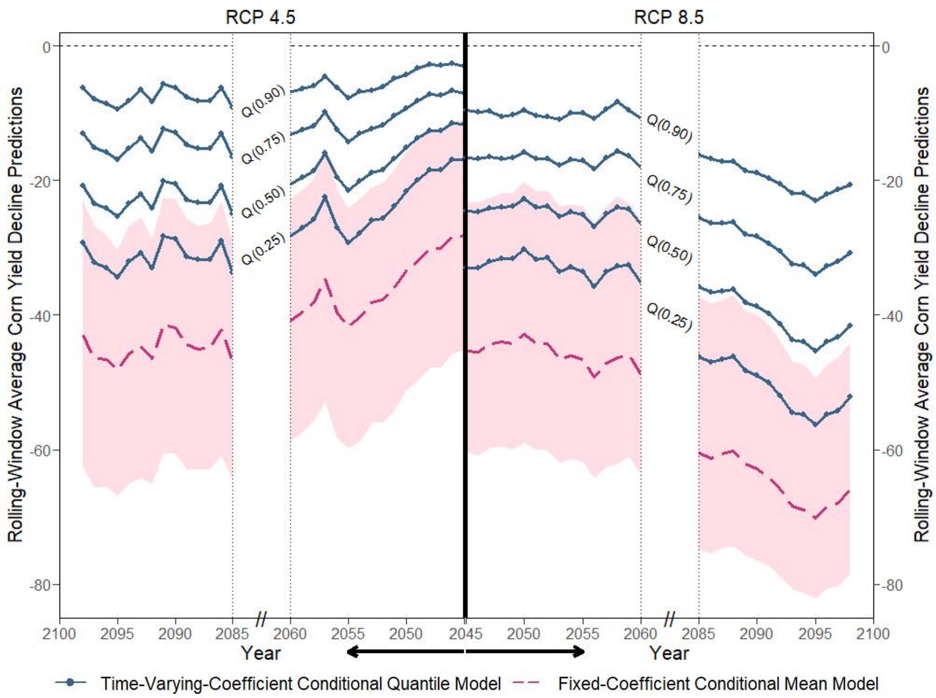

Figure 6. Projections for Future Corn Yield Decline: Time-Varying-Coefficient Conditional Quantile Model vs. Fixed-Coefficient Conditional Mean Model (in %)

Notes: This figure depicts projections of corn yield decline under future climate. The left half of the figure shows projections under RCP4.5 (a moderate warming scenario) and the right half shows projections under RCP8.5 (a severe warming scenario). Solid blue lines correspond to the estimates from our time-varying-coefficient conditional *quantile* model. From top to bottom, the solid blue lines are projections for the 0.90^{th}, 0.75^{th}, 0.50^{th}, and the 0.25^{th} conditional yield quantile. Dashed pink lines show the projections based on a fixed-coefficient conditional *mean* model, with the shaded areas illustrating their corresponding 95% confidence intervals. To smooth out the annual variation of future weather, we present six-year rolling-window average of the projected yield decline. Future climate data are generated by global climate model HadGEM2-ES365 under future warming scenarios RCP4.5 and RCP8.5, respectively.

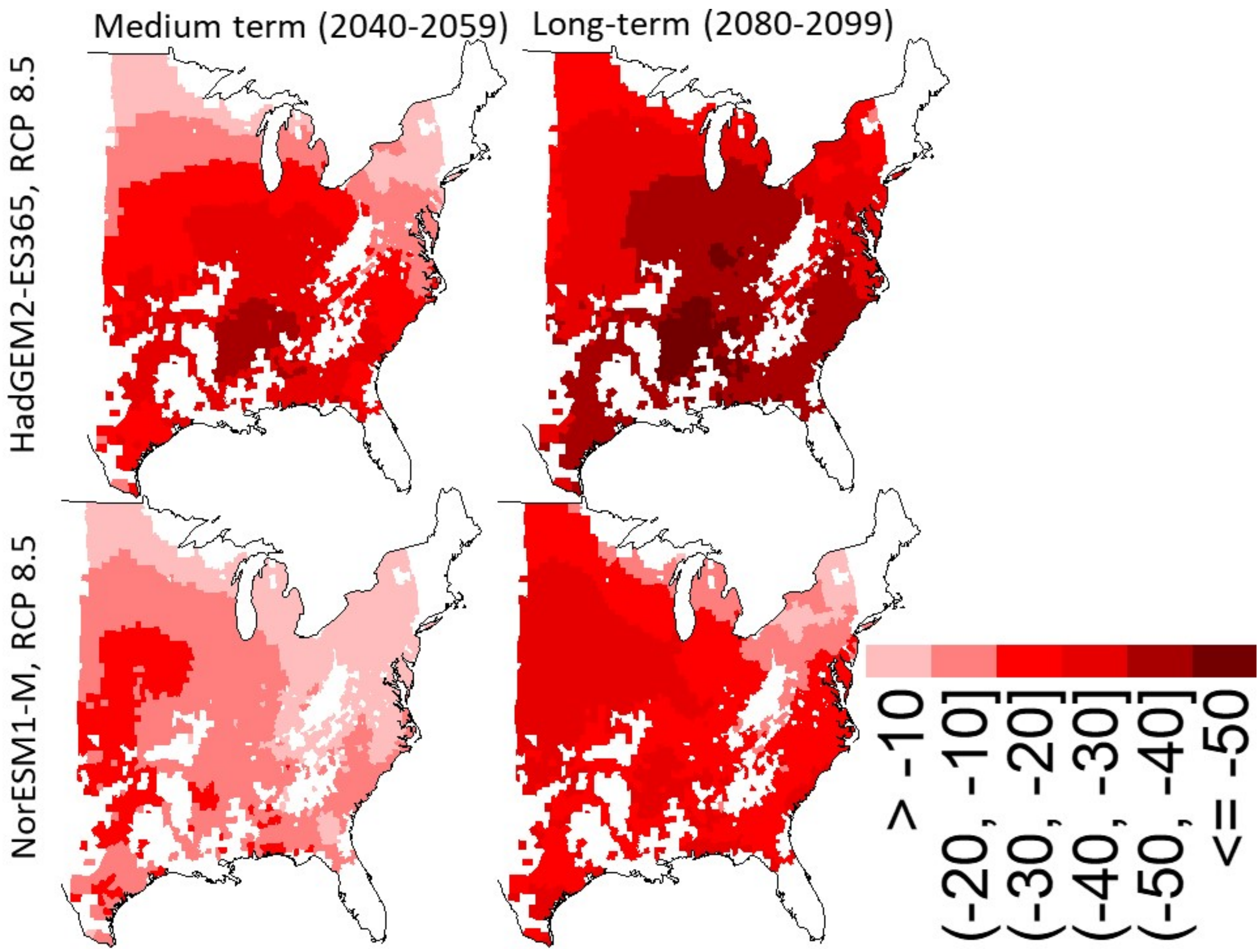

Figure 7. Geographical Configuration of Climate Change Effect on Corn Yields (in %)
Notes: Negative values indicate yield reduction. Maps are based on the time-varying-coefficient median regression. Climate change scenario considered is RCP8.5.

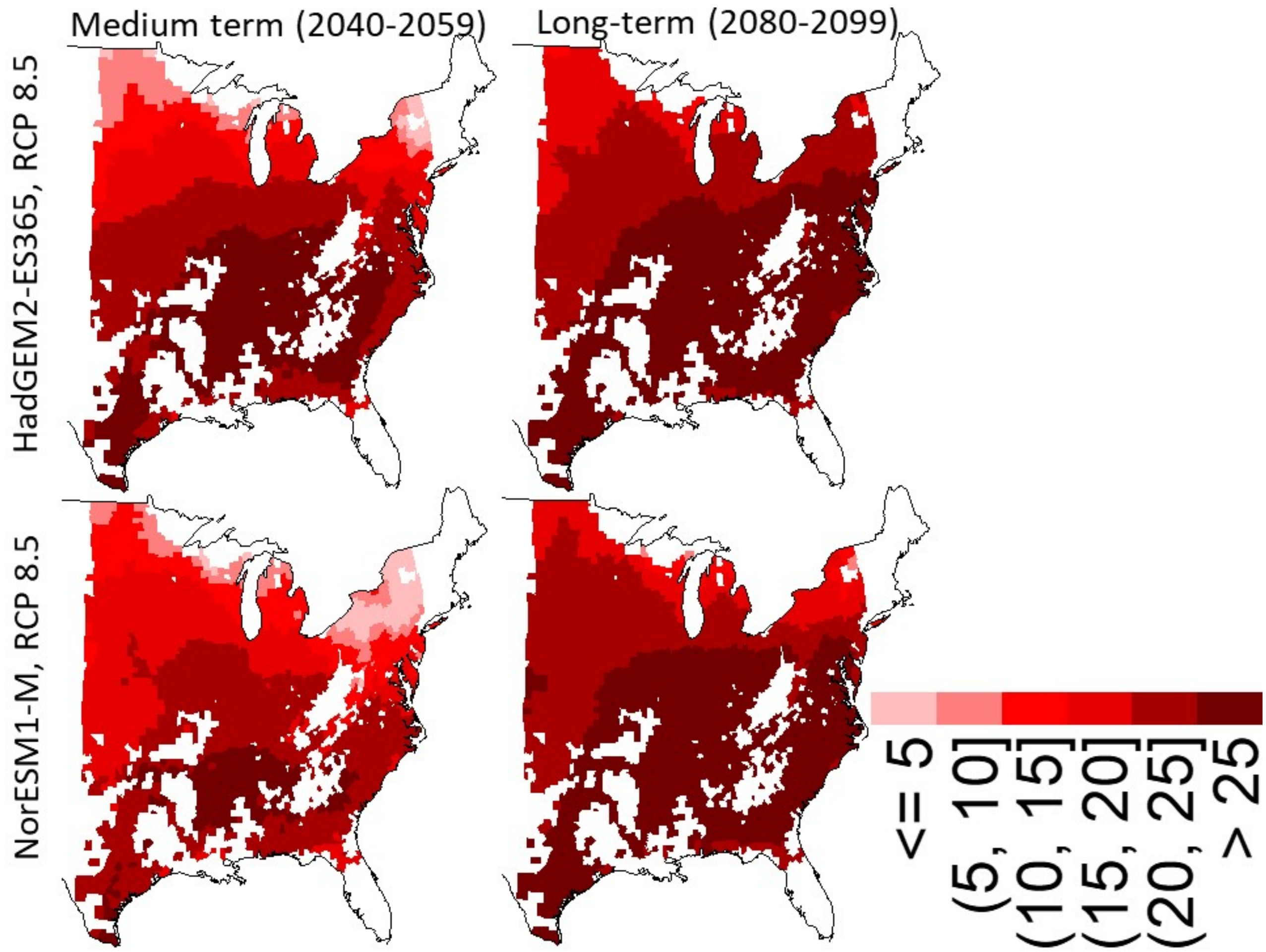

Figure 8. Spatial Differences in Corn Yield Decline Projections between the Time-Varying-Coefficient and Fixed-Coefficient Models (in percentage point)

Notes: The difference is calculated by using the absolute value of reductions projected by the fixed-coefficient models minus those projected by the time-varying-coefficient models. The darker the color, the larger the overestimation in yield reduction under the fixed-coefficient model. Maps are based on the median regression and climate change scenario considered is RCP8.5.

Appendices

Contents

A Bootstrap Algorithm

To make matters concrete, define G clusters $\{\mathcal{G}_1, \ldots, \mathcal{G}_G\}$ with each $\mathcal{G}_g$ corresponding to county-years from a given U.S. climate division. Then, the wild cluster bootstrap algorithm is as follows:

(i) Compute the estimator in equations (2.6)–(2.9). Save the estimated coefficients $[\widehat{\boldsymbol{\eta}}', \widehat{\beta}_0, \widehat{\boldsymbol{\beta}}_1', \widehat{\boldsymbol{\varphi}}_1']'$, fixed effects $\{\widehat{\mu}_i\}$ and residuals $\{\widehat{u}_{it}\}$.

(ii) Generate bootstrap weights ω_g^b for all $g = 1, \ldots, G$ from the two-point mass distribution suggested by Mammen (1993):

$$w_g^b = \begin{cases} \left(1+\sqrt{5}\right)/2 & \text{with prob. } \left(\sqrt{5}-1\right)/\left(2\sqrt{5}\right) \\ \left(1-\sqrt{5}\right)/2 & \text{with prob. } \left(\sqrt{5}+1\right)/\left(2\sqrt{5}\right) \end{cases}. \tag{A.1}$$

Next, for each observation (i,t) with $i = 1, \ldots, n$ and $t = 1, \ldots, T$, generate a new bootstrap disturbance as $u_{it}^b = \left(\sum_{g=1}^G \omega_g^b \mathbb{1}\{(i,t) \in \mathcal{G}_g\}\right) \times \widehat{u}_{it}$.

(iii) Construct a new bootstrap outcome variable:

$$\log y_{it}^b = \widehat{\mu}_i + \widehat{\beta}_0 + \sum_\kappa \widehat{\eta}_\kappa d_{\kappa,t} + \mathbf{x}_{it}' \left[\widehat{\boldsymbol{\beta}}_1 + \widehat{\boldsymbol{\varphi}}_1 \sum_\kappa \widehat{\eta}_\kappa d_{\kappa,t}\right] + u_{it}^b \tag{A.2}$$

for all $i = 1, \ldots, n$ and $t = 1, \ldots, T$.

(iv) Recompute the estimators in equations (2.6)–(2.9) using $\log y_{it}^b$ in place of $\log y_{it}$ to obtain bootstrap estimates of the location-function coefficients and the fixed effects. Signify these by the superscript "b." Then, compute the bootstrap estimate of the residual $\widehat{u}_{it}^b = y_{it} - \widehat{\mu}_i^b - \widehat{\beta}_0^b - \sum_\kappa \widehat{\eta}_\kappa^b d_{\kappa,t} - \mathbf{x}_{it}' \left(1 + \sum_\kappa \widehat{\eta}_\kappa^b d_{\kappa,t}\right) \widehat{\boldsymbol{\beta}}_1^b$. Reestimate the estimators in (2.11) and (2.13) using $\widehat{u}_{it}^b$ in place of $\widehat{u}_{it}$ to obtain bootstrap estimates of the scale function coefficients and q_τ.

(v) Repeat bootstrap steps (ii)–(iv) M times ($M = 500$ in this study). Use the empirical distribution of M bootstrap replicas of some estimand of interest (say, a coefficient or a quantile-specific function thereof) to construct bias-corrected confidence intervals for this estimand.

B Additional Descriptive Statistics of Data

This appendix includes additional descriptive statistics for both the historical data as well as future climate projections for corn- and soybean-producing counties.

Table B.1. Correlation Coefficients between Historical Weather Variables (1948–2010)

Corn	$GDD_{8-29°C}$	$GDD_{29°C+}$	Precip.	Wind	Hum.	L.-Wave	S.-Wave	Press.
Total $GDD_{8-29°C}$	1							
Total $GDD_{29°C+}$	0.8196	1						
Total Precipitation (mm)	0.3531	0.0015	1					
Ave. Wind Speed (m/s)	–0.3543	–0.1278	–0.3585	1				
Ave. Humidity (kg/kg)	0.9105	0.6433	0.5070	–0.5683	1			
Ave. Long-Wave Radiation (W/m^2)	0.9556	0.7202	0.4587	–0.3528	0.9097	1		
Ave. Short-Wave Radiation (W/m^2)	0.6616	0.6915	–0.0236	–0.0567	0.4275	0.5448	1	
Ave. Surface Pressure (kPa)	0.5789	0.3443	0.3794	–0.3275	0.6381	0.6131	0.1262	1
Soybeans	$GDD_{8-30°C}$	$GDD_{30°C+}$	Precip.	Wind	Hum.	L.-Wave	S.-Wave	Press.
Total $GDD_{8-30°C}$	1							
Total $GDD_{30°C+}$	0.7754	1						
Total Precipitation (mm)	0.4184	0.0550	1					
Ave. Wind Speed (m/s)	–0.4163	–0.1956	–0.3294	1				
Ave. Humidity (kg/kg)	0.9188	0.6190	0.5333	–0.6017	1			
Ave. Long-Wave Radiation (W/m^2)	0.9523	0.6655	0.5237	–0.4135	0.9158	1		
Ave. Short-Wave Radiation (W/m^2)	0.6423	0.6777	0.0025	–0.0741	0.4041	0.5137	1	
Ave. Surface Pressure (kPa)	0.5955	0.3110	0.4181	–0.4554	0.6724	0.6322	0.1101	1

Note: The numbers of observations for the corn and soybean datasets are 118,134 and 91,977, respectively. All weather variables are measured within the growing season (March to August). Average weather variables are simple averages of their daily values across the growing season.

Table B.2. Summary Statistics of Future Climate Data Predicted by HadGEM2-ES365 for Corn-Producing Counties

	Medium Term (2040–2059)						*Long Term* (2080–2099)						
Variable	Mean	Min.	1st Qu.	Median	3rd Qu.	Max.	Std.	Mean	Min.	1st Qu.	Median	3rd Qu.	Max.	Std.
RCP4.5														
Total $GDD_{8-29°C}$	2,346	1,206	2,003	2,328	2,676	3,589	446	2,500	1,428	2,200	2,481	2,784	3,601	401
Total $GDD_{29°C+}$	186.72	1.17	96.81	168.15	261.14	682.00	110.85	239.84	11.09	152.93	223.78	319.23	736.50	112.99
Total Precipitation (mm)	591	28	462	592	703	1509	182	582	62	461	581	699	1469	173
Ave. Wind Speed (m/s)	2.75	1.78	2.42	2.74	3.06	4.79	0.44	2.70	1.61	2.35	2.70	3.00	4.76	0.45
Ave. Humidity (kg/kg)	0.010	0.005	0.009	0.010	0.011	0.016	0.002	0.011	0.005	0.009	0.011	0.012	0.016	0.002
Ave. Short-Wave Radiation (W/m^2)	236	205	230	235	241	272	9	237	206	231	237	243	276	9
RCP8.5														
Total $GDD_{8-29°C}$	2,439	1,194	2,116	2,439	2,758	3,580	431	2,729	1,780	2,419	2,718	3,016	3,730	388
Total $GDD_{29°C+}$	260.09	6.98	140.15	237.99	367.49	753.39	144.94	442.90	64.95	306.81	429.32	565.59	1039.04	168.68
Total Precipitation (mm)	532	16	415	524	633	1478	172	576	48	452	567	692	1308	175
Ave. Wind Speed (m/s)	2.90	1.86	2.57	2.88	3.19	5.00	0.45	2.77	1.74	2.50	2.76	3.00	4.88	0.38
Ave. Humidity (kg/kg)	0.010	0.006	0.009	0.010	0.011	0.016	0.002	0.011	0.006	0.010	0.011	0.013	0.018	0.002
Ave. Short-Wave Radiation (W/m^2)	239	206	231	239	246	277	11	238	209	232	238	245	271	9

Note: The number of included corn-producing counties is 1,893. All weather variables are measured within the growing season (March to August). Average weather variables are simple averages of their daily values across the growing season.

Table B.3. Summary Statistics of Future Climate Data Predicted by NorESM1-M for Corn-Producing Counties

	Medium Term (2040–2059)							*Long Term* (2080–2099)						
Variable	Mean	Min	1st Qu.	Median	3rd Qu.	Max	Std.	Mean	Min	1st Qu.	Median	3rd Qu.	Max	Std.
RCP4.5														
Total $GDD_{8-29°C}$	2,266	1,179	1,936	2,243	2,576	3,612	429	2,378	1,300	2,071	2,364	2,674	3,629	406
Total $GDD_{29°C+}$	142.74	3.79	70.05	123.20	197.74	739.55	92.76	173.780	8.078	92.923	154.306	236.562	864.771	104.02
Total Precipitation (mm)	618	47	501	613	718	1507	177	622	62	523	612	715	1519	161
Ave. Wind Speed (m/s)	2.79	1.74	2.47	2.78	3.09	4.80	0.42	2.78	1.80	2.45	2.76	3.07	4.84	0.43
Ave. Humidity (kg/kg)	0.010	0.005	0.008	0.010	0.011	0.015	0.002	0.010	0.005	0.009	0.010	0.012	0.015	0.002
Ave. Short-Wave radiation (W/m^2)	236	208	230	236	242	275	9	240	211	233	240	246	282	9
RCP8.5														
Total $GDD_{8-29°C}$	2,369	1,237	2,056	2,359	2,673	3,595	422	2,628	1,594	2,347	2,614	2,900	3,783	370
Total $GDD_{29°C+}$	170.19	4.38	89.86	148.67	228.09	824.00	106.82	299.91	27.20	200.4	282.5	379.2	1175.54	137.43
Total Precipitation (mm)	634	61	520	631	737	1334	177	640	100	520	636	744	1646	181
Ave. Wind Speed (m/s)	2.87	1.67	2.54	2.85	3.17	4.95	0.44	2.93	1.90	2.61	2.91	3.21	5.10	0.44
Ave. Humidity (kg/kg)	0.010	0.005	0.009	0.010	0.012	0.015	0.002	0.011	0.006	0.009	0.011	0.012	0.017	0.002
Ave. Short-Wave radiation (W/m^2)	238	202	232	237	242	275	8	241	192	234	241	247	273	9

Note: The number of included corn-producing counties is 1,893. All weather variables are measured within the growing season (March to August). Average weather variables are simple averages of their daily values across the growing season.

Table B.4. Summary Statistics of Future Climate Data Predicted by HadGEM2-ES365 for Soybean-Producing Counties

	Medium Term (2040–2059)							*Long Term* (2080–2099)						
Variable	Mean	Min	1st Qu.	Median	3rd Qu.	Max	Std.	Mean	Min	1st Qu.	Median	3rd Qu.	Max	Std.
RCP4.5														
Total $GDD_{8-30°C}$	2,373	1,210	2,028	2,363	2,703	3,688	445	2,537	1,448	2,238	2,527	2,820	3,705	398
Total $GDD_{30°C+}$	146.38	1.58	72.58	130.80	205.77	522.47	90.64	192.19	6.09	119.78	178.58	256.06	548.93	93.97
Total Precipitation (mm)	593	28	465	593	704	1509	179	584	84	463	581	699	1687	171
Ave.~Wind Speed (m/s)	2.76	1.78	2.44	2.75	3.05	4.96	0.43	2.71	1.61	2.37	2.71	3.00	4.76	0.44
Ave.~Humidity (kg/kg)	0.010	0.005	0.009	0.010	0.011	0.016	0.002	0.011	0.005	0.009	0.011	0.012	0.016	0.002
Ave.~Short-Wave radiation (W/m^2)	235	205	230	235	240	265	8	237	206	230	236	243	266	9
RCP8.5														
Total $GDD_{8-30°C}$	2,476	1,197	2,152	2,484	2,796	3,677	431	2,784	1,826	2,469	2,779	3,072	3,865	393
Total $GDD_{30°C+}$	212.38	1.75	109.52	191.83	301.72	589.21	123.98	374.56	63.33	256.51	360.83	479.30	854.26	147.62
Total Precipitation (mm)	534	30	419	523	631	1478	168	579	48	456	568	692	1291	172
Ave.~Wind Speed (m/s)	2.91	1.86	2.60	2.89	3.19	4.78	0.44	2.77	1.74	2.52	2.76	2.99	4.80	0.36
Ave.~Humidity (kg/kg)	0.010	0.006	0.009	0.010	0.011	0.016	0.002	0.011	0.006	0.010	0.011	0.013	0.018	0.002
Ave.~Short-Wave radiation (W/m^2)	238	208	230	238	245	269	11	238	212	232	238	244	264	9

Note: The Number of included soybean-producing counties is 1,722. All weather variables are measured within the growing season (March to August). Average weather variables are simple averages of their daily values across the growing season.

Table B.5. Summary Statistics of Future Climate Data Predicted by NorESM1-M for Soybean-Producing Counties

	Medium Term (2040–2059)							*Long Term* (2080–2099)						
Variable	Mean	Min	1st Qu.	Median	3rd Qu.	Max	Std.	Mean	Min	1st Qu.	Median	3rd Qu.	Max	Std.
RCP4.5														
Total $GDD_{8-30°C}$	2,289	1,181	1,961	2,276	2,597	3,715	422	2,407	1,306	2,101	2,403	2,699	3,726	401
Total $GDD_{30°C+}$	107.25	1.62	50.58	91.65	150.42	516.67	72.30	134.49	7.09	69.23	118.060	183.51	564.20	84.98
Total Precipitation (mm)	620	47	505	613	717	1464	172	624	92	526	611	714	1474	155
Ave.∼Wind Speed (m/s)	2.80	1.74	2.49	2.79	3.08	4.80	0.40	2.79	1.80	2.47	2.76	3.07	4.84	0.42
Ave.∼Humidity (kg/kg)	0.010	0.005	0.008	0.010	0.011	0.015	0.002	0.010	0.005	0.009	0.010	0.011	0.015	0.002
Ave.∼Short-Wave radiation (W/m^2)	236	208	229	235	241	265	8	239	206	233	239	245	271	9
RCP8.5														
Total $GDD_{8-30°C}$	2,398	1,241	2,090	2,398	2,697	3,689	415	2,674	1,606	2,395	2,669	2,947	3,919	365
Total $GDD_{30°C+}$	131.20	1.20	67.20	113.21	176.15	692.60	85.72	246.92	18.72	162.21	231.45	312.58	843.11	117.74
Total Precipitation (mm)	635	62	524	631	733	1409	170	641	112	525	635	741	1687	177
Ave.∼Wind Speed (m/s)	2.87	1.67	2.57	2.86	3.16	4.95	0.43	2.94	1.91	2.64	2.92	3.20	4.70	0.43
Ave.∼Humidity (kg/kg)	0.010	0.005	0.009	0.010	0.011	0.016	0.002	0.011	0.006	0.009	0.011	0.012	0.017	0.002
Ave.∼Short-Wave radiation (W/m^2)	237	201	232	237	242	268	8	240	189	234	240	246	269	9

Note: The Number of included soybean-producing counties is 1,722. All weather variables are measured within the growing season (March to August). Average weather variables are simple averages of their daily values across the growing season.

C Results for the Soybean Yield

This appendix reports the results obtained by replicating the estimations and analyses reported in the main text using the soybean log-yields as an outcome.

Table C.1. Time-Varying Quantile Slope Coefficient Estimates for the Soybean Yield

Variable	*All Estimates* Min	1st Qu.	Median	3rd Qu.	Max	*Statistically Significant Estimates* Min	1st Qu.	Median	3rd Qu.	Max	$\neq 0$ (%)
The 0.25th Yield Quantile											
Total $GDD_{8-30°C}$	0.1159	0.1483	0.1656	0.1964	0.2218	0.1159	0.1483	0.1656	0.1964	0.2218	100
Total $GDD_{8-30°C}$ sq. ($\times 10^{-3}$)	–0.0368	–0.0334	–0.0292	–0.0268	–0.0224	–0.0368	–0.0334	–0.0292	–0.0268	–0.0224	100
Total $GDD_{30°C+}$ (square root)	–11.0579	–10.0258	–8.7782	–8.0774	–6.7646	–11.0579	–10.0258	–8.7782	–8.0774	–6.7646	100
Total Precipitation	0.0641	0.1138	0.1403	0.1875	0.2266	0.0641	0.1138	0.1403	0.1875	0.2266	100
Total Precipitation sq. ($\times 10^{-3}$)	–0.1743	–0.14	–0.0985	–0.0752	–0.0316	–0.1743	–0.1401	–0.0987	–0.0764	–0.0491	98.4
Average Wind Speed	–14.9098	–12.0773	–8.6534	–6.7303	–3.1276	–14.9098	–12.1914	–8.6942	–7.3537	–5.4163	93.7
Average Humidity ($\times 10^{3}$)	–0.769	0.1508	1.2626	1.887	3.0569	1.6574	1.9274	2.1253	2.3131	3.0569	31.7
Average Long-Wave Radiation	0.042	0.0807	0.1014	0.1382	0.1687						0
Average Short-Wave Radiation	–0.0143	0.0543	0.0909	0.156	0.2099	0.1224	0.1258	0.1322	0.1566	0.1658	12.7
Average Surface Pressure	–7.4801	–4.3607	–2.6956	0.269	2.7215	–7.4801	–4.9734	–3.687	–2.7922	2.7215	63.5
The 0.50th Yield Quantile											
Total $GDD_{8-30°C}$)	0.0979	0.1303	0.1476	0.1784	0.2039	0.0979	0.1303	0.1476	0.1784	0.2039	100
Total $GDD_{8-30°C}$ sq. ($\times 10^{-3}$)	–0.0318	–0.0284	–0.0242	–0.0219	–0.0175	–0.0318	–0.0284	–0.0242	–0.0219	–0.0175	100
Total $GDD_{30°C+}$ (square root)	–10.1474	–9.1153	–7.8677	–7.1669	–5.8541	–10.1474	–9.1153	–7.8677	–7.1669	–5.8541	100
Total Precipitation	0.0439	0.0935	0.1201	0.1673	0.2063	0.0639	0.095	0.1203	0.1675	0.2063	98.4
Total Precipitation sq. ($\times 10^{-3}$)	–0.1603	–0.126	–0.0845	–0.0612	–0.0176	–0.1603	–0.1262	–0.0847	–0.0625	–0.0352	98.4
Average Wind Speed	–15.428	–12.5956	–9.1717	–7.2485	–3.6458	–15.428	–12.6233	–9.2096	–7.4322	–5.1155	96.8
Average Humidity ($\times 10^{3}$)	–0.7763	0.1434	1.2552	1.8797	3.0495	1.5983	1.9044	2.1009	2.3056	3.0495	33.3
Average Long-Wave Radiation	–0.0386	0.0002	0.0208	0.0577	0.0881						0
Average Short-Wave Radiation	–0.0106	0.058	0.0946	0.1598	0.2137	0.1218	0.1305	0.1598	0.1685	0.2137	28.6
Average Surface Pressure	–8.1764	–5.057	–3.3919	–0.4273	2.0252	–8.1764	–5.6697	–4.3833	–3.4885	2.0252	63.5

Note: The left panel summarizes all point estimates, whereas the right panel summarizes only statistically significant point estimates of time-varying slope coefficients. The last column reports the share of sample period for which time-varying slope coefficients are statistically significant. Statistical significance is assessed using two-sided 95% bias-corrected percentile confidence intervals. The reported estimates are measured in % of yield per unit in the corresponding regressor.

Table C.1. Time-Varying Quantile Slope Coefficient Estimates for the Soybean Yield (cont.)

	All Estimates					*Statistically Significant Estimates*					
Variable	Min	1st Qu.	Median	3rd Qu.	Max	Min	1st Qu.	Median	3rd Qu.	Max	$\neq 0$ (%)
The 0.75th Yield Quantile											
Total $GDD_{8-39°C}$	0.0823	0.1147	0.132	0.1628	0.1883	0.0823	0.1147	0.132	0.1628	0.1883	100
Total $GDD_{8-30°C}$ sq. ($\times 10^{-3}$)	–0.0275	–0.0241	–0.0199	–0.0176	–0.0132	–0.0275	–0.0241	–0.0199	–0.0176	–0.0132	100
Total $GDD_{30°C+}$ (square root)	–9.3562	–8.3241	–7.0765	–6.3758	–5.063	–9.3562	–8.3241	–7.0765	–6.3758	–5.063	100
Total Precipitation	0.0263	0.076	0.1025	0.1497	0.1887	0.0463	0.0774	0.1027	0.1499	0.1887	98.4
Total Precipitation sq. ($\times 10^{-3}$)	–0.1482	–0.1139	–0.0724	–0.0491	–0.0054	–0.1482	–0.1152	–0.0729	–0.0566	–0.0332	93.7
Average Wind Speed	–15.8783	–13.0459	–9.622	–7.6988	–4.0961	–15.8783	–13.0597	–9.6409	–7.8017	–5.5476	98.4
Average Humidity ($\times 10^3$)	–0.7827	0.1371	1.2488	1.8733	3.0432	1.5919	1.9137	2.1116	2.2994	3.0432	31.7
Average Long-Wave Radiation	–0.1086	–0.0698	–0.0491	–0.0123	0.0181						0
Average Short-Wave Radiation	–0.0073	0.0612	0.0978	0.163	0.2169	0.1154	0.1343	0.167	0.1843	0.2169	38.1
Average Surface Pressure	–8.7815	–5.6621	–3.9969	–1.0323	1.4202	–8.7815	–6.2364	–4.9117	–3.9805	–2.328	68.3
The 0.90th Yield Quantile											
Total $GDD_{8-30°C}$)	0.0693	0.1016	0.1189	0.1497	0.1752	0.0693	0.1016	0.1189	0.1497	0.1752	100
Total $GDD_{8-30°C}$ sq. ($\times 10^{-3}$)	–0.0239	–0.0205	–0.0163	–0.0139	–0.0095	–0.0239	–0.0205	–0.0163	–0.0139	–0.0095	100
Total $GDD_{30°C+}$ (square root)	–8.6936	–7.6615	–6.4139	–5.7131	–4.4004	–8.6936	–7.6615	–6.4139	–5.7131	–4.4004	100
Total Precipitation	0.0116	0.0612	0.0878	0.135	0.174	0.0431	0.0698	0.0883	0.1365	0.174	93.7
Total Precipitation sq. ($\times 10^{-3}$)	–0.138	–0.1037	–0.0622	–0.0389	0.0047	–0.138	–0.1061	–0.0697	–0.0492	–0.023	90.5
Average Wind Speed	–16.2555	–13.423	–9.9991	–8.0759	–4.4732	–16.2555	–13.4368	–10.0181	–8.1788	–5.9248	98.4
Average Humidity ($\times 10^3$)	–0.788	0.1317	1.2435	1.868	3.0378	1.6928	1.9156	2.1234	2.2943	3.0378	30.2
Average Long-Wave Radiation	–0.1672	–0.1284	–0.1078	–0.0709	–0.0405						0
Average Short-Wave Radiation	–0.0046	0.0639	0.1005	0.1657	0.2196	0.1122	0.1361	0.1695	0.1905	0.2196	42.9
Average Surface Pressure	–9.2882	–6.1688	–4.5036	–1.5391	0.9134	–9.2882	–6.7277	–5.2927	–4.4684	–2.4118	71.4

Note: The left panel summarizes all point estimates, whereas the right panel summarizes only statistically significant point estimates of time-varying slope coefficients. The last column reports the share of sample period for which time-varying slope coefficients are statistically significant. Statistical significance is assessed using two-sided 95% bias-corrected percentile confidence intervals. The reported estimates are measured in % of yield per unit in the corresponding regressor.

Table C.2. Soybean Yield Change Predictions Based on Various Climate Forecasts (%)

	RCP4.5 Scenario				*RCP8.5 Scenario*			
Horizon	0.25th Quant.	0.50th Quant.	0.75th Quant.	0.90th Quant.	0.25th Quant.	0.50th Quant.	0.75th Quant.	0.90th Quant.
Based on HadGEM2-ES365 Forecasts								
2040–2049	–25.1	–21.3	–17.7	–14.6	–39.8	–34.6	–29.6	–25.1
	(–31.2, –18.8)	(–26.8, –14.5)	(–23.6, –10.7)	(–20.8, –7.2)	(–45.5, –32.7)	(–40.7, –27.1)	(–36.2, –21.5)	(–32.2, –16.4)
2050–2059	–34.5	–29.5	–24.8	–20.5	–40.5	–35	–29.8	–25
	(–40.5, –27.3)	(–35.7, –21.7)	(–31.4, –16.6)	(–27.5, –11.9)	(–46.3, –33.4)	(–41.3, –27.3)	(–36.6, –21.3)	(–32.4, –15.8)
2040–2059	–29.8	–25.4	–21.3	–17.6	–40.2	–34.8	–29.7	–25
	(–35.7, –23.2)	(–31.3, –18)	(–27.5, –13.6)	(–24.1, –9.6)	(–45.9, –33.3)	(–41, –27.2)	(–36.4, –21.5)	(–32.2, –16.2)
2080–2089	–37.7	–31.8	–26.1	–21	–51.4	–44.3	–37.2	–30.5
	(–43.9, –30)	(–38.5, –23.4)	(–33.4, –17.2)	(–28.9, –11.3)	(–57.3, –43.7)	(–51, –35.5)	(–44.8, –27.4)	(–39.1, –19.9)
2090–2099	–35.9	–30	–24.4	–19.3	–57.9	–50.8	–43.5	–36.4
	(–42.3, –28)	(–36.9, –21.4)	(–31.8, –15.4)	(–27.1, –9.5)	(–63.6, –50.4)	(–57.4, –42)	(–51.1, –33.6)	(–45.1, –25.5)
2080–2099	–36.8	–30.9	–25.2	–20.1	–54.7	–47.5	–40.3	–33.4
	(–43, –29)	(–37.7, –22.5)	(–32.5, –16.2)	(–28.1, –10.4)	(–60.5, –47.1)	(–54.2, –38.7)	(–48, –30.5)	(–42.1, –22.7)
Based on NorESM1-M Forecasts								
2040–2049	–22.5	–19	–15.9	–13.1	–27.8	–23.4	–19.3	–15.7
	(–28.4, –16.1)	(–24.4, –12.3)	(–21.6, –8.9)	(–19.2, –5.8)	(–33.6, –20.7)	(–29.5, –15.8)	(–25.8, –11.5)	(–22.6, –7.7)
2050–2059	–26.5	–22.5	–18.8	–15.5	–31.1	–26.1	–21.4	–17.2
	(–32.5, –19.8)	(–28.4, –15.2)	(–25.1, –11.2)	(–22.1, –7.7)	(–37, –24.1)	(–32.2, –18.5)	(–28, –13.4)	(–24.3, –8.8)
2040–2059	–24.5	–20.8	–17.3	–14.3	–29.4	–24.7	–20.4	–16.4
	(–30.5, –17.9)	(–26.4, –13.8)	(–23.3, –10.1)	(–20.6, –6.8)	(–35.3, –22.4)	(–30.8, –17.2)	(–26.9, –12.5)	(–23.4, –8.3)
2080–2089	–23.5	–19.3	–15.5	–12.1	–41.2	–34.7	–28.4	–22.6
	(–29.4, –16.4)	(–25.3, –11.9)	(–21.9, –7.9)	(–18.9, –4.3)	(–47.3, –33.4)	(–41.5, –26)	(–35.9, –19.1)	(–30.8, –12.7)
2090–2099	–32	–26.9	–22.1	–17.7	–52.4	–45.4	–38.4	–31.8
	(–38, –24.5)	(–33.2, –18.8)	(–28.9, –13.6)	(–25.1, –8.8)	(–58.4, –45.3)	(–52, –37)	(–46, –29.2)	(–40.3, –21.5)
2080–2099	–27.7	–23.1	–18.8	–14.9	–46.8	–40	–33.4	–27.2
	(–33.6, –20.4)	(–29.3, –15.4)	(–25.4, –10.8)	(–22, –6.6)	(–52.8, –39.6)	(–46.8, –31.6)	(–40.9, –24)	(–35.5, –17.1)

Note: Reported are the aggregate averages of point estimates of county-level yield declines predicted using future climate forecasts and using the estimated average 2001–2010 time-varying coefficients representative of the most recently available technology. The average is weighted by the average 2001-2010 county-level acreage for the crop in question. Two-sided 95% bias-corrected percentile confidence intervals are in parentheses. The reported estimates are measured in % of yield.

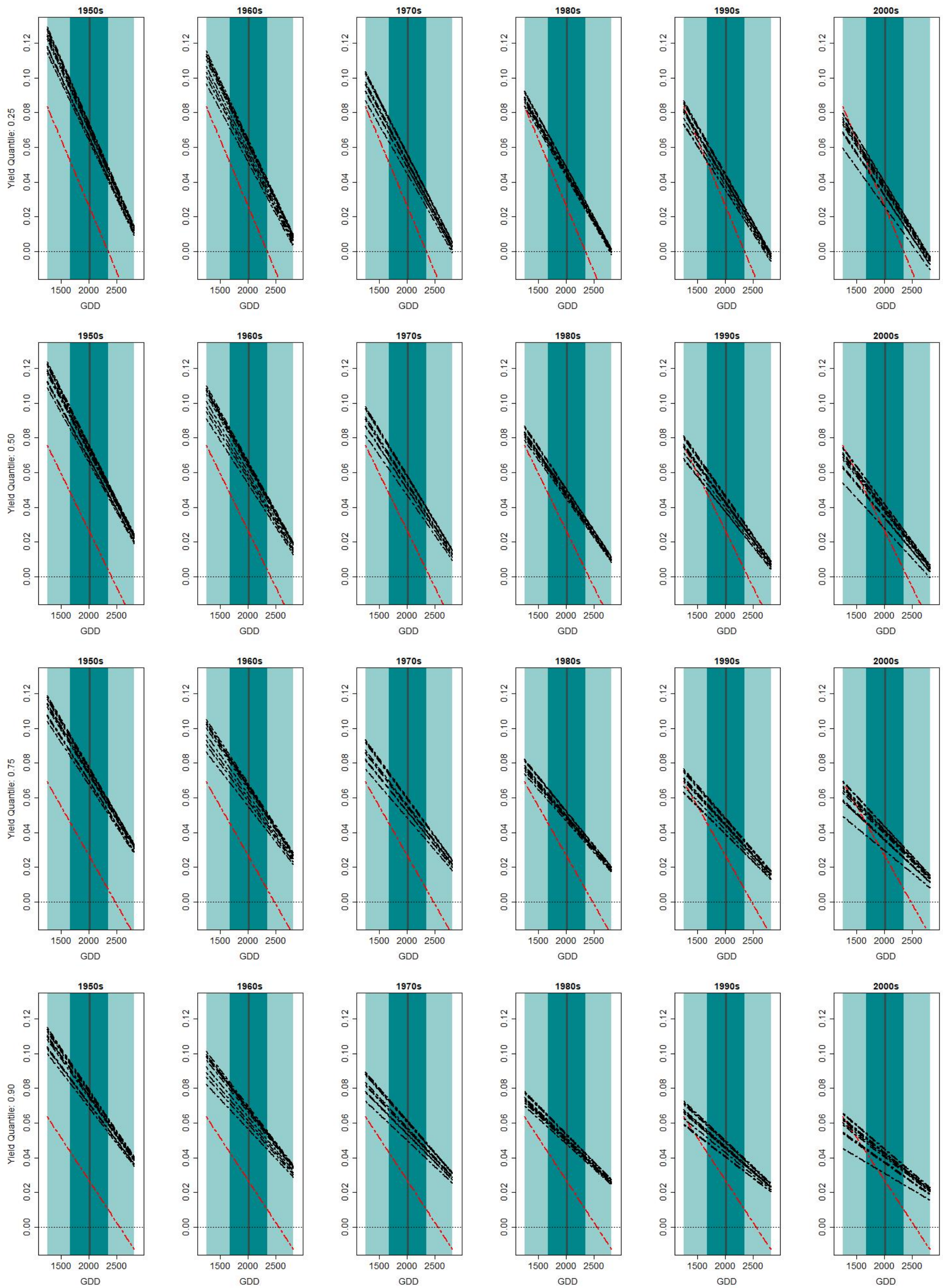

Figure C.1. Marginal-Effect Function Estimates of Total $\text{GDD}_{8-30^{\circ}\text{C}}$ for the Soybean Yield (in % per GDD)

Note: Dashed black (solid pink) lines correspond to the estimates from a time-varying coefficient (fixed-coefficient) model. Dark (light) shaded areas illustrate the inter-quartile (middle 95%) ranges of total GDD in each decade.

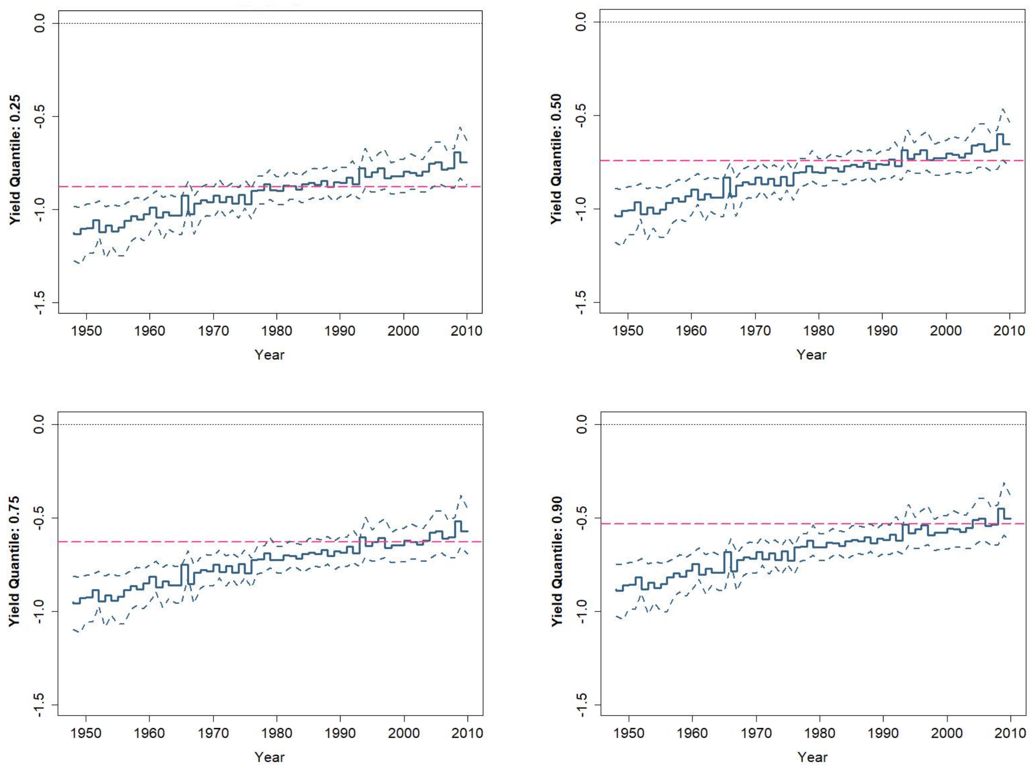

Figure C.2. Marginal Effect Estimates of Total $GDD_{30^{\circ}C+}$ for the Soybean Yield with Two-Sided 95% Confidence Intervals (in % per GDD)

Note: The estimates are evaluated at the median $GDD_{30^{\circ}C+}$. Horizontal dashed pink lines correspond to the estimates from a fixed-coefficient model.

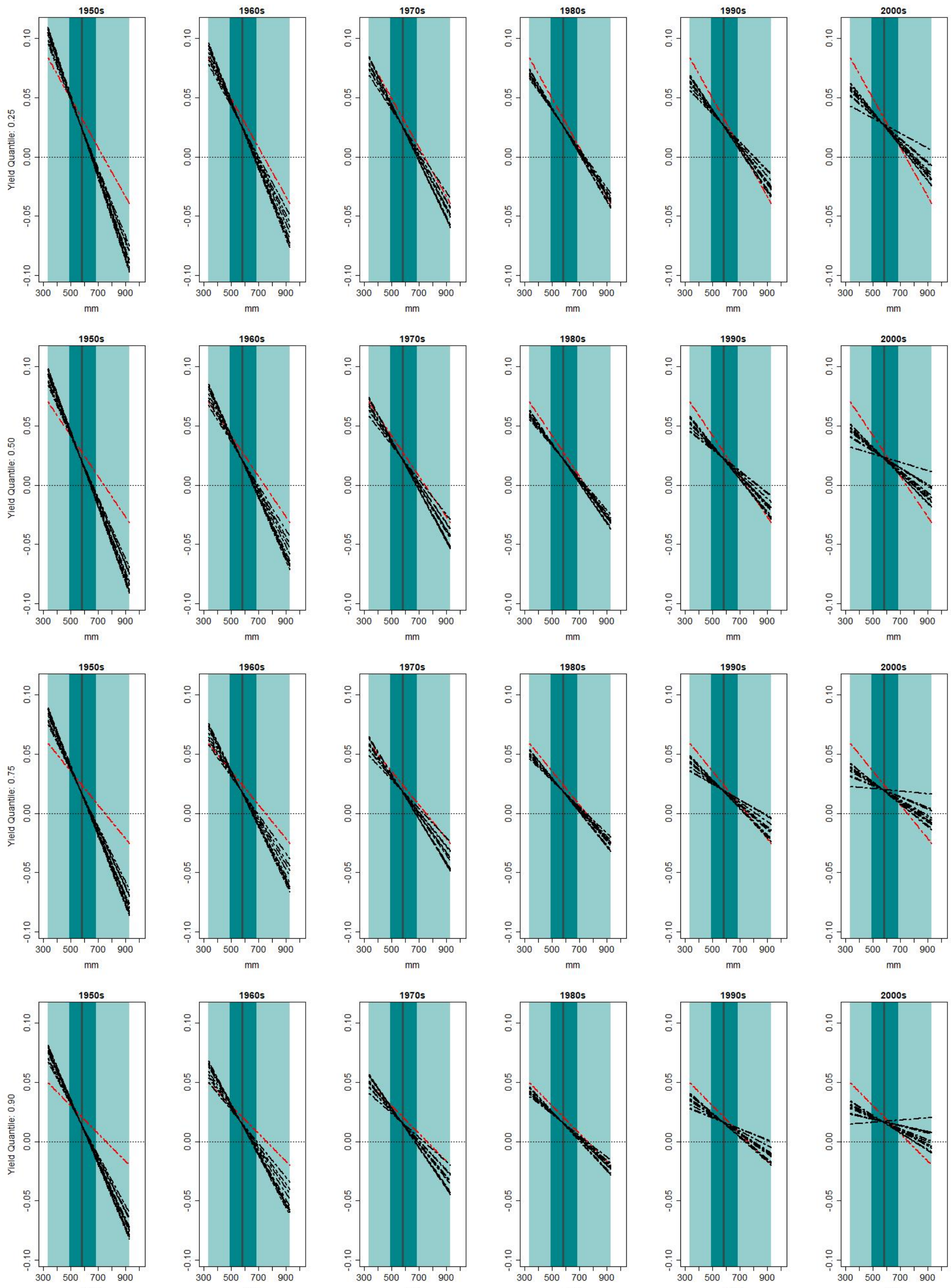

Figure C.3. Marginal-Effect Function Estimates of Total Precipitation for the Soybean Yield (in % per mm)

Note: Dashed black (solid pink) lines correspond to the estimates from a time-varying coefficient (fixed-coefficient) model. Dark (light) shaded areas illustrate the inter-quartile (middle 95%) ranges of total precipitation in each decade.

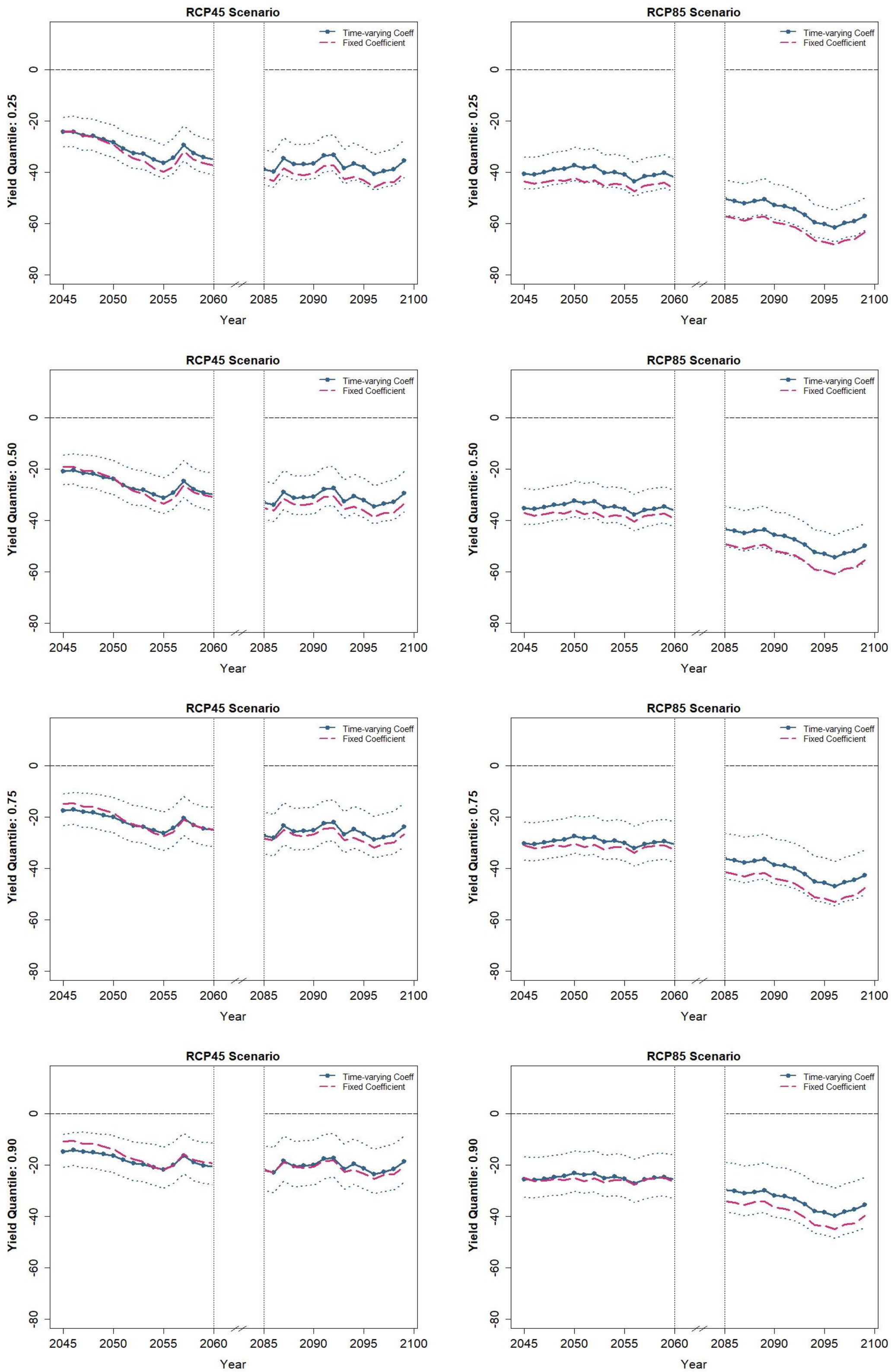

Figure C.4. Rolling-Window Average Soybean Yield Decline Predictions using the HadGEM2-ES365 Forecasts with Two-Sided 95% Confidence Intervals (in %)

Note: Solid blue lines correspond to the estimates from our time-varying coefficient model. The dotted blue lines depict the 95% confidence intervals. Dashed pink lines correspond to the estimates from a fixed-coefficient model.

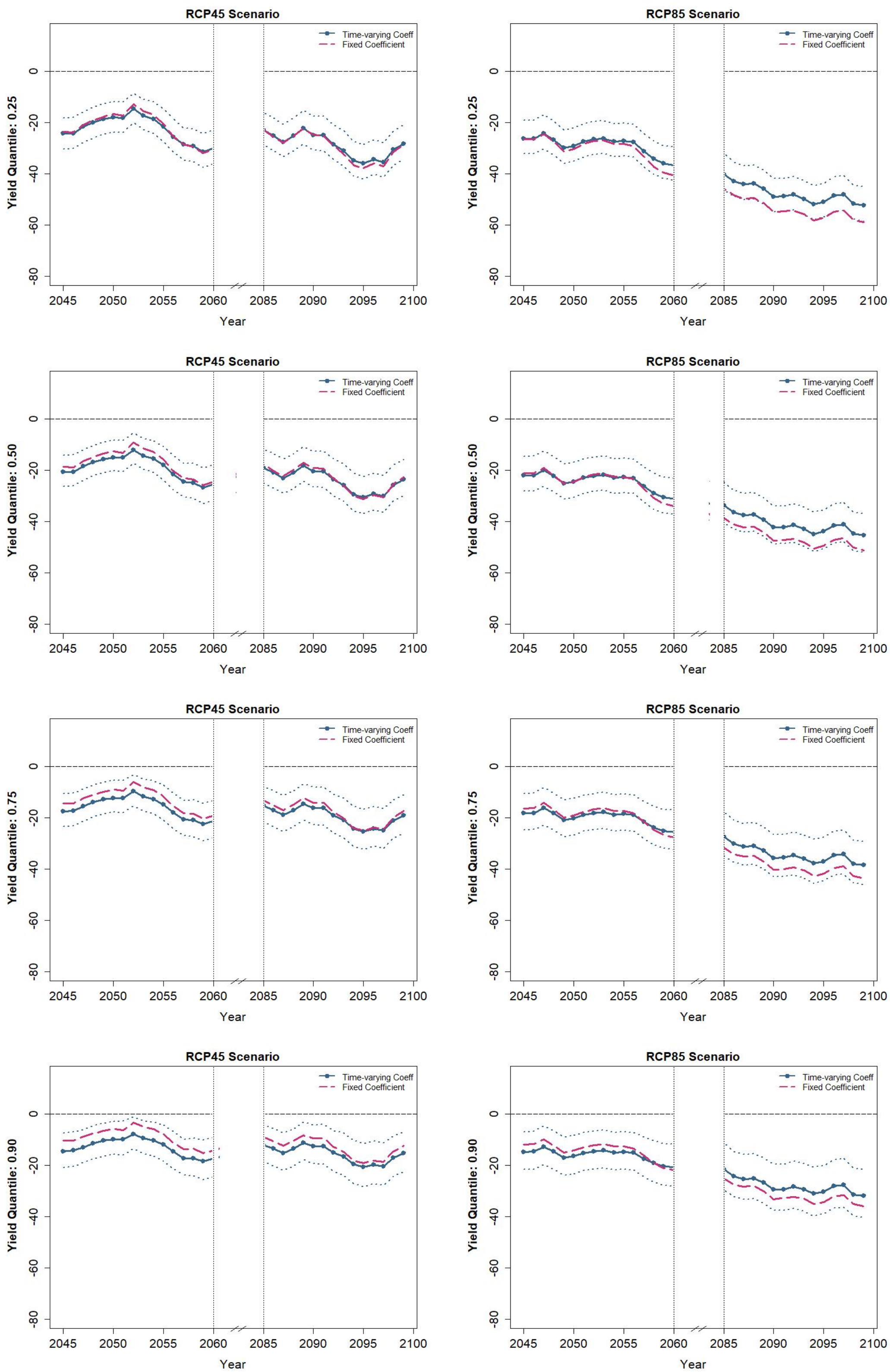

Figure C.5. Rolling-Window Average Soybean Yield Decline Predictions using the NorESM1-M Forecasts with Two-Sided 95% Confidence Intervals (in %)

Note: Solid blue lines correspond to the estimates from our time-varying coefficient model. The dotted blue lines depict the 95% confidence intervals. Dashed pink lines correspond to the estimates from a fixed-coefficient model.

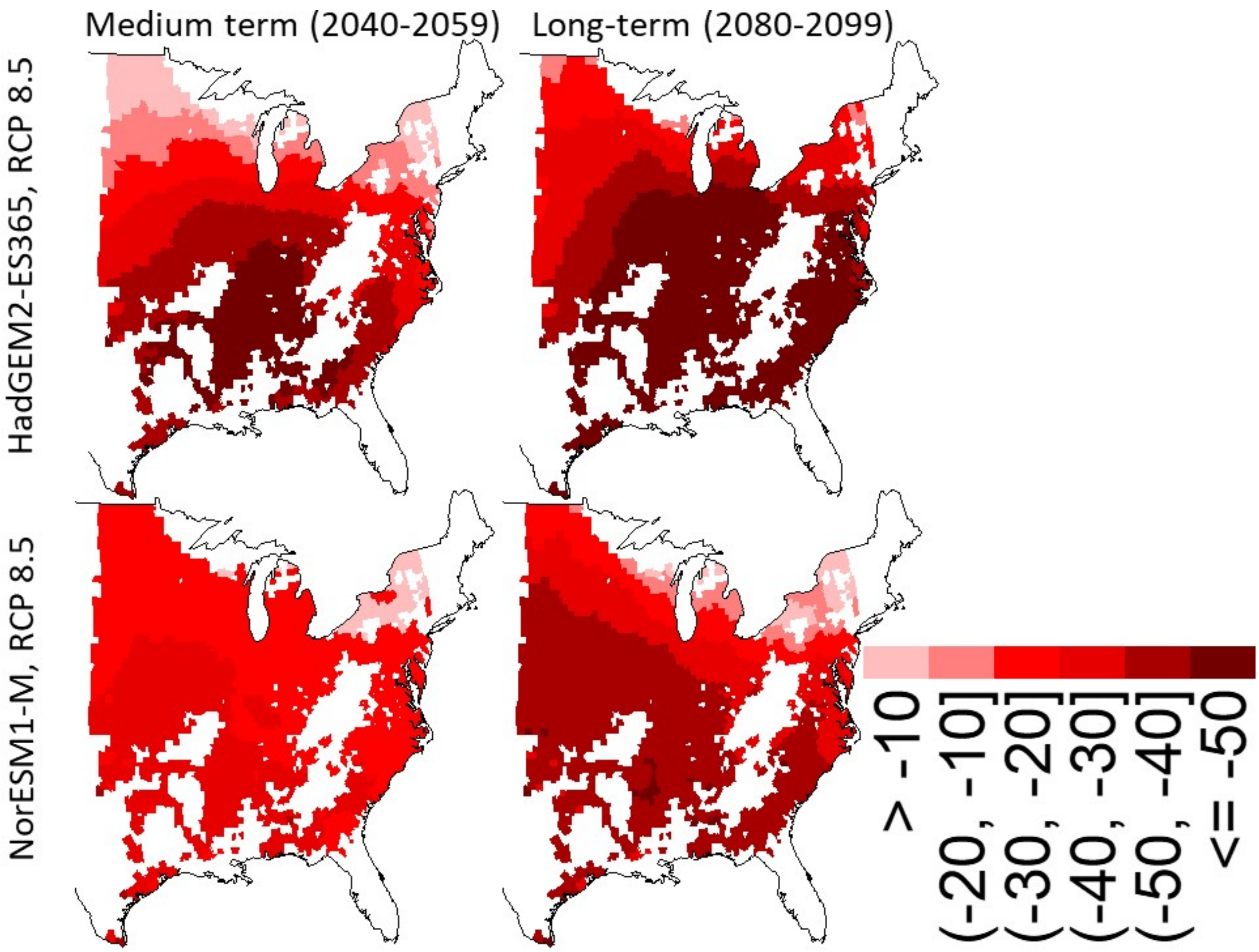

Figure C.6. Geographical Configuration of Climate Change Effect on Soybean Yields (in %)
Note: Negative values indicate yield reduction. Maps are based on the time-varying-coefficient median regression. Climate change scenario considered is RCP8.5.

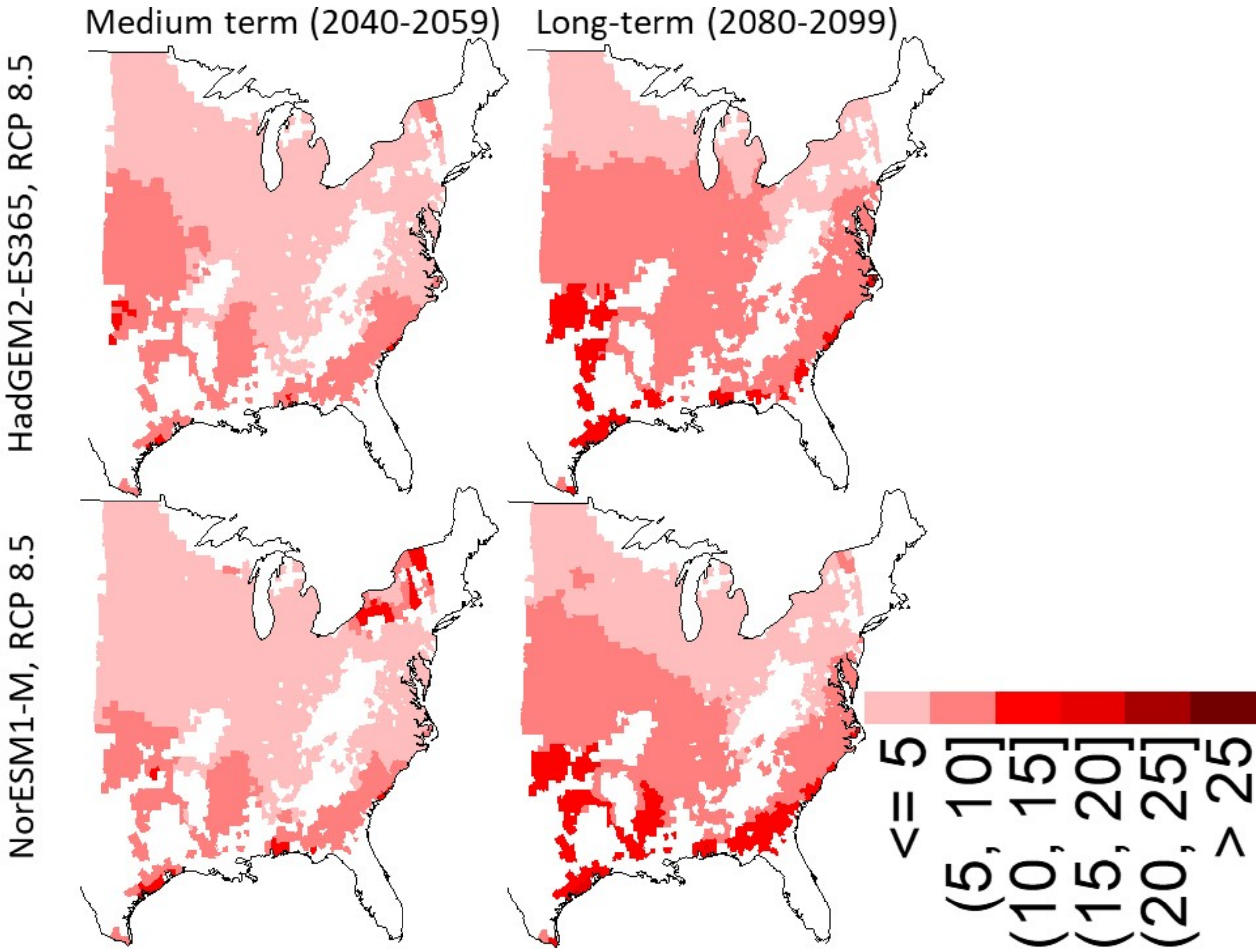

Figure C.7. Spatial Differences in Soybean Yield Decline Projections between the Time-Varying-Coefficient and Fixed-Coefficient Models (in percentage point)

Note: The difference is calculated by using the absolute value of reductions projected by the fixed-coefficient models minus those projected by the time-varying-coefficient models. The darker the color, the larger the overestimation in yield reduction under the fixed-coefficient model. Maps are based on the median regression and climate change scenario considered is RCP8.5.

D Results for the Fixed-Coefficient Models

This appendix reports parameter point estimates for fixed-coefficient models (i.e., a model with the additive linear time trend and another with both the linear and quadratic time trends), followed by the summary of future yield change projections estimated using these parameter estimates, for both the corn and soybeans.

Table D.1. Fixed Slope Coefficient Estimates for the Corn Yield (model with the additive linear time trend)

	Yield Quantiles			
Variable	**0.25th**	**0.50th**	**0.75th**	**0.90th**
Total $GDD_{8-29°C}$	0.1592	0.1396	0.123	0.11
	(0.0656, 0.25)	(0.0445, 0.2409)	(0.0268, 0.236)	(0.0124, 0.2355)
Total $GDD_{8-29°C}$ sq. ($\times 10^{-3}$)	–0.0284	–0.0246	–0.0214	–0.0189
	(–0.0482, –0.0072)	(–0.0449, –0.0036)	(–0.0444, –5e-04)	(–0.0434, 0.0028)
Total $GDD_{29°C+}$ (square root)	–11.0589	–9.3057	–7.8146	–6.6519
	(–13.1006, –8.2733)	(–11.3834, –6.8271)	(–10.0965, –5.6209)	(–9.2836, –4.4336)
Total Precipitation	0.1242	0.0954	0.0709	0.0518
	(0.0613, 0.1966)	(0.037, 0.1647)	(0.0142, 0.1325)	(–0.0033, 0.1136)
Total Precipitation sq. ($\times 10^{-3}$)	–0.099	–0.0756	–0.0556	–0.0401
	(–0.1494, –0.0592)	(–0.1226, –0.0376)	(–0.0984, –0.0164)	(–0.0821, –0.0015)
Average Wind Speed	–6.0665	–5.3883	–4.8115	–4.3618
	(–20.7075, 6.0915)	(–19.7165, 6.5079)	(–18.9406, 6.775)	(–18.5912, 6.9714)
Average Humidity ($\times 10^{3}$)	–0.0935	–0.0291	0.0256	0.0683
	(–7.0673, 7.4991)	(–7.4313, 7.8048)	(–7.7018, 8.5507)	(–8.3052, 8.6598)
Average Long-Wave Radiation	–0.1188	–0.1824	–0.2365	–0.2786
	(–0.7651, 0.5327)	(–0.806, 0.4671)	(–0.8347, 0.4164)	(–0.849, 0.3834)
Average Short-Wave Radiation	–0.0023	0.0445	0.0843	0.1154
	(–0.4748, 0.4022)	(–0.4046, 0.4078)	(–0.3396, 0.435)	(–0.2863, 0.4713)
Average Surface Pressure	0.5622	0.2112	–0.0873	–0.3201
	(–1.2486, 2.6819)	(–1.4515, 2.2878)	(–1.6793, 1.882)	(–1.959, 1.6435)
Time trend	2.1093	2.1383	2.1629	2.1822
	(1.7352, 2.6013)	(1.7178, 2.6546)	(1.701, 2.6984)	(1.6916, 2.7333)

Note: Reported are the point estimates of parameters from a fixed-coefficient model along with the corresponding two-sided 95% bias-corrected accelerated percentile confidence intervals in parentheses. Estimates are measured in % of yield per unit in the corresponding regressor.

Table D.2. Fixed Slope Coefficient Estimates for the Corn Yield (model with both the additive linear and quadratic time trends)

	Yield Quantiles			
Variable	**0.25th**	**0.50th**	**0.75th**	**0.90th**
Total $\text{GDD}_{8-29^{\circ}\text{C}}$	0.1531	0.1328	0.1154	0.0974
	(0.0602, 0.2388)	(0.039, 0.2302)	(0.0153, 0.2141)	(–0.0094, 0.1974)
Total $\text{GDD}_{8-29^{\circ}\text{C}}$ sq. ($\times 10^{-3}$)	–0.0242	–0.0208	–0.0178	–0.0148
	(–0.0423, –0.0028)	(–0.0399, –2e-04)	(–0.0394, 0.0025)	(–0.0366, 0.006)
Total $\text{GDD}_{29^{\circ}\text{C}+}$ (square root)	–10.4379	–9.024	–7.8071	–6.548
	(–12.3278, –7.3703)	(–11.0442, –6.5548)	(–10.0947, –5.7186)	(–9.0538, –4.5164)
Total Precipitation	0.1106	0.099	0.089	0.0787
	(0.039, 0.1689)	(0.0421, 0.1711)	(0.0421, 0.1596)	(0.0468, 0.1426)
Total Precipitation sq. ($\times 10^{-3}$)	–0.0906	–0.0791	–0.0691	–0.0588
	(–0.1339, –0.0425)	(–0.127, –0.0408)	(–0.1139, –0.0382)	(–0.0988, –0.033)
Average Wind Speed	–10.7579	–10.0598	–9.459	–8.8374
	(–24.933, 0.9741)	(–23.9422, 1.7707)	(–23.2699, 2.5547)	(–22.4686, 3.0641)
Average Humidity ($\times 10^{3}$)	–1.6469	–1.0384	–0.5147	0.0272
	(–9.3638, 5.907)	(–8.9393, 6.9767)	(–8.5915, 8.4018)	(–8.0495, 9.509)
Average Long-Wave Radiation	–0.097	–0.1661	–0.2255	–0.2871
	(–0.7317, 0.5731)	(–0.7931, 0.4917)	(–0.8262, 0.4262)	(–0.9007, 0.3606)
Average Short-Wave Radiation	–0.2134	–0.1526	–0.1003	–0.0462
	(–0.6203, 0.1422)	(–0.5446, 0.189)	(–0.5026, 0.2296)	(–0.4714, 0.2973)
Average Surface Pressure	0.4637	0.1653	–0.0916	–0.3574
	(–1.361, 2.5929)	(–1.5019, 2.222)	(–1.6835, 1.9413)	(–2.0601, 1.4712)
Time Trend	4.5404	3.1873	2.0229	0.818
	(4.0852, 6.512)	(1.468, 4.4465)	(0.951, 2.2454)	(0.644, 0.6504)
Time Trend sq.	–0.0367	–0.0166	7.00E–04	0.0185
	(–0.062, –0.0321)	(–0.0323, 0.0076)	(–0.0032, 0.0118)	(0.0184, 0.0185)

Note: Reported are the point estimates of parameters from a fixed-coefficient model along with the corresponding two-sided 95% bias-corrected accelerated percentile confidence intervals in parentheses. Estimates are measured in % of yield per unit in the corresponding regressor.

Table D.3. Fixed Slope Coefficient Estimates for the Soybean Yield (model with the additive linear time trend)

	Yield Quantiles			
Variable	**0.25th**	**0.50th**	**0.75th**	**0.90th**
Total $GDD_{8-30°C}$	0.1798	0.1584	0.1406	0.1254
	(0.121, 0.2358)	(0.0997, 0.2147)	(0.0824, 0.1977)	(0.0673, 0.1833)
Total $GDD_{8-30°C}$ sq. ($\times 10^{-3}$)	–0.0383	–0.0329	–0.0284	–0.0245
	(–0.0501, –0.0262)	(–0.0446, –0.0204)	(–0.0396, –0.0157)	(–0.0357, –0.0117)
Total $GDD_{30°C+}$ (square root)	–8.5847	–7.2534	–6.1405	–5.1961
	(–9.8881, –7.2057)	(–8.548, –5.9549)	(–7.4173, –4.8467)	(–6.4713, –3.9442)
Total Precipitation	0.1533	0.1281	0.1069	0.089
	(0.1087, 0.2077)	(0.0873, 0.18)	(0.0681, 0.1534)	(0.0503, 0.1322)
Total Precipitation sq. ($\times 10^{-3}$)	–0.1037	–0.086	–0.0712	–0.0586
	(–0.1424, –0.0744)	(–0.1197, –0.0579)	(–0.1019, –0.0444)	(–0.0868, –0.0328)
Average Wind Speed	–15.0287	–15.5673	–16.0175	–16.3996
	(–24.6531, –5.9577)	(–25.0466, –6.7137)	(–25.358, –7.4754)	(–25.6639, –8.0643)
Average Humidity ($\times 10^{3}$)	1.4703	1.2327	1.0342	0.8656
	(–2.8661, 5.4568)	(–3.2443, 5.126)	(–3.7017, 4.9697)	(–3.9182, 4.8407)
Average Long-Wave Radiation	0.353	0.2858	0.2296	0.1819
	(–0.0823, 0.7078)	(–0.1283, 0.6524)	(–0.1662, 0.6017)	(–0.1974, 0.5697)
Average Short-Wave Radiation	0.3904	0.357	0.3291	0.3054
	(0.1394, 0.624)	(0.1188, 0.5803)	(0.1133, 0.5479)	(0.0907, 0.5161)
Average Surface Pressure	–1.7979	–2.5219	–3.1271	–3.6406
	(–3.1248, –0.0238)	(–3.7687, –0.8064)	(–4.2855, –1.4536)	(–4.7519, –1.9895)
Time Trend	1.2706	1.2818	1.2912	1.2992
	(1.0216, 1.5918)	(1.0282, 1.5932)	(1.0338, 1.5949)	(1.037, 1.5943)

Note: Reported are the point estimates of parameters from a fixed-coefficient model along with the corresponding two-sided 95% bias-corrected accelerated percentile confidence intervals in parentheses. Estimates are measured in % of yield per unit in the corresponding regressor.

Table D.4. Fixed Slope Coefficient Estimates for the Soybean Yield (model with both the additive linear and quadratic time trends)

	Yield Quantiles			
Variable	**0.25th**	**0.50th**	**0.75th**	**0.90th**
Total $GDD_{8-30^\circ C}$	0.1747	0.1602	0.1479	0.1353
	(0.1153, 0.2226)	(0.1036, 0.2182)	(0.0927, 0.2116)	(0.0869, 0.2021)
Total $GDD_{8-30^\circ C}$ sq. ($\times 10^{-3}$)	–0.0358	–0.0325	–0.0297	–0.0269
	(–0.0457, –0.0215)	(–0.0445, –0.0205)	(–0.0412, –0.0188)	(–0.0427, –0.0179)
Total $GDD_{30^\circ C+}$ (square root)	–8.0247	–7.2765	–6.6397	–5.9936
	(–8.9524, –6.2999)	(–8.533, –5.9482)	(–8.3036, –5.7021)	(–7.4688, –5.4469)
Total Precipitation	0.1501	0.1296	0.1121	0.0943
	(0.0992, 0.198)	(0.0882, 0.182)	(0.0738, 0.1628)	(0.0598, 0.1457)
Total Precipitation sq. ($\times 10^{-3}$)	–0.1024	–0.0874	–0.0747	–0.0617
	(–0.1366, –0.0718)	(–0.1218, –0.0589)	(–0.1088, –0.0503)	(–0.0933, –0.0395)
Average Wind Speed	–17.8952	–16.8763	–16.009	–15.1292
	(–28.852, –10.1969)	(–26.5812, –8.1587)	(–24.4542, –6.072)	(–21.5541, –5.1948)
Average Humidity ($\times 10^{3}$)	0.3851	0.8618	1.2676	1.6793
	(–5.2285, 4.1686)	(–3.8206, 5.3455)	(–3.2015, 6.1943)	(–2.4151, 7.1355)
Average Long-Wave Radiation	0.3978	0.2798	0.1794	0.0776
	(0.0255, 0.7826)	(–0.1409, 0.6454)	(–0.2985, 0.4999)	(–0.436, 0.3553)
Average Short-Wave Radiation	0.2952	0.2852	0.2767	0.2681
	(0.101, 0.4792)	(0.0852, 0.464)	(0.0749, 0.4514)	(0.0682, 0.4395)
Average Surface Pressure	–1.9963	–2.6006	–3.1149	–3.6367
	(–3.3326, –0.1985)	(–3.7963, –0.8442)	(–4.1645, –1.4935)	(–4.6947, –2.0066)
Time Trend	2.5276	1.5908	0.7934	–0.0154
	(2.0429, 3.7071)	(0.6778, 2.5877)	(0.1438, 1.0205)	(–0.092, –0.0911)
Time Trend sq.	–0.0186	–0.0048	0.0069	0.0188
	(–0.0288, –0.014)	(–0.0163, 0.0068)	(0.004, 0.0125)	(0.0187, 0.0188)

Note: Reported are the point estimates of parameters from a fixed-coefficient model along with the corresponding two-sided 95% bias-corrected accelerated percentile confidence intervals in parentheses. Estimates are measured in % of yield per unit in the corresponding regressor.

Table D.5. Fixed-Slope-Coefficients-Based Corn Yield Change Predictions (model with the additive linear time trend)

	RCP45 Scenario				*RCP85 Scenario*			
Horizon	0.25th Quant.	0.50th Quant.	0.75th Quant.	0.90th Quant.	0.25th Quant.	0.50th Quant.	0.75th Quant.	0.90th Quant.
				HadGEM2-ES365 Forecasts				
2040–2049	–33.5	–28.5	–23.9	–20	–49.9	–43.7	–37.6	–32.3
	(–47.1, –11.9)	(–44.9, –7.3)	(–41.2, –1.3)	(–38.1, 3.8)	(–64.2, –30)	(–59.4, –21.2)	(–54.8, –13.1)	(–50.7, –6)
2050–2059	–44.8	–38.9	–33.2	–28.2	–51.6	–45.2	–38.9	–33.4
	(–57.7, –22.3)	(–54.9, –16.3)	(–50.6, –8.5)	(–46.8, –2)	(–65.4, –31)	(–60.6, –22.3)	(–55.9, –13.9)	(–51.9, –6.9)
2040–2059	–39.2	–33.7	–28.5	–24.1	–50.8	–44.4	–38.2	–32.8
	(–52.1, –16.9)	(–49.7, –11.7)	(–45.7, –4.9)	(–42.3,0.6)	(–63.7, –28.8)	(–59.9, –22)	(–55.3, –13.5)	(–51.3, –6.2)
2080–2089	–50.6	–44.1	–37.7	–32.1	–66.3	–59.4	–52.2	–45.7
	(–63.4, –26.8)	(–60.6, –20.3)	(–55.5, –11.5)	(–50.9, –3.9)	(–78.6, –45.6)	(–73.8, –36.2)	(–69.1, –25.8)	(–64.6, –17)
2090–2099	–48.9	–42.3	–36	–30.6	–72.3	–65.6	–58.5	–51.8
	(–62.9, –24.3)	(–59.5, –16.4)	(–54.8, –7.8)	(–50.6, –0.8)	(–83.2, –53)	(–78.7, –43.4)	(–74.1, –32.7)	(–69.7, –23.2)
2080–2099	–49.7	–43.2	–36.9	–31.4	–69.3	–62.5	–55.3	–48.8
	(–63, –25.6)	(–60, –18.1)	(–55.2, –9.6)	(–51, –2)	(–79.7, –47.9)	(–76.2, –39.8)	(–71.7, –29.3)	(–67.1, –20.1)
				NorESM1-M Forecasts				
2040–2049	–29.9	–25.4	–21.2	–17.7	–38.1	–32.5	–27.2	–22.8
	(–44, –7.8)	(–42.2, –4.1)	(–39, 1.7)	(–36.2, 6.1)	(–52.8, –14.2)	(–49.9, –8.4)	(–45.9, –2)	(–42.7, 3.6)
2050–2059	–35.6	–30.3	–25.4	–21.3	–43	–36.9	–31.2	–26.3
	(–50.3, –13.1)	(–47.6, –7.5)	(–44.1, –0.7)	(–40.8, 4.7)	(–56.8, –18.9)	(–53.5, –12.8)	(–49.1, –5.4)	(–45.4, 0.6)
2040–2059	–32.7	–27.9	–23.3	–19.5	–40.5	–34.7	–29.2	–24.5
	(–46.9, –10.2)	(–44.9, –5.8)	(–41.5, 0.7)	(–38.5, 5.3)	(–54.7, –16.7)	(–51.7, –10.6)	(–47.5, –3.8)	(–43.9, 1.9)
2080–2089	–33.6	–28.4	–23.5	–19.5	–55.7	–48.7	–41.8	–35.8
	(–47.7, –10.1)	(–45.8, –5.3)	(–42.1, 1)	(–39, 6.1)	(–69, –30.8)	(–65.1, –21.9)	(–60.1, –12.6)	(–55.8, –4.7)
2090–2099	–43.6	–37.5	–31.7	–26.7	–67.9	–60.8	–53.6	–46.9
	(–57.3, –18.9)	(–54.4, –12.5)	(–50.1, –4.5)	(–46.4, 1.7)	(–78.7, –45.7)	(–75.1, –37.1)	(–69.7, –26.8)	(–65.2, –17.6)
2080–2099	–38.6	–32.9	–27.6	–23.1	–61.8	–54.8	–47.7	–41.3
	(–52.6, –14.7)	(–50, –8.9)	(–46, –1.7)	(–42.5, 3.7)	(–74, –38)	(–70, –29.6)	(–65, –19.6)	(–60.2, –11.2)

Note: Reported are the aggregate averages of point estimates of county-level yield declines predicted using future climate forecasts and using the parameter estimates from a fixed-coefficient model. The average is weighted by the average 2001-2010 county-level acreage for the crop in question. Two-sided 95% bias-corrected percentile confidence intervals are in parentheses. The reported estimates are measured in % of yield.

Table D.6. Fixed-Slope-Coefficients-Based Corn Yield Change Predictions (model with both the additive linear and quadratic time trends)

	RCP45 Scenario				*RCP85 Scenario*			
Horizon	0.25th Quant.	0.50th Quant.	0.75th Quant.	0.90th Quant.	0.25th Quant.	0.50th Quant.	0.75th Quant.	0.90th Quant.
				HadGEM2-ES365 Forecasts				
2040–2049	–27.7	–24.5	–21.6	–18.4	–43.6	–39.4	–35.4	–31
	(–42.7, –4.5)	(–42.6, –0.7)	(–39, 5.3)	(–35.8, 10.6)	(–61.2, –21.8)	(–56.7, –13.1)	(–52.3, –4.1)	(–48.1, 3.2)
2050–2059	–38.4	–34.3	–30.6	–26.4	–45.5	–40.9	–36.6	–31.8
	(–52.9, –11.3)	(–52, –7.9)	(–47.8, 0.6)	(–43.9, 7)	(–62.9, –23.1)	(–58.1, –14.4)	(–53.2, –5.2)	(–48.8, 3.6)
2040–2059	–33	–29.4	–26.1	–22.4	–44.5	–40.1	–36	–31.4
	(–47.7, –8.3)	(–47.2, –4.3)	(–43.3, 2.9)	(–39.8, 8.6)	(–59.3, –18.2)	(–57.3, –13.6)	(–52.8, –4.4)	(–48.3, 3.4)
2080–2089	–44	–39.2	–34.8	–29.7	–60.4	–54.7	–49.2	–42.7
	(–58.4, –12.5)	(–56.5, –12.5)	(–51.7, –3)	(–47, 5.2)	(–75, –39.1)	(–69.7, –29)	(–64.2, –17.8)	(–58.4, –7.4)
2090–2099	–42	–37.4	–33.1	–28.3	–66.7	–61.2	–55.6	–48.9
	(–57.6, –10.1)	(–55.7, –8.8)	(–51.1, 0.7)	(–46.7, 9)	(–79.9, –46.6)	(–75, –35.7)	(–69.5, –24)	(–63.9, –12.8)
2080–2099	–43	–38.3	–33.9	–29	–63.5	–58	–52.4	–45.8
	(–58.1, –11.7)	(–56.1, –10.7)	(–51.4, –0.9)	(–46.9, 7.3)	(–75.3, –36.5)	(–72.4, –32.3)	(–66.9, –20.8)	(–61.1, –10.1)
				NorESM1-M Forecasts				
2040–2049	–24	–21.3	–18.8	–16.1	–32.2	–28.5	–25.2	–21.5
	(–39.3, –0.6)	(–39.8, 2.4)	(–36.7, 8.2)	(–34, 13.2)	(–48.8, –6.4)	(–47.4, –1.6)	(–43.4, 5.8)	(–39.9, 12.6)
2050–2059	–29.8	–26.5	–23.5	–20.2	–37.1	–32.9	–29	–24.8
	(–45.6, –5)	(–45.4, –1)	(–41.8, 5.7)	(–38.6, 12.7)	(–52.8, –10.2)	(–50.9, –6.4)	(–46.5, 1.9)	(–42.7, 9.7)
2040–2059	–26.9	–23.9	–21.1	–18.1	–34.6	–30.7	–27.1	–23.1
	(–42.6, –2.9)	(–42.7, 0.6)	(–39.3, 7)	(–36.4, 12.6)	(–50.8, –8.7)	(–49.1, –4.2)	(–44.8,4.1)	(–41.2, 11.3)
2080–2089	–27.8	–24.3	–21.2	–17.8	–49.6	–44.4	–39.5	–33.9
	(–43.8, –2)	(–43.2, 1.4)	(–39.4, 8.5)	(–36.1, 14)	(–64.9, –20.8)	(–62, –16.6)	(–56.8, –6.2)	(–51.7, 3.7)
2090–2099	–37.5	–33.3	–29.4	–25	–62.6	–57	–51.4	–44.9
	(–53.6, –10.5)	(–51.9, –6)	(–47.4, 2.7)	(–43.5, 10.7)	(–75.1, –34.6)	(–72.1, –31.1)	(–66.3, –20.3)	(–61.1, –8.5)
2080–2099	–32.6	–28.8	–25.3	–21.4	–56.1	–50.7	–45.5	–39.4
	(–48.7, –6.2)	(–47.5, –2.3)	(–43.6, 5.7)	(–39.9, 12.2)	(–70.1, –27.9)	(–67, –23.6)	(–61.7, –12.9)	(–56.5, –2.6)

Note: Reported are the aggregate averages of point estimates of county-level yield declines predicted using future climate forecasts and using the parameter estimates from a fixed-coefficient model. The average is weighted by the average 2001-2010 county-level acreage for the crop in question. Two-sided 95% bias-corrected percentile confidence intervals are in parentheses. The reported estimates are measured in % of yield.

Table D.7. Fixed-Slope-Coefficients-Based Soybean Yield Change Predictions (model with the additive linear time trend)

	RCP45 Scenario				*RCP85 Scenario*			
Horizon	0.25th Quant.	0.50th Quant.	0.75th Quant.	0.90th Quant.	0.25th Quant.	0.50th Quant.	0.75th Quant.	0.90th Quant.
				HadGEM2-ES365 Forecasts				
2040–2049	–25.3	–20.2	–15.6	–11.3	–43.9	–37.5	–31.4	–25.7
	(–35.8, –11.3)	(–32.3, –7.6)	(–28, –2.3)	(–24.2, 2.7)	(–54.3, –32.2)	(–48.9, –24.5)	(–43.8, –17.5)	(–38.9, –10.8)
2050–2059	–37.3	–31.1	–25.3	–19.8	–44.6	–37.9	–31.5	–25.5
	(–47.4, –24.2)	(–43.3, –18.1)	(–38.5, –11.1)	(–33.8, –4.8)	(–55.4, –32.3)	(–49.8, –24.3)	(–44.2, –16.8)	(–39.1, –9.8)
2040–2059	–31.3	–25.6	–20.4	–15.6	–44.2	–37.7	–31.5	–25.6
	(–41.5, –17.9)	(–37.9, –13.1)	(–33.3, –6.6)	(–29, –1)	(–54, –31.8)	(–49.4, –24.3)	(–44.1, –17.1)	(–39, –10.3)
2080–2089	–41.4	–34.2	–27.5	–21.2	–58	–50.2	–42.4	–34.8
	(–52.3, –27.7)	(–46.7, –19.8)	(–41, –11.8)	(–35.6, –4)	(–67.4, –46.2)	(–61.1, –36.7)	(–54.7, –27.1)	(–48.2, –17.9)
2090–2099	–40.5	–33.6	–27	–20.9	–64.6	–56.9	–49	–41.1
	(–51.6, –26.6)	(–46.2, –18.9)	(–40.6, –11.3)	(–35.4, –4.2)	(–73.1, –53.4)	(–67, –43.8)	(–60.6, –33.9)	(–53.9, –24)
2080–2099	–40.9	–33.9	–27.3	–21.1	–61.3	–53.5	–45.7	–38
	(–51.9, –27.1)	(–46.4, –19.3)	(–40.8, –11.4)	(–35.5, –4.2)	(–70.1, –49.2)	(–64.1, –40.2)	(–57.7, –30.5)	(–51.1, –21)
				NorESM1-M Forecasts				
2040–2049	–21.9	–17.2	–13.1	–9.3	–28.6	–23	–17.9	–13.2
	(–32.5, –7.5)	(–29.4, –4.2)	(–25.6, 0.5)	(–22.2, 5.1)	(–39.7, –13.6)	(–35.6, –8.6)	(–31, –2.6)	(–27.1, 2.7)
2050–2059	–26.1	–20.9	–16.1	–11.7	–33.2	–27.1	–21.5	–16.3
	(–36.8, –10.8)	(–33.4, –7.3)	(–29.2, –1.5)	(–25.5, 3.6)	(–44, –19.5)	(–39.6, –13.2)	(–34.7, –6.7)	(–30.2, –0.7)
2040–2059	–24	–19.1	–14.6	–10.5	–30.9	–25	–19.7	–14.7
	(–34.5, –8.7)	(–31.4, –6)	(–27.3, –0.4)	(–23.8, 4.2)	(–41.8, –16.6)	(–37.6, –11)	(–32.8, –4.7)	(–28.5, 1)
2080–2089	–23.3	–18.1	–13.3	–8.9	–46.8	–39.5	–32.5	–25.9
	(–34.8, –9.1)	(–30.9, –4.4)	(–26.5, 1.2)	(–22.5, 6.3)	(–57.2, –33.3)	(–51.4, –25.1)	(–45.4, –16.8)	(–39.7, –8.8)
2090–2099	–33.1	–26.8	–21	–15.6	–58.7	–51	–43.3	–35.8
	(–44.2, –18.5)	(–40, –12.5)	(–35, –5.4)	(–30.3, 1)	(–68.1, –46.9)	(–62, –37.5)	(–55.7, –28.1)	(–49.7, –19.1)
2080–2099	–28.2	–22.4	–17.1	–12.3	–52.8	–45.3	–37.9	–30.8
	(–39.4, –13.7)	(–35.4, –8.5)	(–30.6, –2)	(–26.4, 3.6)	(–62.7, –40.2)	(–56.6, –31.4)	(–50.4, –22.7)	(–44.6, –14.1)

Note: Reported are the aggregate averages of point estimates of county-level yield declines predicted using future climate forecasts and using the parameter estimates from a fixed-coefficient model. The average is weighted by the average 2001-2010 county-level acreage for the crop in question. Two-sided 95% bias-corrected percentile confidence intervals are in parentheses. The reported estimates are measured in % of yield.

Table D.8. Fixed-Coefficients-Based Soybean Yield Change Predictions (model with both the additive linear and quadratic time trends)

	RCP45 Scenario				*RCP85 Scenario*			
Horizon	0.25th Quant.	0.50th Quant.	0.75th Quant.	0.90th Quant.	0.25th Quant.	0.50th Quant.	0.75th Quant.	0.90th Quant.
HadGEM2-ES365 Forecasts								
2040–2049	–20.6	–19	–17.7	–16.2	–39	–36.3	–34	–31.4
	(–30.3,0.1)	(–30.7, –4)	(–26.6, 1.3)	(–23.1, 6)	(–52.3, –29.4)	(–47.2, –21.7)	(–42.2, –14.3)	(–37.7, –7.6)
2050–2059	–32.2	–29.8	–27.7	–25.4	–39.6	–36.7	–34.2	–31.5
	(–41.2, –12)	(–41.3, –14.9)	(–36.6, –7.9)	(–32.3, –1.2)	(–53.4, –29.4)	(–48, –21.3)	(–42.9, –13.5)	(–38, –6.1)
2040–2059	–26.4	–24.4	–22.7	–20.8	–39.3	–36.5	–34.1	–31.4
	(–35.5, –6.1)	(–36, –9.7)	(–31.7, –3.6)	(–27.7, 2.3)	(–47.8, –19.7)	(–47.5, –21.5)	(–42.5, –13.9)	(–37.9, –6.8)
2080–2089	–35.9	–32.9	–30.2	–27.3	–52.8	–49	–45.4	–41.4
	(–44.7, –14.5)	(–45, –17.1)	(–39.6, –8.6)	(–34.6, –0.6)	(–65.9, –43.1)	(–59.5, –33.7)	(–53.3, –24.1)	(–47.2, –14.5)
2090–2099	–35.1	–32.2	–29.6	–26.8	–59.7	–55.7	–52.1	–48
	(–44.3, –13.2)	(–44.4, –15.7)	(–39.1, –7.8)	(–34.2, –0.3)	(–71.8, –50.4)	(–65.7, –40.8)	(–59.5, –30.8)	(–53.3, –20.5)
2080–2099	–35.5	–32.5	–29.9	–27.1	–56.2	–52.4	–48.7	–44.7
	(–44.7, –14)	(–44.7, –16.4)	(–39.4, –8.1)	(–34.4, –0.4)	(–63.6, –36.3)	(–62.6, –37.3)	(–56.3, –27.4)	(–50.3, –17.5)
NorESM1-M Forecasts								
2040–2049	–17.2	–16	–15	–13.9	–23.7	–21.9	–20.2	–18.6
	(–27.3,3.9)	(–28, –0.5)	(–24.3, 4.6)	(–21.1, 8.9)	(–34.5, –2)	(–34.3, –6.2)	(–29.8, 0.1)	(–26.1, 5.9)
2050–2059	–21.3	–19.8	–18.4	–17	–28.3	–26	–24	–21.8
	(–32, 0.5)	(–32.1, –3.4)	(–27.9, 2.1)	(–24.2, 7)	(–37.5, –7.4)	(–37.8, –10.5)	(–33.2, –3.5)	(–28.8, 2.9)
2040–2059	–19.2	–17.9	–16.7	–15.5	–26	–23.9	–22.1	–20.2
	(–29.8, 2)	(–30, –1.9)	(–26.1, 3.4)	(–22.7, 8)	(–35.9, –5)	(–35.9, –8.2)	(–31.6, –1.5)	(–27.4, 4.6)
2080–2089	–18.5	–16.9	–15.5	–14	–41.7	–38.4	–35.4	–32.2
	(–29,2.9)	(–29.1, –1.7)	(–25, 4.2)	(–21.5, 9.5)	(–50.9, –20.3)	(–50, –21.9)	(–44.2, –12.9)	(–38.7, –4.5)
2090–2099	–28	–25.7	–23.7	–21.5	–53.9	–50	–46.5	–42.7
	(–37.9, –5.7)	(–38.1, –9.3)	(–33.3, –1.9)	(–28.9, 4.9)	(–61.9, –32.8)	(–60.5, –34.4)	(–54.3, –24.3)	(–48.3, –14.5)
2080–2099	–23.2	–21.3	–19.6	–17.8	–47.8	–44.2	–41	–37.4
	(–33.5, –1.7)	(–33.6, –5.5)	(–29.2, 1.1)	(–25.3, 7.2)	(–56.6, –26.5)	(–55.2, –28.1)	(–49.2, –18.6)	(–43.5, –9.4)

Note: Reported are the aggregate averages of point estimates of county-level yield declines predicted using future climate forecasts and using the parameter estimates from a fixed-coefficient model. The average is weighted by the average 2001-2010 county-level acreage for the crop in question. Two-sided 95% bias-corrected percentile confidence intervals are in parentheses. The reported estimates are measured in % of yield.

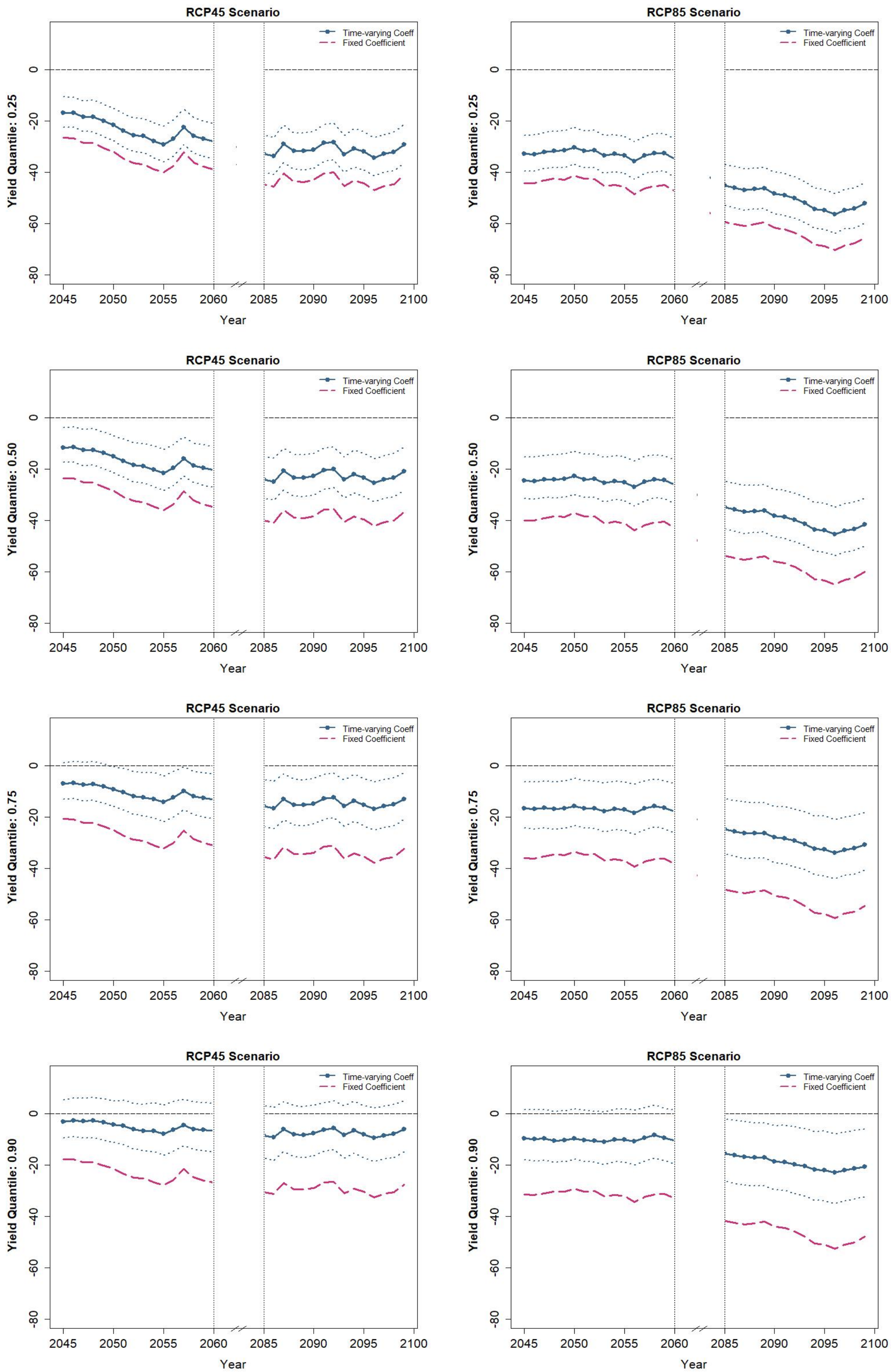

Figure D.1. Rolling-Window Average Corn Yield Decline Predictions using the HadGEM2-ES365 Forecasts with Two-Sided 95% Confidence Intervals (in %) (time-varying coefficient model and fixed-coefficient model with both the additive linear and quadratic time trends)

Note: Solid blue lines correspond to the estimates from our time-varying coefficient model. The dotted blue lines depict the 95% confidence intervals. Dashed pink lines correspond to the estimates from a fixed-coefficient model with both the additive linear and quadratic time trends.

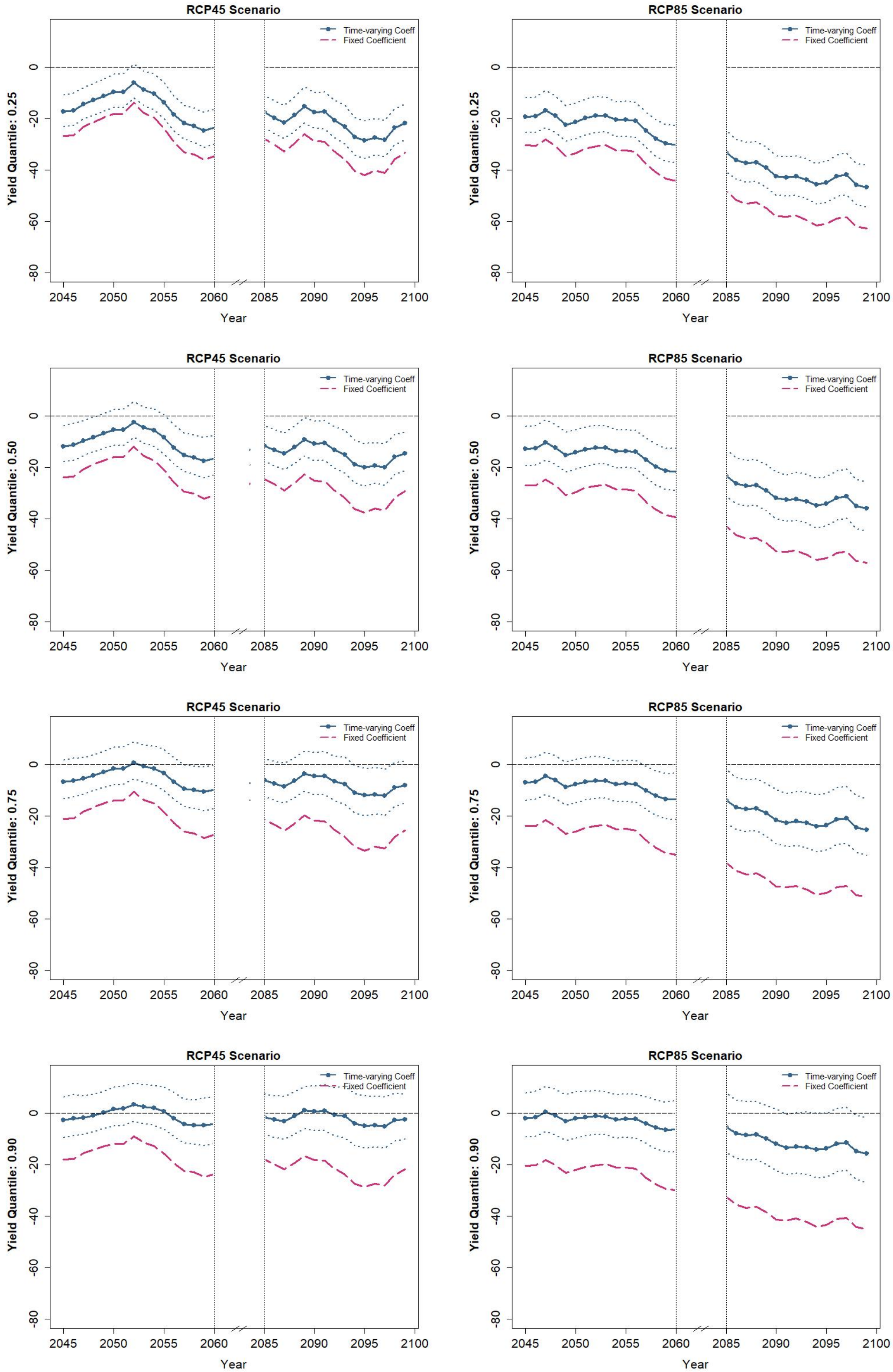

Figure D.2. Rolling-Window Average Corn Yield Decline Predictions using the NorESM1-M Forecasts with Two-Sided 95% Confidence Intervals (in %) (time-varying coefficient model and fixed-coefficient model with both the additive linear and quadratic time trends)

Note: Solid blue lines correspond to the estimates from our time-varying coefficient model. The dotted blue lines depict the 95% confidence intervals. Dashed pink lines correspond to the estimates from a fixed-coefficient model with both the additive linear and quadratic time trends.

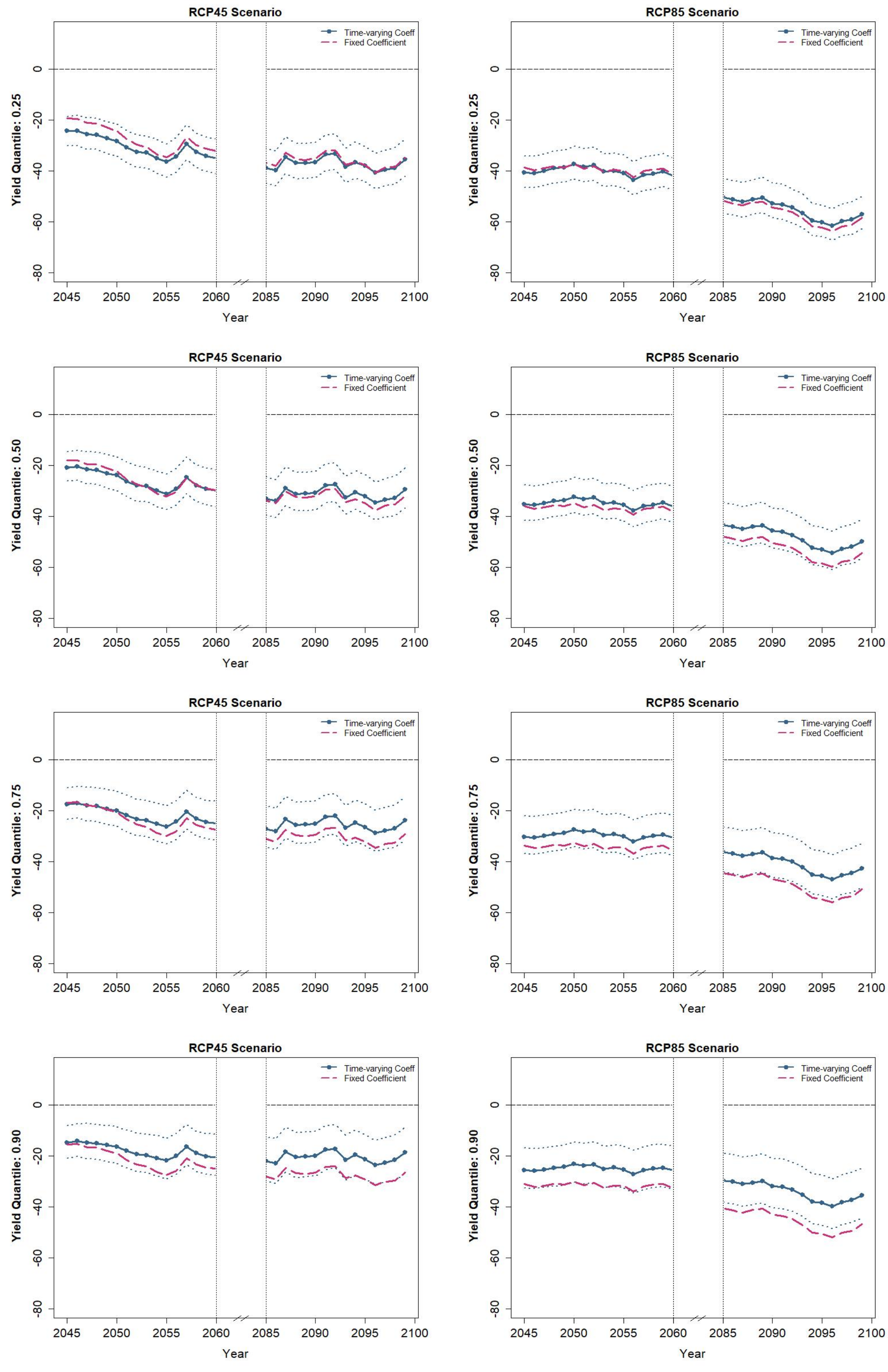

Figure D.3. Rolling-Window Average Soybean Yield Decline Predictions using the HadGEM-2-ES365 Forecasts with Two-Sided 95% Confidence Intervals (in %) (time-varying coefficient model and fixed-coefficient model with both the additive linear and quadratic time trends)

Note: Solid blue lines correspond to the estimates from our time-varying coefficient model. The dotted blue lines depict the 95% confidence intervals. Dashed pink lines correspond to the estimates from a fixed-coefficient model with both the additive linear and quadratic time trends.

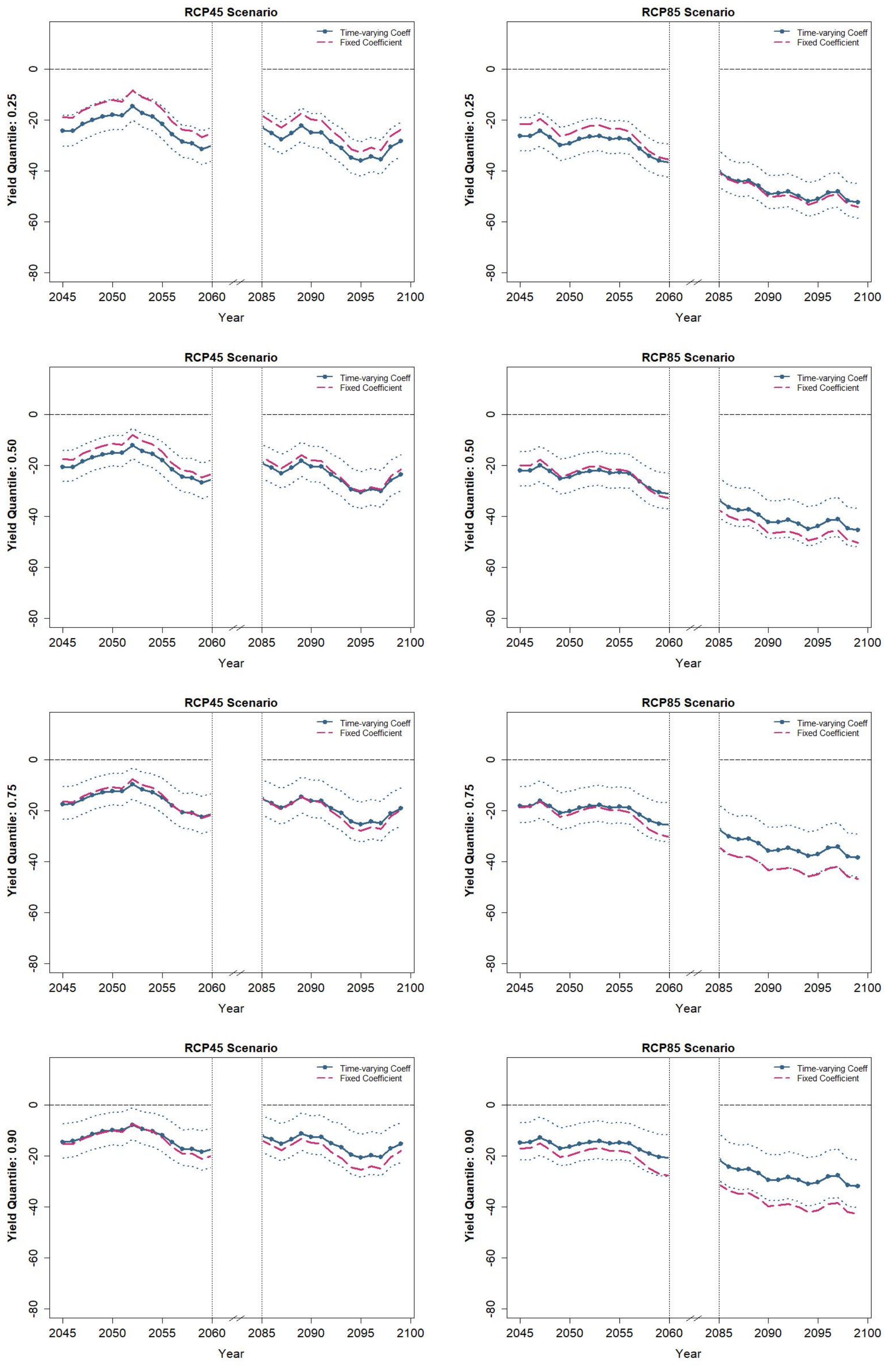

Figure D.4. Rolling-Window Average Soybean Yield Decline Predictions using the NorESM1-M Forecasts with Two-Sided 95% Confidence Intervals (in %) (time-varying coefficient model and fixed-coefficient model with both the additive linear and quadratic time trends)

Note: Solid blue lines correspond to the estimates from our time-varying coefficient model. The dotted blue lines depict the 95% confidence intervals. Dashed pink lines correspond to the estimates from a fixed-coefficient model with both the additive linear and quadratic time trends.

E Modeling Temperature à la Schlenker & Roberts (2009)

This appendix includes the robustness check results where the nonlinear relationship between the crop yield and temperature is modeled using a series of discretized measures of the exposure time à la Schlenker & Roberts (2009) within five-degree Celsius intervals.

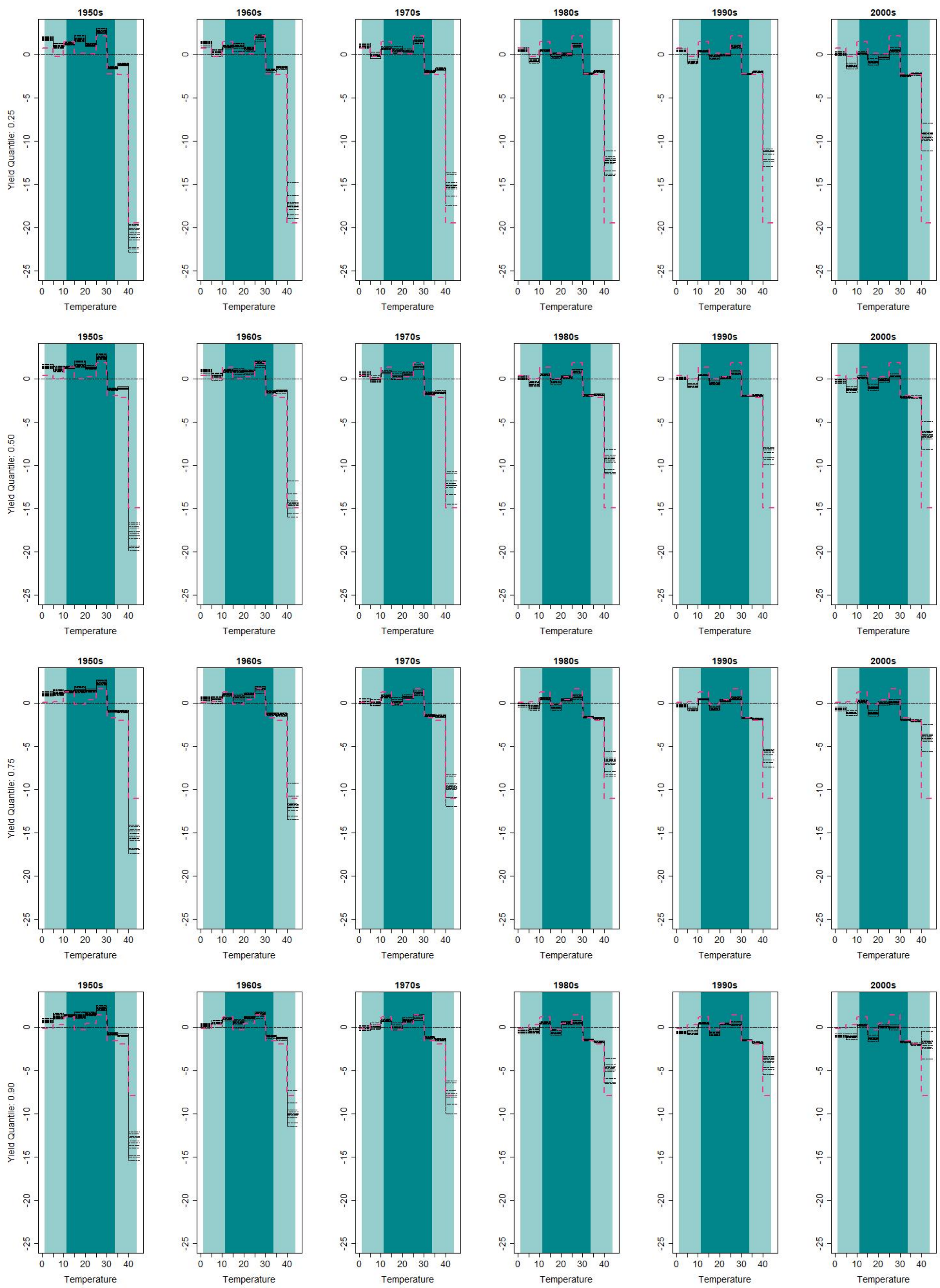

Figure E.1. Marginal Effect Estimates of One-day Exposure under a Specific 5°C-Temperature Interval for the Corn Yield (in %)

Note: A dashed black line corresponds to the estimates in a year from the time-varying coefficient model. A dashed pink line corresponds to the estimates from the fixed-coefficient model with the additive liner time trend. Dark (light) shaded areas illustrate the inter-quartile (middle 95%) ranges of temperature in each decade.

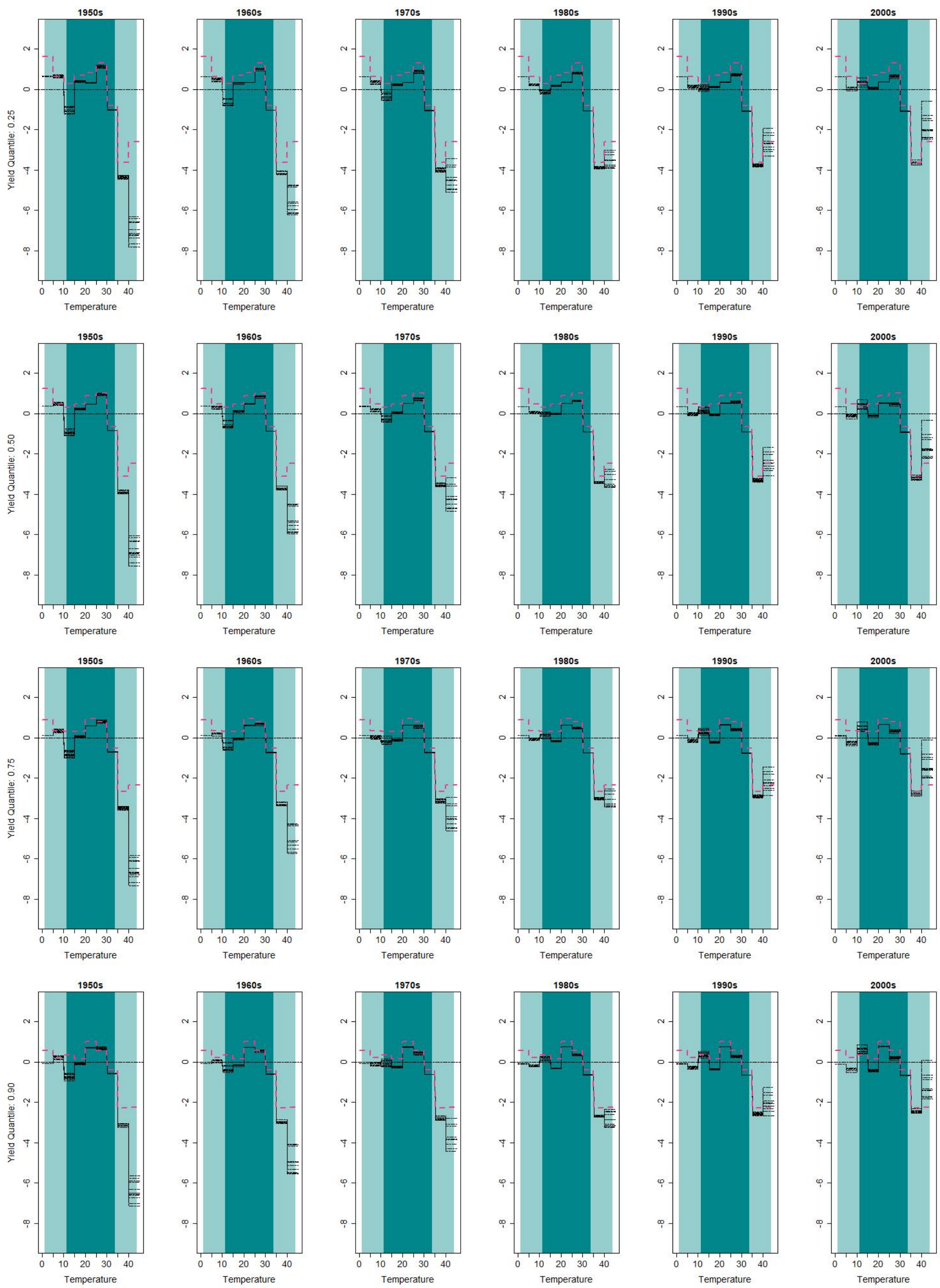

Figure E.2. Marginal Effect Estimates of One-day Exposure under a Specific 5°C-Temperature Interval for the Soybean Yield (in %)

Note: A dashed black line corresponds to the estimates in a year from the time-varying coefficient model. A dashed pink line corresponds to the estimates from the fixed-coefficient model with the additive liner time trend. Dark (light) shaded areas illustrate the inter-quartile (middle 95%) ranges of temperature in each decade.

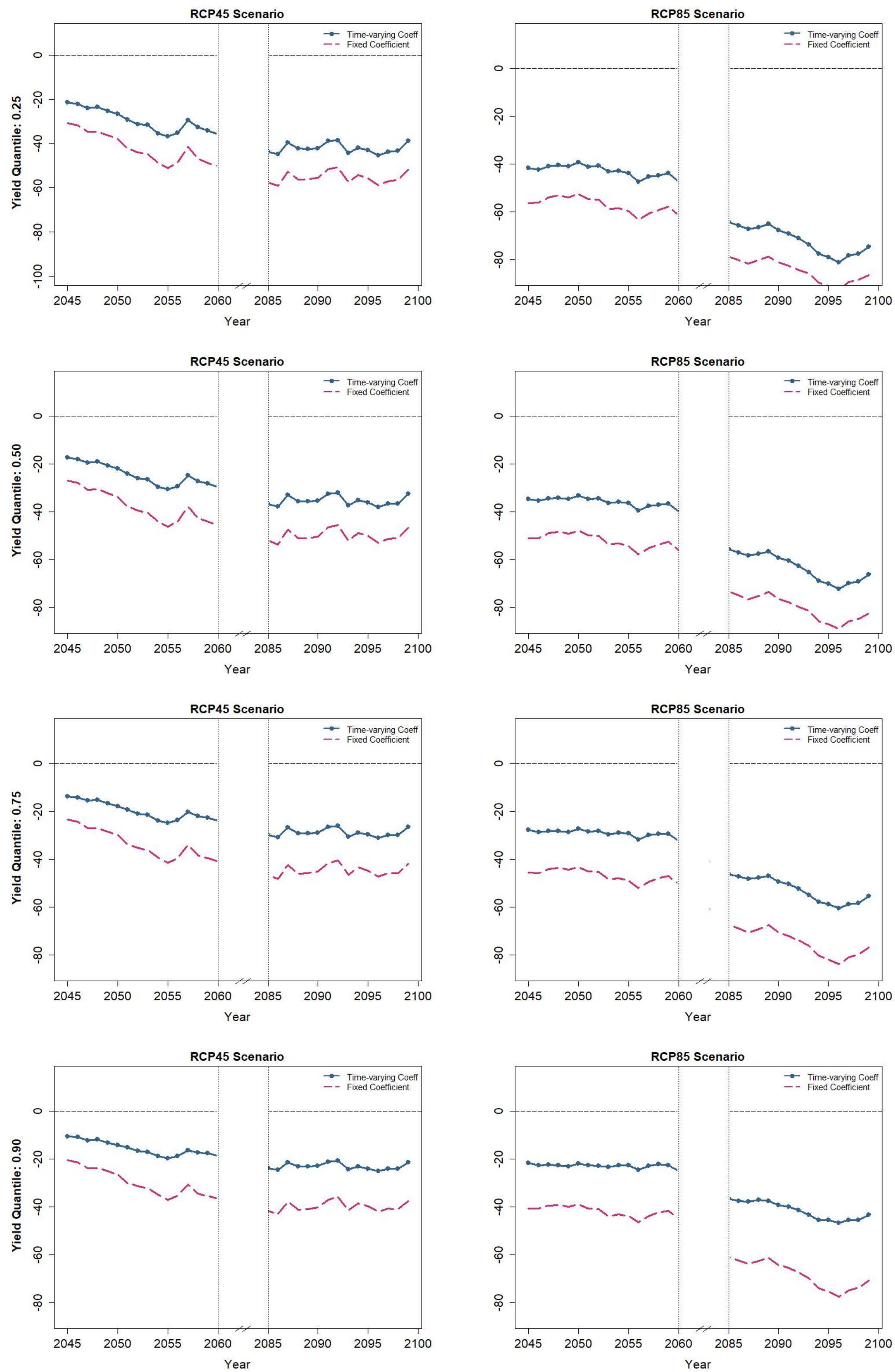

Figure E.3. Rolling-Window Average Corn Yield Decline Predictions Based on the HadGEM2-ES365 Forecasts When Using the Temperature Exposure Intervals as Temperature Variables (in %)

Note: Solid blue lines correspond to the estimates from our time-varying coefficient model. Dashed pink lines correspond to the estimates from the fixed-coefficient model with an additive linear time trend.

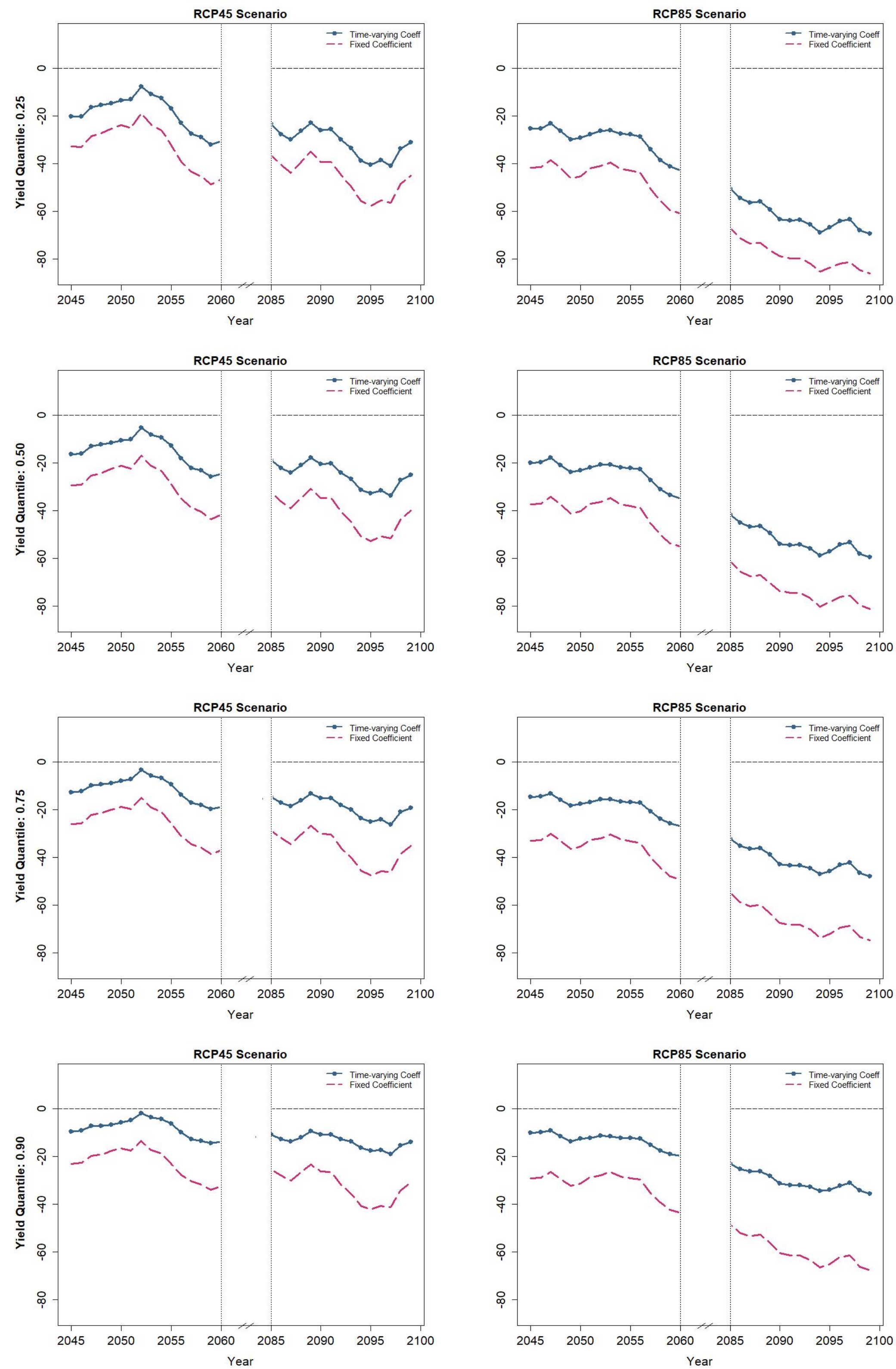

Figure E.4. Rolling-Window Average Corn Yield Decline Predictions Based on the NorESM1-M Forecasts When Using the Temperature Exposure Intervals as Temperature Variables (in %)
Note: Solid blue lines correspond to the estimates from our time-varying coefficient model. Dashed pink lines correspond to the estimates from the fixed-coefficient model with an additive linear time trend.

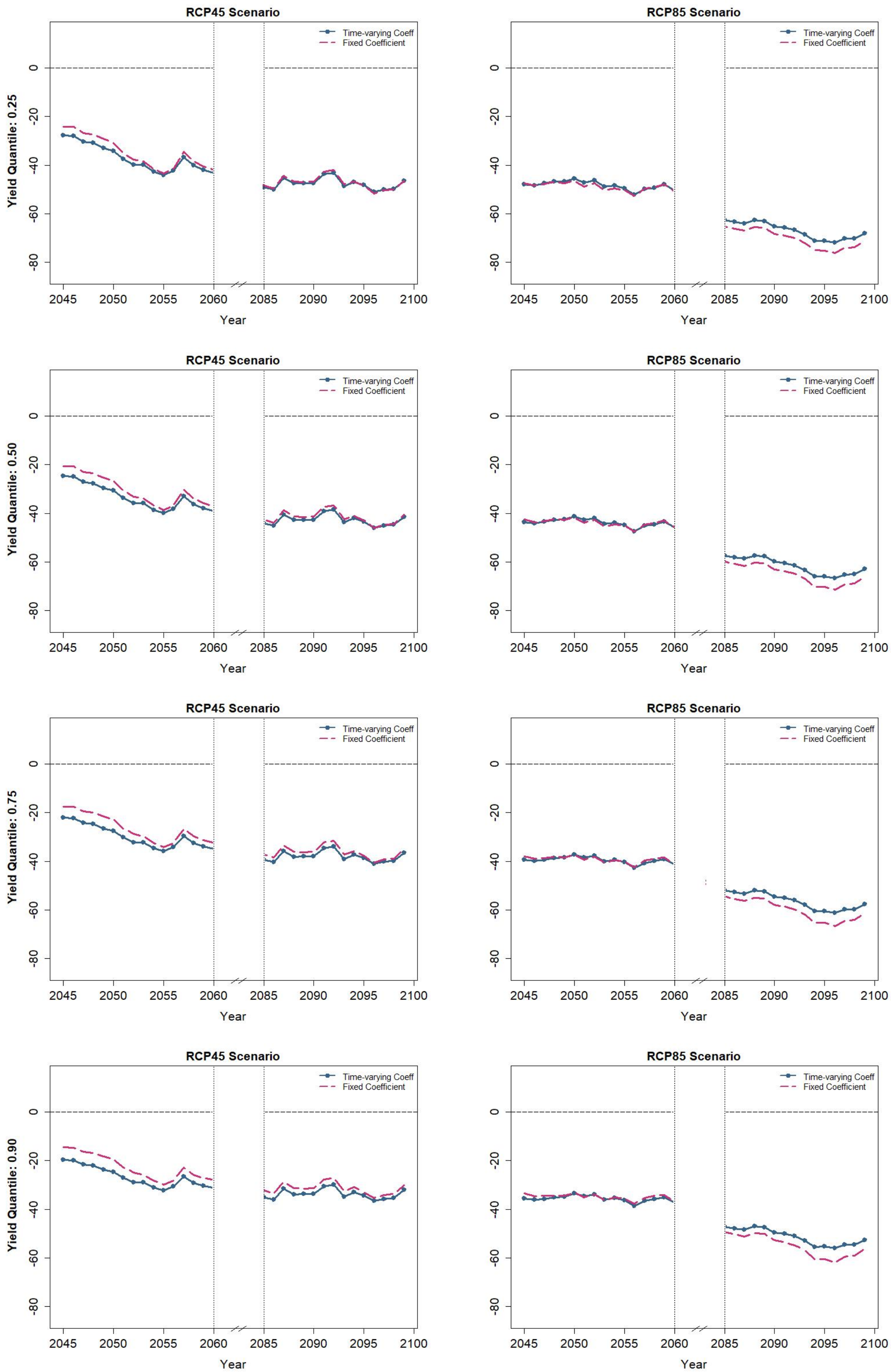

Figure E.5. Rolling-Window Average Soybean Yield Decline Predictions Based on the HadGEM2-ES365 Forecasts When Using the Temperature Exposure Intervals as Temperature Variables (in %)

Note: Solid blue lines correspond to the estimates from our time-varying coefficient model. Dashed pink lines correspond to the estimates from the fixed-coefficient model with an additive linear time trend.

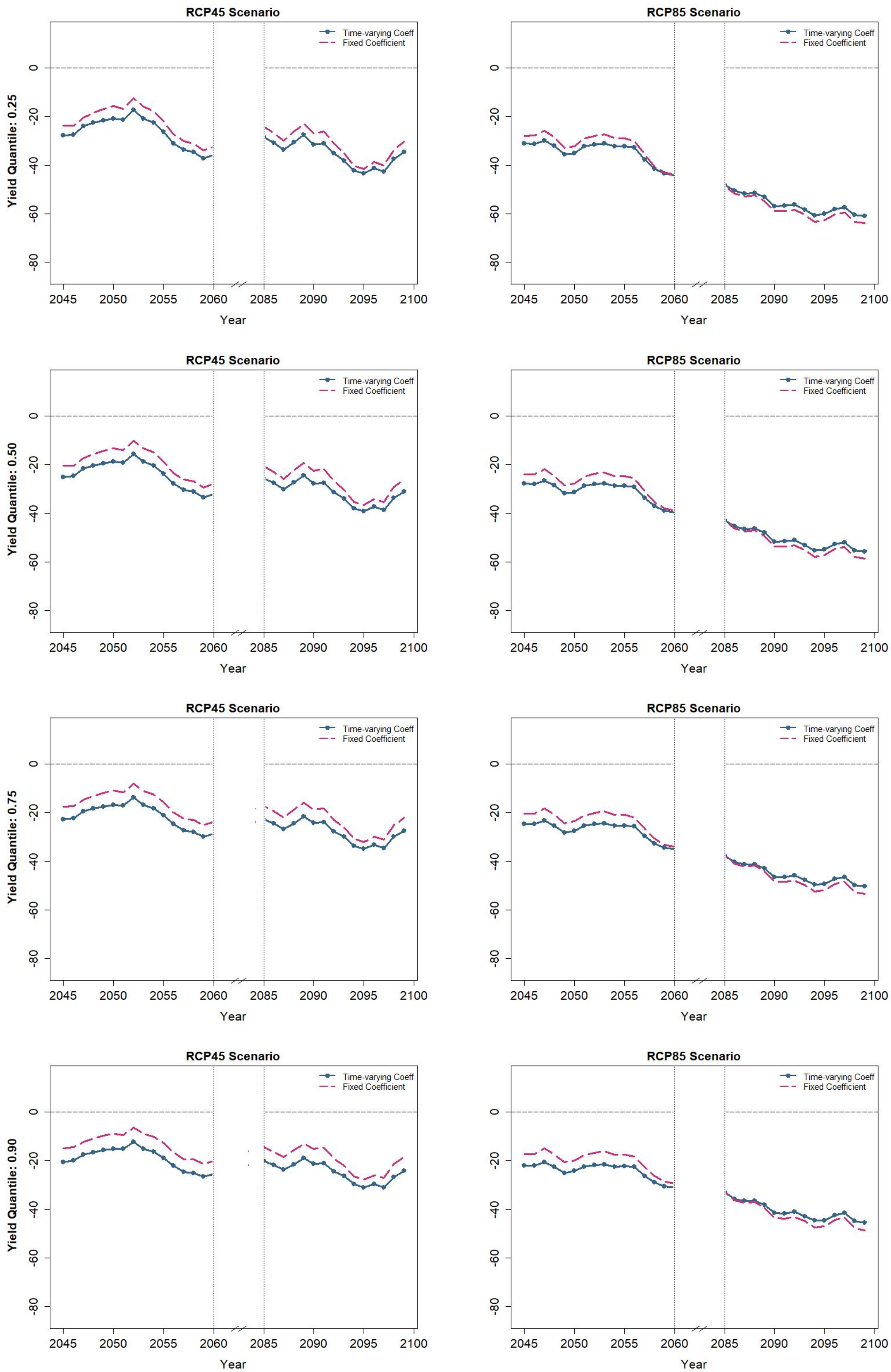

Figure E.6. Rolling-Window Average Soybean Yield Decline Predictions Based on the NorESM1-M Forecasts When Using the Temperature Exposure Intervals as Temperature Variables (in %)
Note: Solid blue lines correspond to the estimates from our time-varying coefficient model. Dashed pink lines correspond to the estimates from the fixed-coefficient model with an additive linear time trend.

F Results for the Weighted Estimations

This appendix includes the robustness check results where the regressions are weighted using the harvested acreage of a crop.

Table F.1. Time-Varying Quantile Slope Coefficient Estimates for the Corn Yield (Weighted Estimation)

	All Estimates					*All Estimates*				
Variable	Min	1st Qu.	Median	3rd Qu.	Max	Min	1st Qu.	Median	3rd Qu.	Max
	The 0.25th Yield Quantile					**The 0.50th Yield Quantile**				
Total $GDD_{8-29^\circ C}$	0.0446	0.1133	0.1604	0.2388	0.3511	0.0174	0.0861	0.1331	0.2116	0.3238
Total $GDD_{8-29^\circ C}$ sq. ($\times 10^{-3}$)	–0.0652	–0.0420	–0.0258	–0.0161	–0.0019	–0.0605	–0.0373	–0.0211	–0.0114	0.0028
Total $GDD_{29^\circ C+}$ (square root)	–13.3258	–10.7229	–8.9031	–7.8113	–6.2189	–11.3861	–8.7833	–6.9635	–5.8716	–4.2793
Total Precipitation	0.1274	0.1843	0.2233	0.2884	0.3814	0.0746	0.1315	0.1705	0.2356	0.3286
Total Precipitation sq. ($\times 10^{-3}$)	–0.3322	–0.2406	–0.1765	–0.1381	–0.0820	–0.2906	–0.1990	–0.1349	–0.0965	–0.0405
Average Wind Speed	–6.3083	–6.2472	–6.2045	–6.1789	–6.1416	–5.8130	–5.7520	–5.7093	–5.6837	–5.6463
Average Humidity ($\times 10^{3}$)	–7.1315	–5.9507	–5.1251	–4.6297	–3.9073	–6.8597	–5.6788	–4.8532	–4.3579	–3.6355
Average Long-Wave Radiation	0.0237	0.0455	0.0608	0.0699	0.0832	–0.0113	0.0105	0.0257	0.0349	0.0482
Average Short-Wave Radiation	–1.1675	–0.5734	–0.1581	0.0911	0.4545	–1.1151	–0.5210	–0.1057	0.1435	0.5069
Average Surface Pressure	2.1717	3.0247	3.6095	4.5843	5.9786	2.1803	3.0332	3.6181	4.5929	5.9871
	The 0.75th Yield Quantile					**The 0.90th Yield Quantile**				
Total $GDD_{8-29^\circ C}$	–0.0053	0.0634	0.1105	0.1890	0.3012	–0.0227	0.0460	0.0931	0.1715	0.2838
Total $GDD_{8-29^\circ C}$ sq. ($\times 10^{-3}$)	–0.0566	–0.0334	–0.0172	–0.0075	0.0067	–0.0536	–0.0304	–0.0142	–0.0044	0.0098
Total $GDD_{29^\circ C+}$ (square root)	–9.7740	–7.1712	–5.3514	–4.2595	–2.6672	–8.5331	–5.9303	–4.1105	–3.0186	–1.4263
Total Precipitation	0.0307	0.0876	0.1267	0.1917	0.2848	–0.0030	0.0539	0.0929	0.1580	0.2510
Total Precipitation sq. ($\times 10^{-3}$)	–0.2561	–0.1644	–0.1004	–0.0620	–0.0059	–0.2295	–0.1379	–0.0738	–0.0354	0.0207
Average Wind Speed	–5.4014	–5.3404	–5.2977	–5.2721	–5.2347	–5.0846	–5.0235	–4.9808	–4.9552	–4.9179
Average Humidity ($\times 10^{3}$)	–6.6338	–5.4529	–4.6273	–4.1319	–3.4095	–6.4599	–5.2790	–4.4534	–3.9580	–3.2356
Average Long-Wave Radiation	–0.0405	–0.0187	–0.0034	0.0057	0.0191	–0.0629	–0.0411	–0.0258	–0.0167	–0.0033
Average Short-Wave Radiation	–1.0715	–0.4774	–0.0621	0.1871	0.5505	–1.0380	–0.4439	–0.0286	0.2206	0.5840
Average Surface Pressure	2.1873	3.0403	3.6252	4.6000	5.9942	2.1928	3.0458	3.6306	4.6054	5.9997

Note: The panel summarizes all point estimates. The reported estimates are measured in % of yield per unit in the corresponding regressor.

Table F.2. Time-Varying Quantile Slope Coefficient Estimates for the Soybean Yield (Weighted Estimation)

	All Estimates					*All Estimates*				
Variable	Min	1st Qu.	Median	3rd Qu.	Max	Min	1st Qu.	Median	3rd Qu.	Max
	The 0.25th Yield Quantile					**The 0.50th Yield Quantile**				
Total $GDD_{8-30°C}$	0.1263	0.1843	0.2174	0.2757	0.3335	0.1002	0.1583	0.1913	0.2496	0.3074
Total $GDD_{8-30°C}$ sq. ($\times 10^{-3}$)	–0.0566	–0.0475	–0.0384	–0.0332	–0.0241	–0.0505	–0.0414	–0.0323	–0.0271	–0.0180
Total $GDD_{30°C+}$ (square root)	–12.0109	–10.3289	–8.6342	–7.6734	–5.9866	–10.6646	–8.9826	–7.2878	–6.3271	–4.6402
Total Precipitation	0.0843	0.1054	0.1174	0.1386	0.1596	0.0759	0.0970	0.1090	0.1301	0.1511
Total Precipitation sq. ($\times 10^{-3}$)	–0.1305	–0.1103	–0.0901	–0.0786	–0.0584	–0.1226	–0.1025	–0.0822	–0.0707	–0.0505
Average Wind Speed	–6.1611	–5.9087	–5.7650	–5.5115	–5.2598	–6.2088	–5.9564	–5.8127	–5.5591	–5.3075
Average Humidity ($\times 10^{3}$)	–0.8211	–0.1250	0.5763	0.9739	1.6719	–1.4031	–0.7071	–0.0057	0.3919	1.0899
Average Long-Wave Radiation	–0.2949	–0.1673	–0.0389	0.0340	0.1618	–0.3125	–0.1850	–0.0566	0.0163	0.1442
Average Short-Wave Radiation	–0.1109	–0.0877	–0.0643	–0.0511	–0.0278	–0.1369	–0.1137	–0.0903	–0.0770	–0.0538
Average Surface Pressure	–6.0595	–3.4835	–2.0163	0.5718	3.1404	–6.0698	–3.4938	–2.0267	0.5614	3.1301
	The 0.75th Yield Quantile					**The 0.90th Yield Quantile**				
Total $GDD_{8-30°C}$	0.0782	0.1362	0.1693	0.2275	0.2854	0.0597	0.1177	0.1508	0.2091	0.2669
Total $GDD_{8-30°C}$ sq. ($\times 10^{-3}$)	–0.0453	–0.0363	–0.0271	–0.0220	–0.0129	–0.0410	–0.0319	–0.0228	–0.0176	–0.0086
Total $GDD_{30°C+}$ (square root)	–9.5260	–7.8440	–6.1493	–5.1885	–3.5017	–8.5719	–6.8898	–5.1951	–4.2343	–2.5475
Total Precipitation	0.0687	0.0898	0.1018	0.1230	0.1440	0.0628	0.0838	0.0958	0.1170	0.1380
Total Precipitation sq. ($\times 10^{-3}$)	–0.1159	–0.0958	–0.0756	–0.0641	–0.0439	–0.1104	–0.0903	–0.0700	–0.0585	–0.0383
Average Wind Speed	–6.2491	–5.9968	–5.8530	–5.5995	–5.3478	–6.2829	–6.0306	–5.8868	–5.6333	–5.3816
Average Humidity ($\times 10^{3}$)	–1.8953	–1.1993	–0.4979	–0.1003	0.5977	–2.3078	–1.6118	–0.9104	–0.5128	0.1852
Average Long-Wave Radiation	–0.3275	–0.2000	–0.0715	0.0013	0.1292	–0.3400	–0.2125	–0.0840	–0.0112	0.1167
Average Short-Wave Radiation	–0.1589	–0.1356	–0.1123	–0.0990	–0.0757	–0.1773	–0.1541	–0.1307	–0.1174	–0.0941
Average Surface Pressure	–6.0786	–3.5026	–2.0354	0.5527	3.1213	–6.0859	–3.5099	–2.0427	0.5454	3.1140

Note: The panel summarizes all point estimates. The reported estimates are measured in % of yield per unit in the corresponding regressor.

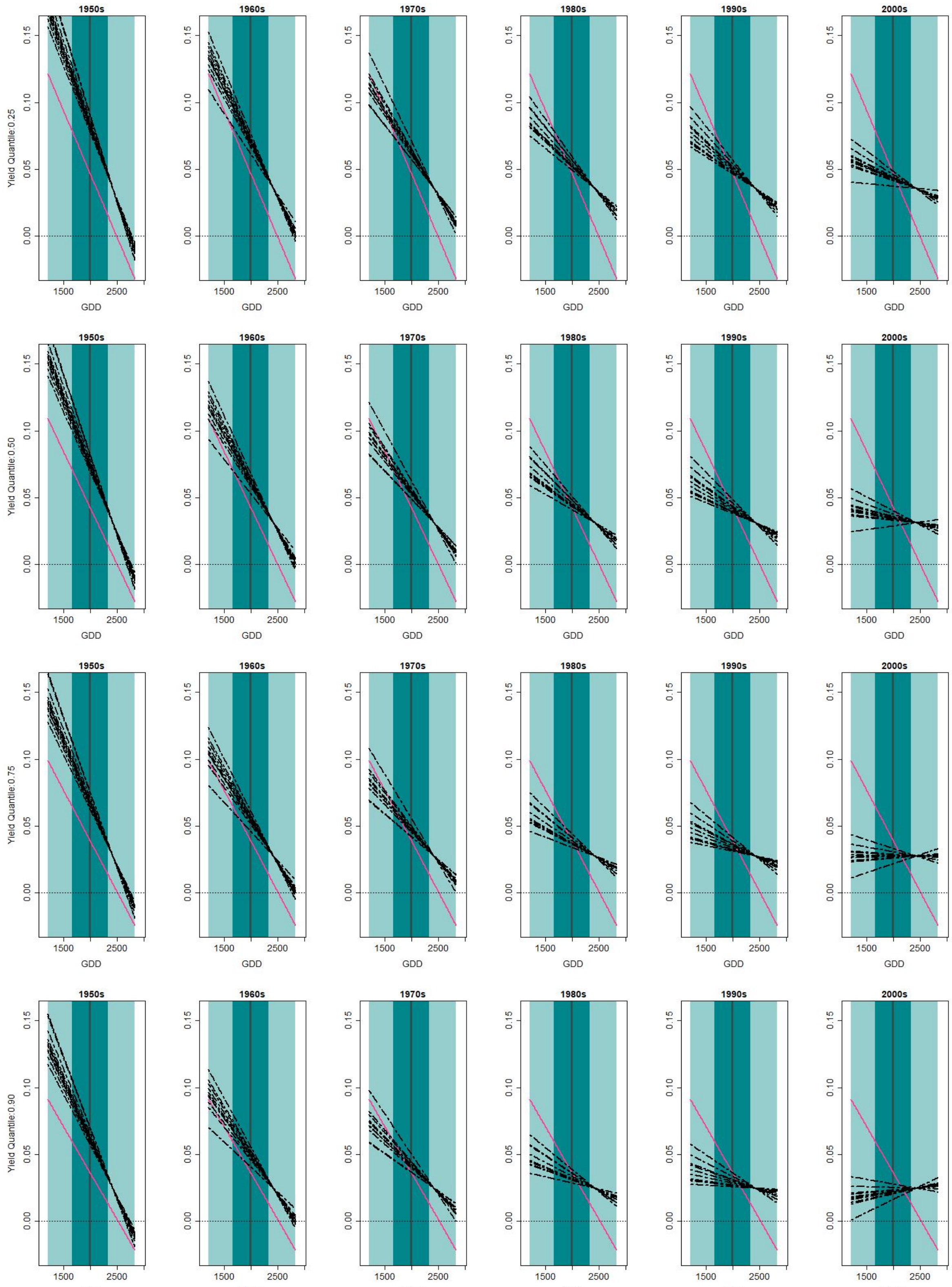

Figure F.1. Marginal-Effect Function Estimates of Total GDD$_{8-29°C}$ for the Corn Yield based on the Weighted Estimation (in % per GDD)

Note: Dashed black (solid pink) lines correspond to the estimates from a time-varying coefficient (fixed-coefficient) model. Dark (light) shaded areas illustrate the inter-quartile (middle 95%) ranges of total GDD in each decade.

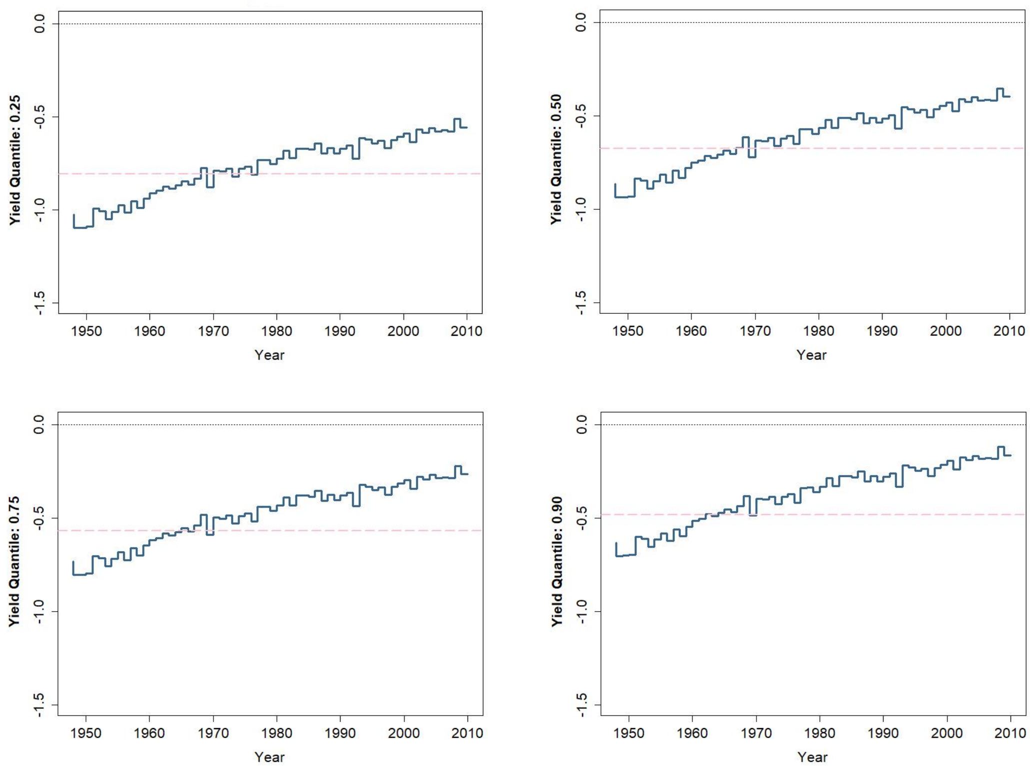

Figure F.2. Marginal Effect Estimates of Total $GDD_{29^{\circ}C+}$ for the Corn Yield based on the Weighted Estimation (in % per GDD)

Note: Horizontal dashed pink lines correspond to the estimates from a fixed-coefficient model.

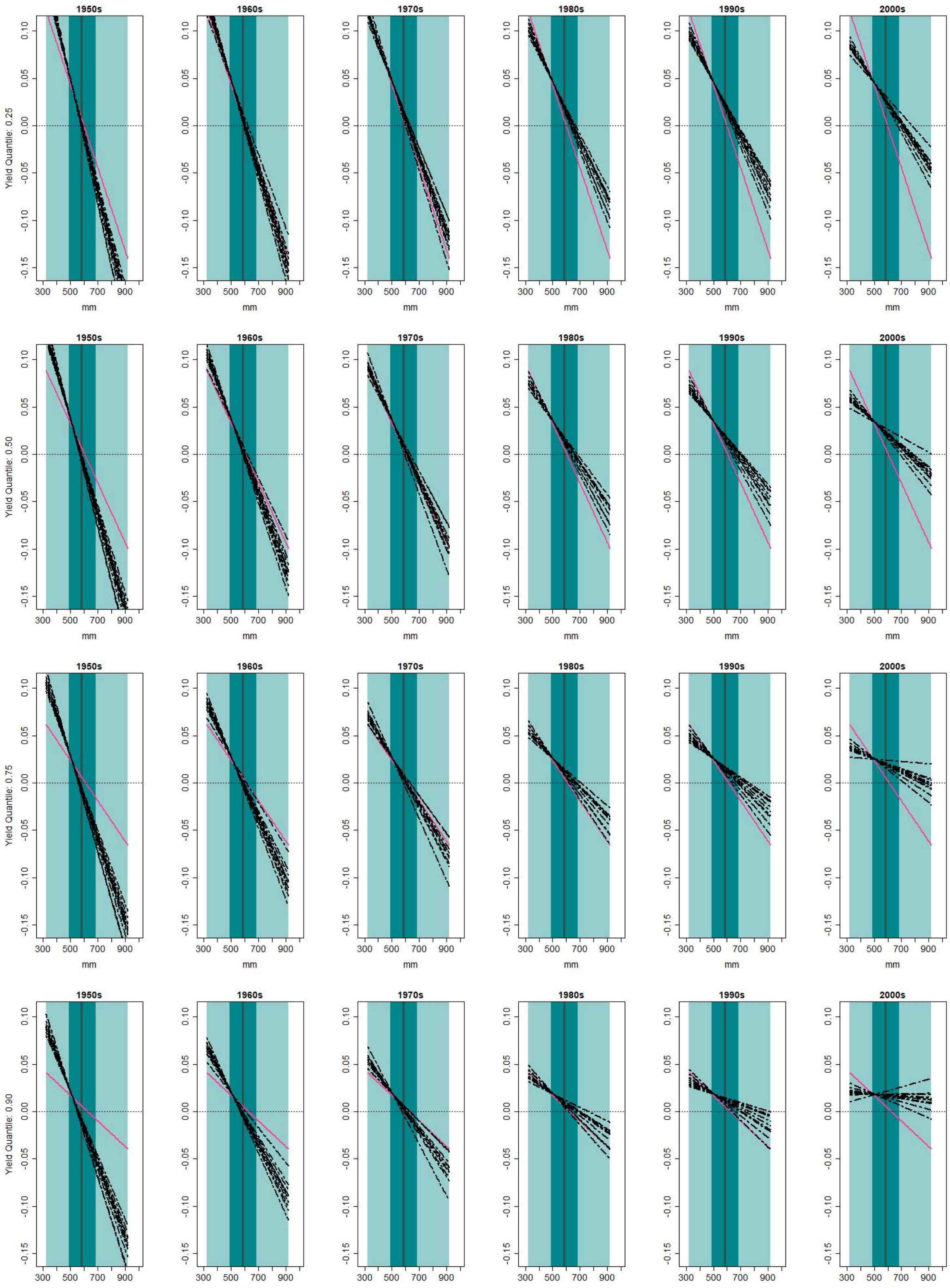

Figure F.3. Marginal-Effect Function Estimates of Total Precipitation for the Corn Yield based on the Weighted Estimation (in % per mm)

Note: Dashed black (solid pink) lines correspond to the estimates from a time-varying coefficient (fixed-coefficient) model. Dark (light) shaded areas illustrate the inter-quartile (middle 95%) ranges of total precipitation in each decade.

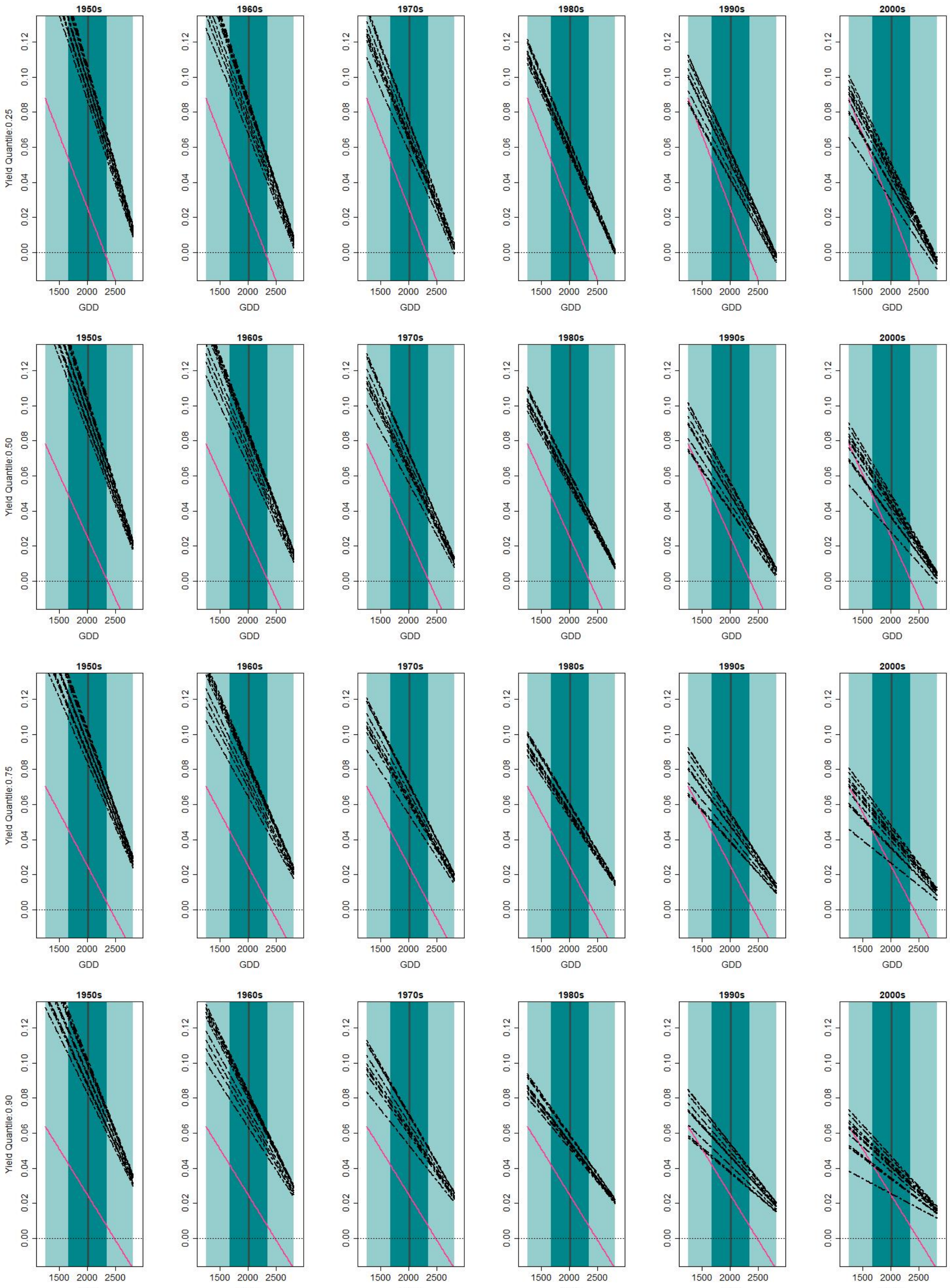

Figure F.4. Marginal-Effect Function Estimates of Total $GDD_{8-30°C}$ for the Soybean Yield based on the Weighted Estimation (in % per GDD)

Note: Dashed black (solid pink) lines correspond to the estimates from a time-varying coefficient (fixed-coefficient) model. Dark (light) shaded areas illustrate the inter-quartile (middle 95%) ranges of total GDD in each decade.

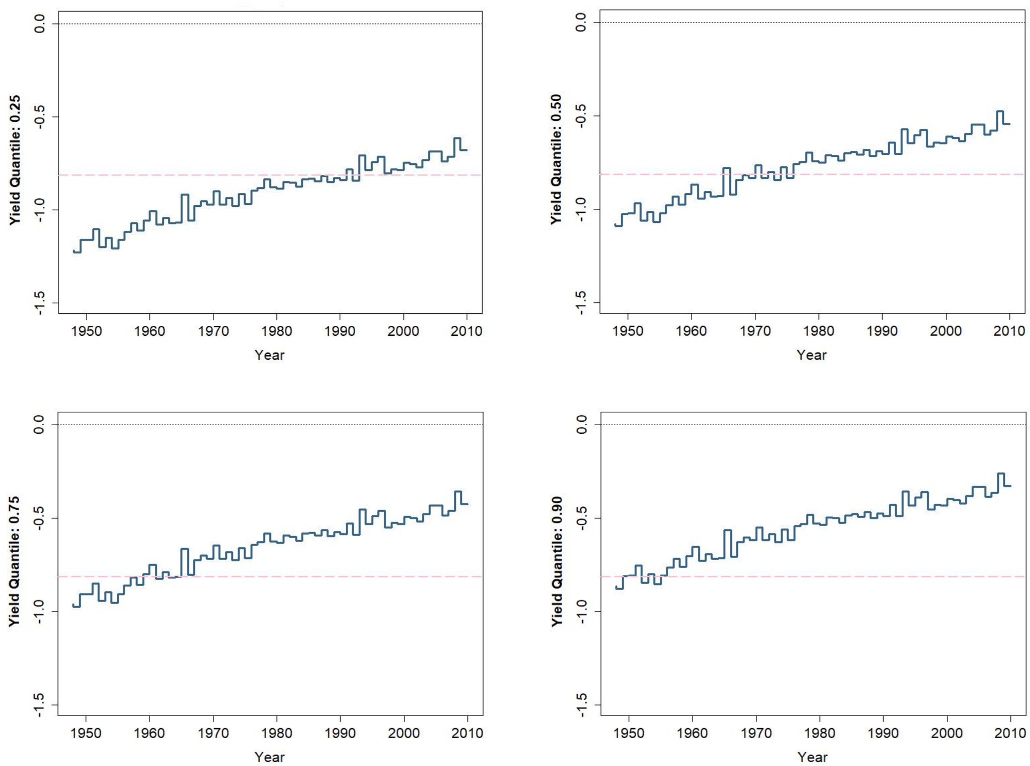

Figure F.5. Marginal Effect Estimates of Total $GDD_{30^{\circ}C+}$ for the Soybean Yield based on the Weighted Estimation (in % per GDD)

Note: Horizontal dashed pink lines correspond to the estimates from a fixed-coefficient model.

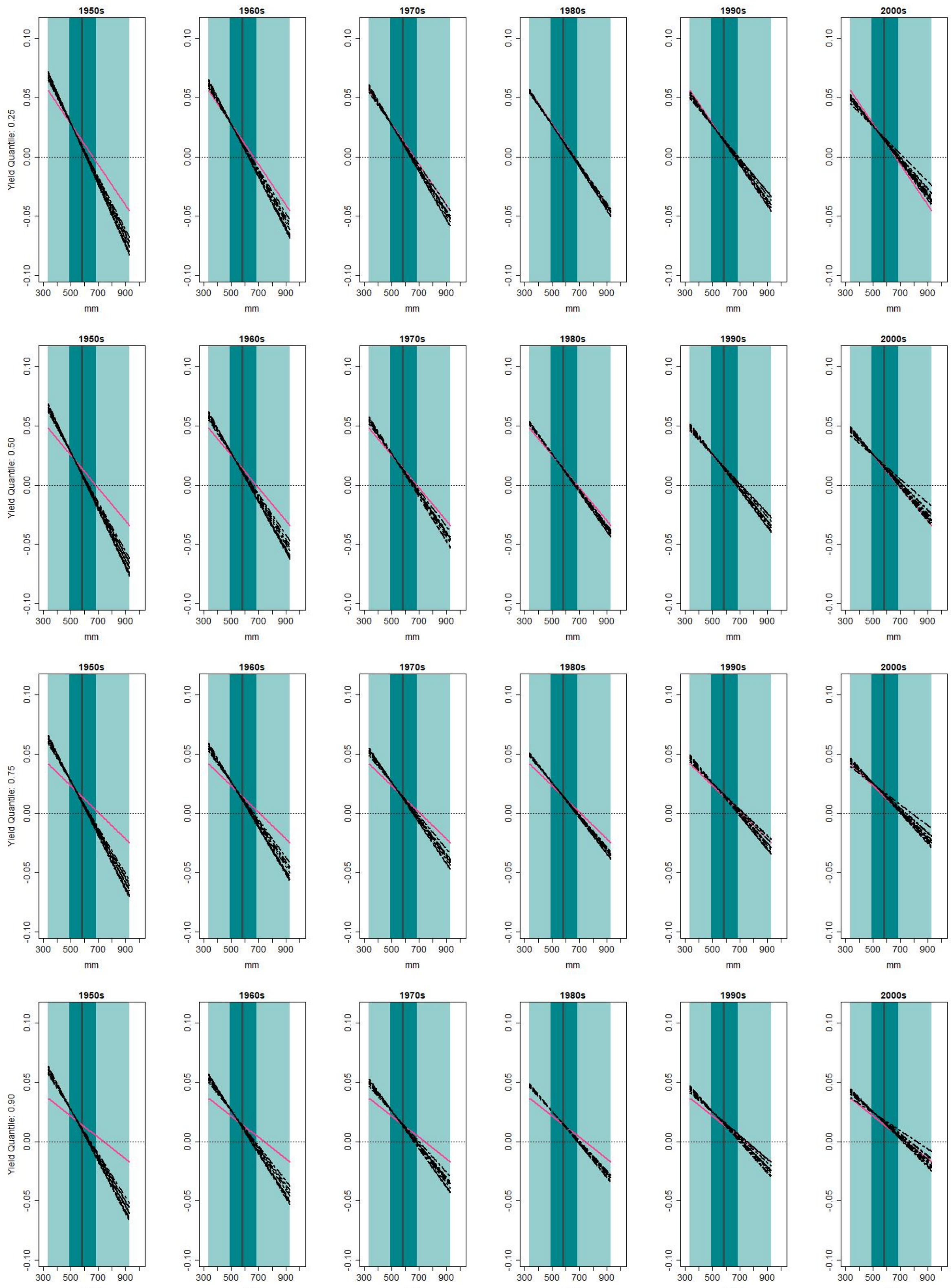

Figure F.6. Marginal-Effect Function Estimates of Total Precipitation for the Soybean Yield based on the Weighted Estimation (in % per mm)

Note: Dashed black (solid pink) lines correspond to the estimates from a time-varying coefficient (fixed-coefficient) model. Dark (light) shaded areas illustrate the inter-quartile (middle 95%) ranges of total precipitation in each decade.

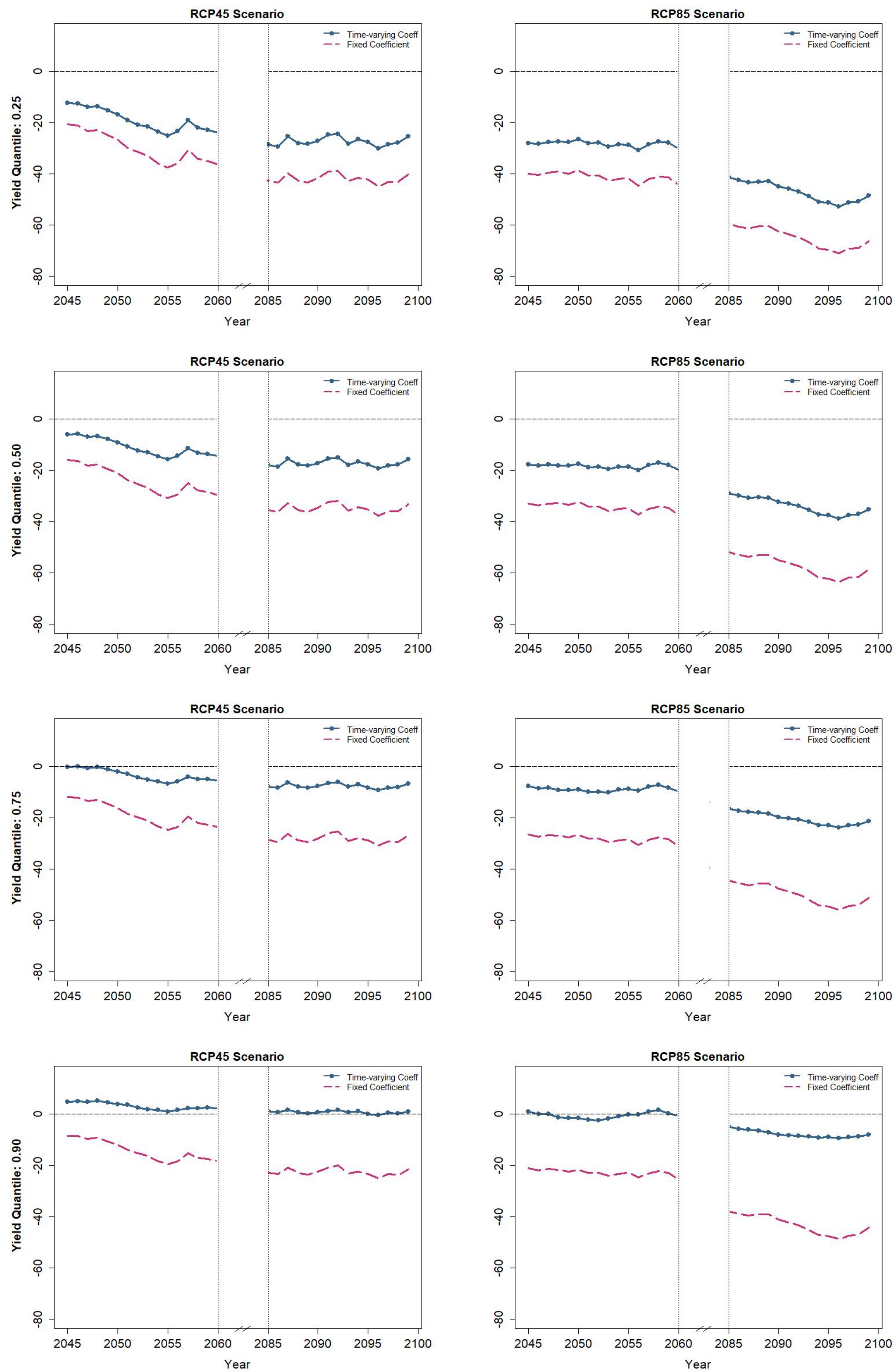

Figure F.7. Rolling-Window Average Corn Yield Decline Predictions using the HadGEM2-ES365 Forecasts based on the Weighted Estimation (in %)

Note: Solid blue lines correspond to the estimates from our time-varying coefficient model. Dashed pink lines correspond to the estimates from a fixed-coefficient model.

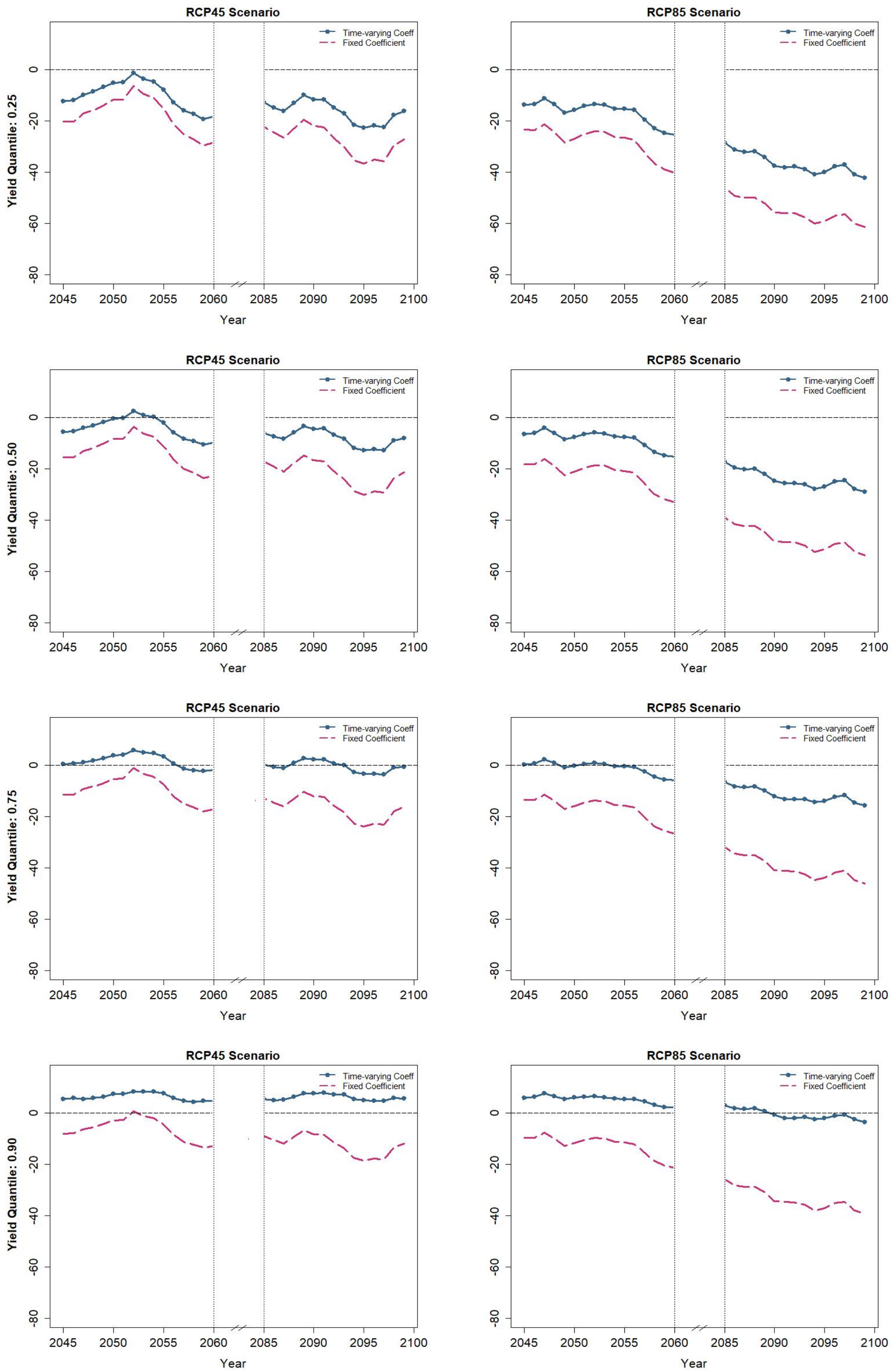

Figure F.8. Rolling-Window Average Corn Yield Decline Predictions using the NorESM1-M Forecasts based on the Weighted Estimation (in %)
Note: Solid blue lines correspond to the estimates from our time-varying coefficient model. Dashed pink lines correspond to the estimates from a fixed-coefficient model.

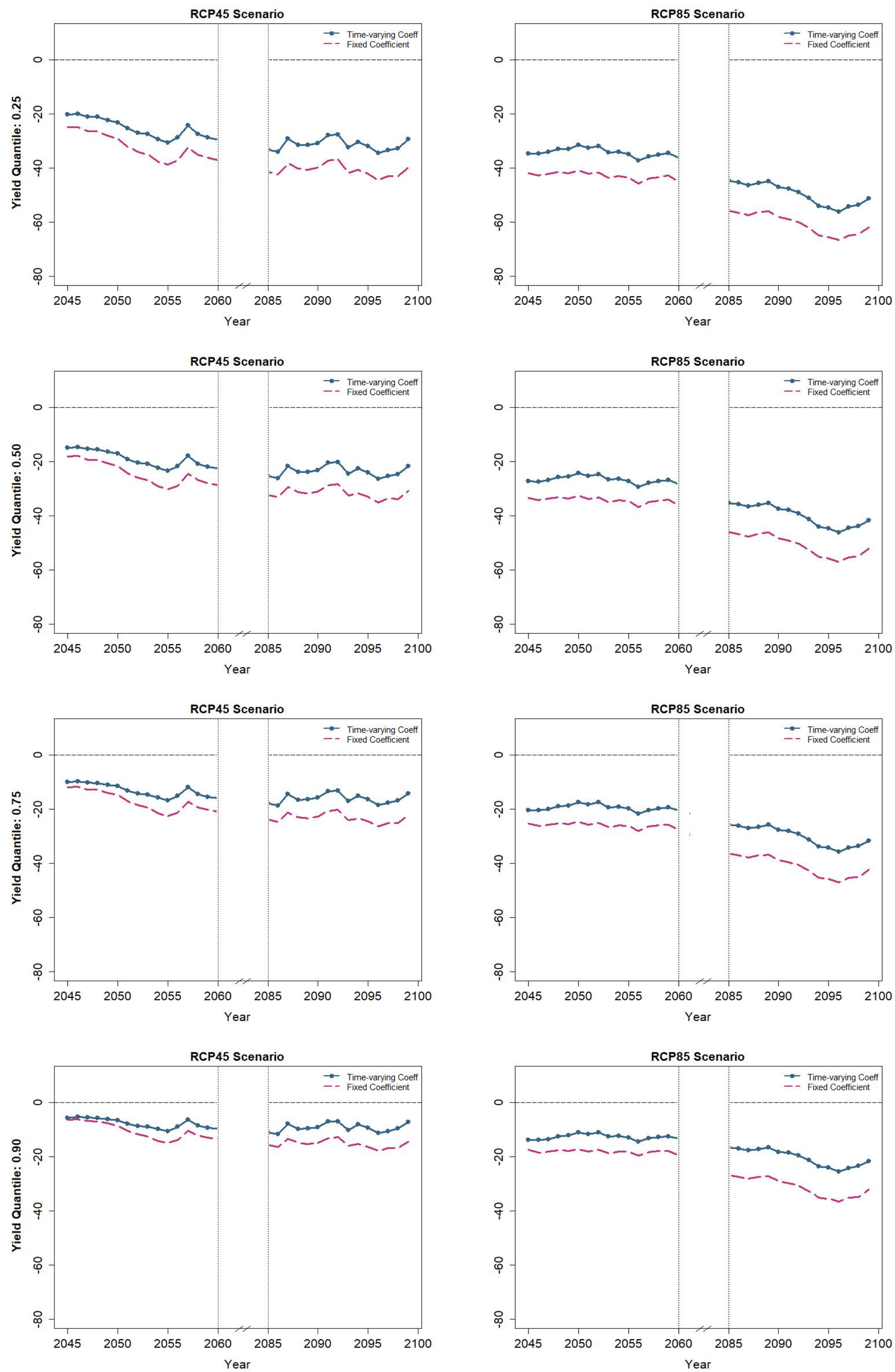

Figure F.9. Rolling-Window Average Soybean Yield Decline Predictions using the HadGEM2-ES365 Forecasts based on the Weighted Estimation (in %)

Note: Solid blue lines correspond to the estimates from our time-varying coefficient model. Dashed pink lines correspond to the estimates from a fixed-coefficient model.

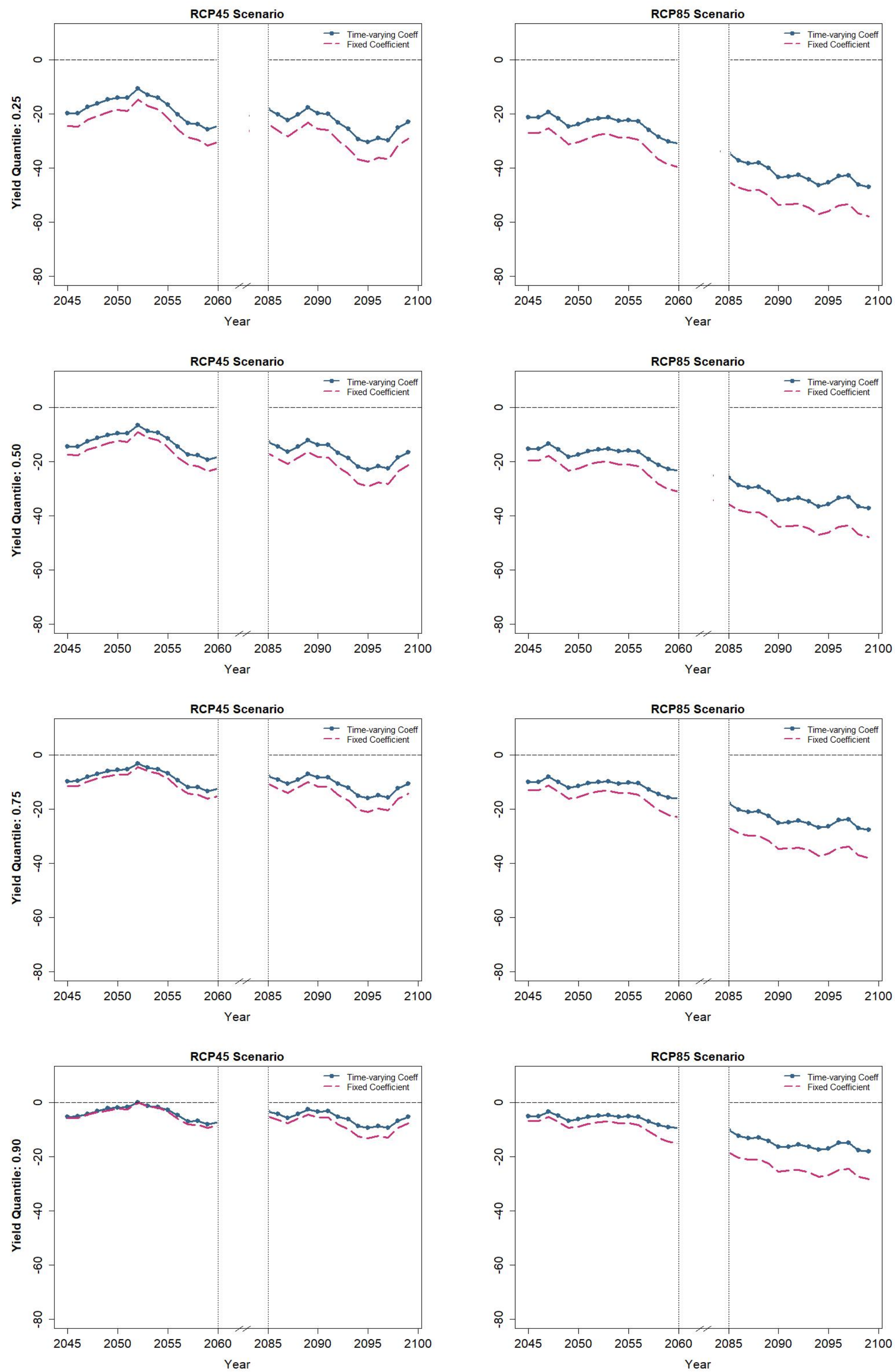

Figure F.10. Rolling-Window Average Soybean Yield Decline Predictions using the NorESM1-M Forecasts based on the Weighted Estimation (in %)

Note: Solid blue lines correspond to the estimates from our time-varying coefficient model. Dashed pink lines correspond to the estimates from a fixed-coefficient model.

References

Mammen, E. 1993. “Bootstrap and wild bootstrap for high dimensional linear models.” Annals of Statistics. 21 (1): 255—285.

Schlenker, W. and M.J. Roberts. 2009. “Nonlinear Temperature Effects Indicate Severe Damages to U.S. Crop Yields under Climate Change.” Proceedings of the National Academy of Sciences 106 (37): 15594-–15598.